LIU, CHENG-KUANG

STUDY OF NUCLEAR BREMSSTRAHLUNG IN THE MODEL INDEPENDENT APPROACH

City University of New York PH.D. 1980

STUDY OF NUCLEAR BREMSSTRAHLUNG IN THE MODEL INDEPENDENT APPROACH

by

CHENG-KUANG LIU

A dissertation submitted to the Graduate Faculty in Physics in partial fulfillment of the requirements for the degree of Doctor of Philosophy, the City University of New York.

1980

This manuscript has been read and accepted for the Graduate Faculty in Physics in satisfaction of the dissertation requirement for the degree of Doctor of Philosophy.

M. K. Liou

July 14, 1980
date

Professor M. K. Liou
Chairman of Examining Committee

Frank Martino

July 15, 1980
date

Professor F. Martino
Executive Officer

Professor C. Shakin

Professor M. I. Sobel

Professor A. Mukerji

Dr. B. F. Gibson
Supervisory Committee

The City University of New York

ABSTRACT

STUDY OF NUCLEAR BREMSSTRAHLUNG IN THE MODEL-INDEPENDENT APPROACH

by

Cheng-Kuang Liu

Advisor: Professor Ming-Kung Liou

The proton-carbon, pion-proton and proton-proton bremsstrahlung processes have been theoretically studied by using two different model-independent approaches, the soft-photon approximation and the Feshbach-Yennie approximation.

The bremsstrahlung cross section for the scattering of protons by ^{12}C near the 1.7-MeV resonance has been measured by the Bologna group and the Brooklyn group. These data have been analyzed by some authors using only the principal term of the Feshbach-Yennie approximation. In this study, we have included in our calculations the correction terms and have extracted the time delay in the p-^{12}C reaction from the data of the Brooklyn group. Our calculation shows that the structure due to the 1.7-MeV resonance can be described successfully by the Feshbach-Yennie approximation only if the correction terms are included.

The $\pi^{\pm}p\gamma$ process near the $\Delta(1236)$ has been systematically studied by an experimental group at UCLA. Many calculations have been performed, but, only the calculation of Nefkens et al. agrees well with the experimental data in most cases. Recently, Liou and Nutt reported a calculation using the soft-photon approximation and their results agree very well with experiment for coplanar events. We have extended their calculation to noncoplanar cases and have found that the soft-photon approximation of Liou and Nutt can describe the experimental data very well not only for coplanar cases but also for noncoplanar cases for most photon angles. In addition, we have also used the Feshbach-Yennie approximation to calculate the $\pi^{\pm}p\gamma$ cross sections. This approximation always predicts a bump in the bremsstrahlung spectrum, although the bump may be small for some photon angles. In most cases, the predicted cross sections are in good agreement with the UCLA data. However, the data for some angles can only be described by the Feshbach-Yennie approximation, and the peak cross section is too large at some angles.

We have applied the soft-photon approximation of Liou and Nutt to calculate the proton-proton bremsstrahlung ($pp\gamma$) cross section and have compared our results with the experimental data at 730, 157, 48 and 42 MeV. We have found that we can use the soft-photon approximation to calculate

the R-type cross section without any difficulty, but we cannot use the same approximation to predict the H-type cross section without some ambiguity. Our result for the R-type cross section at low photon energy is in very good agreement with experiment, but the result at high photon energy is lower than the experimental data for some photon angles. This indicates that other contributions or higher order terms are important for these photon angles. We have also applied the Feshbach-Yennie approximation to the ppγ process at 730-MeV taking into account the principal and correction terms. As a result, we have found that the Feshbach-Yennie approximation gives results which are in very good agreement with experiment for low phton energy. For high photon energy, the agreement with data is also good for most cases, but the predictions are lower than the experimental data for some photon angles.

ACKNOWLEDGEMENTS

I would like to thank Professor Ming-Kung Liou for providing me with the opportunity and guidance to complete this work. I would also like to thank Professor Carl Shakin, Professor Michael I. Sobel, Professor Ambuj Mukerji, and Doctor Benjamin F. Gibson for helpful comments and useful discussions. I also wish to acknowledge the financial assistance provided by the Physics Department, Graduate Center and Research Foundation of the CUNY, and the arrangement of computer time made by the Computer Center. Finally, special thanks are to be given to my parents for their encouragement, to my wife, Li-Sha, and our daughter, Julia, for their patience and understanding.

TABLE OF CONTENTS

List of Tables

List of illustrations

CHAPTER I INTRODUCTION

The nucleon-nucleon bremsstrahlung ($NN\gamma$) process has attracted great interest both theoretically and experimentally during the past two decades because of the off-shell information which is not available in the corresponding non-radiative elastic process (1-3). In principle, if one can observe sizable off-shell effects of the nucleon-nucleon interaction in some kinematical region, then it would be possible to differentiate among the many different phenomenological potentials which fit the elastic data equally well. In addition to the interest in the off-shell nature of the NN interaction, the nuclear bremsstrahlung processes have been used as a tool for investigating the electromagnetic properties of Δ-resonance and for studying nuclear reactions (4-6). Moreover, one can develop a better understanding of processes such as neutral pion production through a knowledge of $NN\gamma$, or one can apply soft-photon theorems (7) to other processes such as radiative decay (8,9).

Most of the bremsstrahlung calculations performed in the past were either model independent calculations or potential model calculations. The model independent calculations are based upon a fundamental theorem, known as the soft-photon theorem or Low's theorem or the low energy theorem for photons. It was first derived by Low (7) and was

extended later by Adler and Dothan (9). The theorem states that when the bremsstrahlung cross section, σ , is expanded in powers of photon energy, k,

$$\sigma = \frac{\sigma_{-1}}{k} + \sigma_0 + \sigma_1 k + \cdots, \qquad (I.1)$$

where

$$\sigma_{-1} = \underset{k\to 0}{limit}\,(k\sigma), \quad \sigma_0 = \underset{k\to 0}{limit}\,\frac{\partial}{\partial k}(k\sigma),$$

$$\sigma_1 = \underset{k\to 0}{limit}\,\frac{\partial^2}{\partial k^2}(k\sigma),$$

the first two terms of the expansion can be evaluated from the amplitude of the corresponding nonradiative elastic process and its derivatives. In other words, σ_{-1} and σ_0 are independent of off-shell effects. Moreover, according to Burnett and Kroll (10,11), the radiative cross section for unpolarized particles will depend upon the unpolarized nonradiative cross section only. Thus, a calculation based upon the first two terms of the expansion given by Eq. I.1, which is often called the soft-photon approximation,

$$\sigma \approx \frac{\sigma_{-1}}{k} + \sigma_0 , \qquad (I.2)$$

provides an on-shell and model independent cross section. The soft-photon approximation has been applied to calculate the NNγ cross section by Nyman (12), Fearing (13), and many other authors (14). It has also been applied to predict the cross sections for pion-proton bremsstrahlung processes (15-19). A modified version of the soft-photon approximation was recently proposed by Liou and Nutt (16,24) who

expanded the kinematics and dynamics consistently.

The soft-photon approximation is applicable to all bremsstrahlung processes with no (or little) contribution from resonance effects and the bremsstrahlung spectrum calculated from this approximation has a characteristic 1/k dependence. Since the soft-photon approximation is not valid when a resonance exists and the resonance effects are not negligible in the correponding elastic process, Feshbach and Yennie (5) have proposed another model independent approximation, known as the Feshbach-Yennie approximation, for radiative resonant scattering processes. The Feshbach-Yennie approximation can be written in a form similar to Eq. I.1 except that σ_{-1}, σ_0, and σ_1 are now determined by the elastic scattering amplitudes (and their derivatives with respect to the scattering angle) evaluated at two different energies, the initial and final energies. This approximation is different from the soft-photon approximation in that it predicts structure in the region of resonance. We shall call the leading term, σ_{-1}/k, of the Feshbach-Yennie approximation the principal term and the second and third terms, σ_0 and $\sigma_1 k$, the correction terms.

The model independent approach has played an important role in the study of nuclear bremsstrahlung processes mainly because of the following reasons: (i) It is simple. The input for the calculation can be either the elastic scatter-

ing amplitudes or the elastic scattering cross sections, which are available directly from the elastic scattering experiments. In fact, it is the only way to calculate the bremsstrahlung cross section for a process when a potential description of the interaction is not available. (ii) It is trivially gauge invariant and relativistic invariant. It is therefore applicable to not only the low energy scattering cases but also to the high energy ones. (iii) Since all model dependent calculations must reproduce the result of the model independent calculation in the soft-photon region, the model independent calculations can be used to check the model dependent calculations. (iv) Although the soft-photon approach gives no useful information about off-shell effects or resonance effects, it is essential for the extraction of these effects from experiments. This is simply because the soft-photon approach always provides an on-shell bremsstrahlung spectrum without structure. The difference between the predicted spectrum and the measured spectrum will be the indication of the possible off-shell or resonance effects.

The potential model approach was first introduced and applied to the nucleon-nucleon bremsstrahlung processes by Sobel and Cromer (1). In this approach, the nuclear interaction is treated exactly by using a phenomenological potential and the electromagnetic interaction is treated only to first order as a perturbation. The half-off-shell T-matrix elements which are required for the bremsstrahlung calcula-

tion can be calculated from the potential. Since different potentials will yield different off-shell effects, various phenomenological potentials can be distinguished by means of the bremsstrahlung calculations. When these calculations are compared with bremsstrahlung data, one hopes that the best potential can be selected. This was the original motivation for studying nucleon-nucleon bremsstrahlung. It turns out that more than ten thousand proton-proton bremsstrahlung data were collected but these data did not permit determination of the best potential. Reasons are the following: (i) The off-shell effects are small. (ii) The data are not accurate enough. (iii) The present potential model proton-proton bremsstrahlung (ppγ) calculations do not simutaneously include all posible corrections (such as the rescattering term, relativistic correction, Coulomb correction, exchange current contribution, etc.)

Although some remarkable progress in the study of nuclear bremsstrahlung processes has been made during the past two decades, some difficulties remain and prevent us from obtaining useful information about the off-shell-effects, electromagnetic properties of resonant states, and nuclear time delay. It is obvious that the problem requires further experimental and theoretical study. In this work, we investigate certain nuclear bremsstrahlung processes in the hope that some of these difficulties may be resolved. Specifically, we study, in the model independent approach,

the proton-carbon bremsstrahlung process ($p^{12}C\gamma$), the pion-proton bremsstrahlung process ($\pi^{\pm}p\gamma$), and the nucleon-nucleon bremsstrahlung process ($NN\gamma$).

In Chapt. III we consider the $p^{12}C\gamma$ process (23). The bremsstrahlung cross section for the scattering of protons by ^{12}C near the 1.7-MeV resonance has been measured by the Bologna group (21) and the Brooklyn group (23). Apart from the spectrum with a simple 1/k dependence, spectra with structure due to the contribution from a resonant state have also been observed. These spectra are important because they can be used not only to test the Feshbach-Yennie approximation but also to extract the nuclear time delay. The Bologna data were analyzed by the Bologna group and Jan et al. (22). Both groups have used the principal term of the Feshbach-Yennie approximation to predict the bremsstrahlung cross sections, and they have found poor agreement between the predicted spectrum and the measured spectrum at the bombarding energy of 1.795-MeV. In order to obtain quantitative agreement between theory and experiment, the Bologna group suggested a new set of resonance parameters for elasic $p-^{12}C$ scattering. These new parameters were studied by Perng et al. (22) who found that they lead to poor agreement with the elastic scattering cross sections near the resonance for some scattering angles. We have studied the problem by improving the calculation of the Bologna group and Jan et al. In this study, the Feshbach-Yennie approximation

with some modification is used and two approximations have been used: one with the principal term only and the other with both the principal and correction terms. To avoid the inconsistency with the elastic data as discussed above, we have used the resonance parameters of Armstrong et al. (27). We have found that at an energy very far from any resonance these two approximations give very similar results and that the structure due to the resonance near 1.7-MeV can be described successfully by the Feshbach-Yennie approximation only if the correction terms are included, since these correction terms are important in the region of resonance.

Eisberg et al. (4) and Feshbach et al. (5) have proposed a measurement of time delay in nuclear reactions resulting from the bremsstrahlung process. Recently, Maroni et al. (21) reported the time delay in the scattering of $p-^{12}C$ through the $p\,^{12}C\,\gamma$ process. In these publications, only the leading term in the bremsstrahlung amplitude is considered. Since the correction terms are not negligible in the region of resonance, we suggest a hybrid method to take account of the correction terms in the extraction of the time delay from data. A description of these calculations is given in section III.C.

In Chapt. IV we study the $\pi^{\pm} p\gamma$ process. One of the main reasons for studying the $\pi^{\pm}p\gamma$ process near the $\Delta(1236)$ is to investigate the electromagnetic properties of

the Δ-resonance. These processes have been systematically studied by an experimental group at UCLA (17-19). This group used 19 photon counters at many different angles to measure the bremsstrahlung spectra at three bombarding energies for each of the π^+ and π^- beams in the hope that the resonance structure could be observed in the resonance region. As a result, 108 spectra were obtained. Most of these spectra exhibited a simple 1/k dependence without structure except for some cases which might have indications of showing structure due to resonance. On the theoretical side, some calculations (19) predicted sizable resonance or off-shell effects which have not been observed experimentaly and only the calculation of Nefkens et al. (EED) (15) agrees well with the experimental data in most cases. Recently, the calculation of Liou and Nutt(16) gave very good agreement between theory and experiment for most cases. However, only the coplanar geometry was considered. We have applied their method to calculate for a noncoplanar geometry (25) and have found that most of the $\pi^{\pm}p\gamma$ events can be successfully described by the soft-photon approximation of LN. These analyses suggest that the contribution from the terms of order k and higher is small and imply that the off-shell effects are negligible in most kinematic regions of the UCLA data.

Another approach to the study of the $\pi^{\pm}p\gamma$ process is to calculate the $\pi^{\pm}p\gamma$ cross section using the Feshbach-

Yennie approximation. Since the Feshbach-Yennie approximation works for the bremsstrahlung process of $p^{12}C$ scattering, it is interesting to see if this approximation will give a good fit to the UCLA data. Thus our calculation may serve as a check on the validity of the Feshbach-Yennie approximation. Details of this work are presented in chapter IV.

Finally, in Chapt. V, we study the NNγ process in the model independent approach. During the past two decades, a great number of NNγ experiments have been performed at various bombarding energies (3.5-MeV $\leq$ E $\leq$ 730-MeV), and more than ten thousand bremsstrahlung data have been collected (2). Since the main motivation for study of the NNγ process is to discriminate among various phenomenological potentials, most theoretical calculations are potential-model calculations (1-3). In the model-independent approach, many authors (2,3,9,12) have applied Low's theorem to calculate the NNγ cross sections and Felsner (33) has used the Feshbach-Yennie approximation to calculate the low energy proton-proton bremsstrahlung. The agreement between theory and experiment is generally good except for some forward angle scattering cases (26).

As we have already mentioned, the soft-photon approximation derived by Liou et al. has been applied to predict both the coplanar as well as noncoplanar $\pi^{\pm}p\gamma$ cross sec-

tions for various bombarding energies and the results are in very good agreement with the UCLA data for most cases. This success of the soft-photon approximation in describing the $\pi^{\pm}p\gamma$ process encourages us to make a further test of the appximation by applying it to predict the $NN\gamma$ cross section. It is also important to see whether the approximation works equally well for other nuclear bremsstrahlung processes without a resonant state.

In this study, we are particularly interested in the $pp\gamma$ process, because most of the experimental bremsstrahlung data collected are of $pp\gamma$ and they can provide quite a sensitive test of the approximation. We expect the soft-photon approximation to work well since there is no resonant state for the p-p system in the energy region where $pp\gamma$ cross sections have been measured. Therefore, the difference between the data (if accurate enough) and our soft-photon prediction can be interpreted as being mainly due to off-shell effects. We also hope that the existing large discrepancy between theory and experiment at forward angles can be resolved. Since the contribution of the leading term in the bremsstrahlung amplitude in the $pp\gamma$ process is small (32) and the O(k) terms in the expansion of the amplitude include not only the off-shell terms and the internal radiation but also the on-shell terms, we try to estimate the contribution of the terms of order k in our approach by suppressing the off-shell derivative terms.

Besides the soft-photon approximation, we are also interested in applying the Feshbach-Yennie approximation to the ppγ case. The details of this study is given in chapter V. For convenience, we present the kinematics which is general to all bremsstrahlung processes, together with Low's prescription in next chapter.

CHAPTER II LOW'S PRESCRIPTION AND KINEMATICS

We consider the bremsstrahlung process of the scattering of particles A and B:

$$A(q_i^\mu) + B(p_i^\mu) \rightarrow A(q_f^\mu) + B(p_f^\mu) + \gamma(k^\mu), \qquad \text{(II.1)}$$

where q_i^μ (q_f^μ) and p_i^μ (p_f^μ) are the initial (final) four-momenta of particles A and B, respectively, and k^μ is the four-momentum of the emitted photon. In the laboratory frame, these five four-momenta are defined in terms of spherical coordinates as

$$\begin{aligned}
q_i^\mu &= (E_i, 0, 0, q_i), \\
p_i^\mu &= (M, 0, 0, 0), \\
q_f^\mu &= (E_q, q_f \sin\theta_q \cos\phi_q, \quad q_f \sin\theta_q \sin\phi_q, \; q_f \cos\theta_q), \\
p_f^\mu &= (E_p, p_f \sin\theta_p \cos\phi_p, \quad p_f \sin\theta_p \sin\phi_p, \; p_f \cos\theta_p), \\
k^\mu &= (k, k \sin\theta_\gamma \cos\phi_\gamma, \quad k \sin\theta_\gamma \sin\phi_\gamma, \; k \cos\theta_\gamma),
\end{aligned} \qquad \text{(II.2)}$$

where

$$E_i = (m^2 + \vec{q}_i^{\,2})^{1/2}, \quad E_q = (m^2 + \vec{q}_f^{\,2})^{1/2}, \quad E_p = (M^2 + \vec{p}_f^{\,2})^{1/2},$$

and m (M) is the mass of particle A (B). They satisfy the energy-momentum conservation:

$$q_i^\mu + p_i^\mu = q_f^\mu + p_f^\mu + k^\mu. \qquad \text{(II.3)}$$

For a given E_i, there are nine kinematical variables for

the process and only five of them can be chosen as independent variables. The choice of these independent variables depends on the experimental arrangement. One may choose θ_q, ϕ_q, θ_p, ϕ_p, and θ_γ which lead to an H-type differential cross section (see Axp. B for the definitions of H-type and R-type cross sections), or θ_q, ϕ_q, θ_γ, ϕ_γ, and k which lead to an R-type cross section. Strictly speaking, the soft-photon theorem can not be derived for the H-type cross section without violating energy-momentum conservation. Therefore, the R-type cross section is to be prefered for the study of bremsstrahlung processes in the soft-photon approach.

In this study, we define θ_q, ϕ_q, θ_γ, ϕ_γ, and k as five independent variables. The dependent variables q_f and p_f, which were not expanded in the usual soft-photon approximations, are expanded about the on-shell point, k = 0. With the notation $A\cdot B = A^\circ B^\circ - \vec{A}\cdot\vec{B}$, we define, following Ref. 24,

$$N_R^\mu = \left[m^2 p_i^\mu - (p_i\cdot\bar{q}_f)\,\bar{q}_f^\mu\right] \Big/ \left[(p_i\cdot\bar{q}_f)(\bar{p}_f\cdot\bar{q}_f) - m^2(p_i\cdot\bar{p}_f)\right], \qquad \text{(II.4)}$$

$$R^\mu = (\bar{p}_f\cdot k)\, N_R^\mu , \qquad \text{(II.5)}$$

and obtain the expansions

$$q_f^\mu \approx \bar{q}_f^\mu + R^\mu , \qquad \text{(II.6)}$$

$$p_f^\mu \approx \bar{p}_f^\mu - (R+k)^\mu .$$

Here $\bar{q}_f^\mu = \lim_{k\to 0} q_f^\mu$, and $\bar{p}_f^\mu = \lim_{k\to 0} p_f^\mu$ are four-momenta for

the corresponding elastic process and they obey the energy-momentum conservation

$$q_i^\mu + p_i^\mu = \bar{q}_f^\mu + \bar{p}_f^\mu . \qquad \text{(II.7)}$$

With one particle off-mass-shell, as shown in Fig. II.1, the T-matrices for the scattering process require three Lorentz invariants which can be choosen as: center-of-mass energy squared, s_j, momentum transfer squared, t_j, and off-mass-shell quantity, Δ_j, for the diagram j, j = a, b, c, or d. Explicitly, we have

$$\begin{aligned}
s_a &= s_c = (q_i + p_i)^2 = s , \\
s_b &= s_d = (q_f + p_f)^2 \approx s - 2(\bar{q}_f + \bar{p}_f)\cdot k , \\
t_a &= t_b = (p_f - p_i)^2 \approx t - 2(\bar{p}_f - p_i)\cdot(R+k) + R^2 + 2k\cdot R , \\
t_c &= t_d = (q_f - q_i)^2 \approx t + 2(\bar{q}_f - q_i)\cdot R + R^2 , \\
\Delta_a &= (q_f + k)^2 - m^2 \approx 2\bar{q}_f\cdot k + 2R\cdot k , \qquad \text{(II.8)} \\
\Delta_b &= (q_i - k)^2 - m^2 = -2q_i\cdot k , \\
\Delta_c &= (p_f + k)^2 - M^2 \approx 2\bar{p}_f\cdot k - 2R\cdot k , \\
\Delta_d &= (p_i - k)^2 - M^2 = -2p_i\cdot k ,
\end{aligned}$$

where each invariant has been written explicitly in terms of the center-of-mass energy squared s and the momentum transfer squared t for the corresponding elastic process.

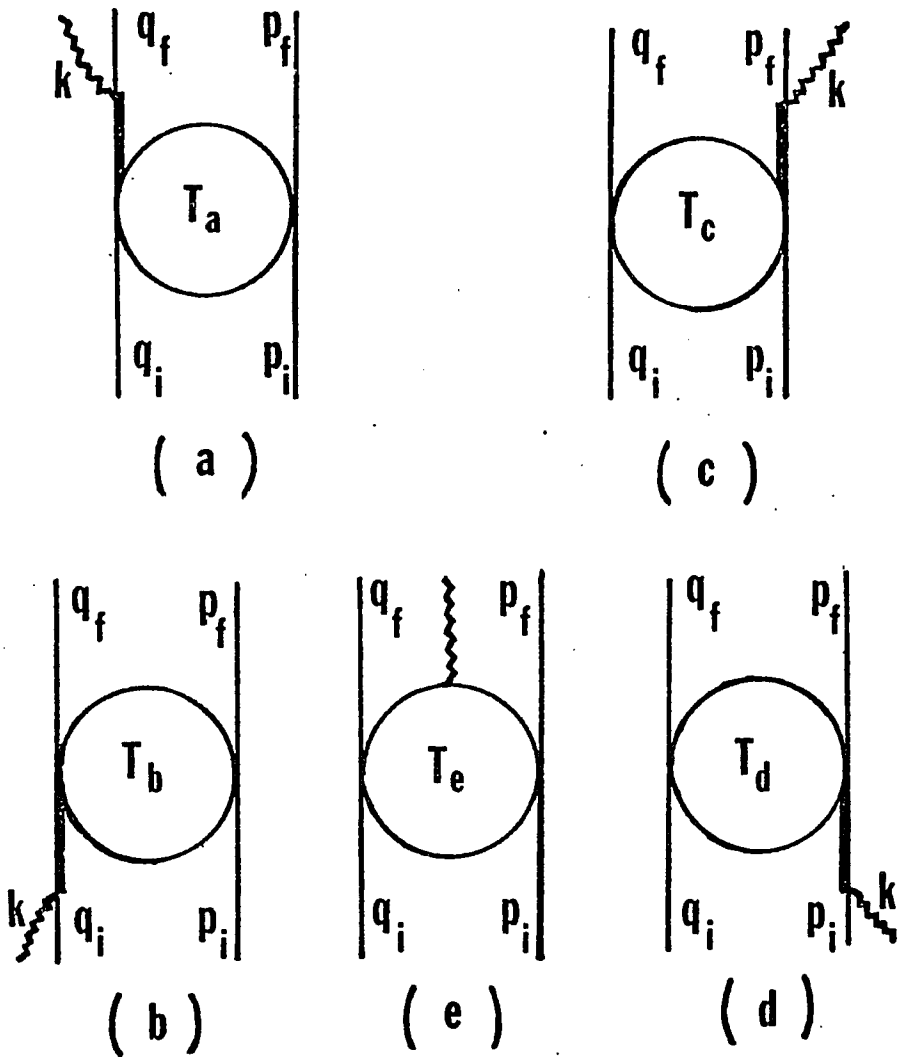

Fig. II.1- Diagrams for the bremsstrahlung process: (a)-(d) the external scattering diagrams; (e) the internal scattering diagram.

The total bremsstrahlung amplitude, $\mathcal{M}_\mu$, may be written as the sum of external amplitude, $\mathcal{M}_\mu^E$, and internal amplitude, $\mathcal{M}_\mu^I$. The radiation which comes from the four off-shell legs of Fig. II.1 contributes to the external amplitude, while the rest comprises the internal amplitude. Low (7) has shown that current conservation enables one to calculate the first two terms of the amplitude up to the order of k^0. Adler and Dothan (9) have written down the following recipe for the calculation of bremsstrahlung amplitude: one first writes down $\mathcal{M}_\mu^E$, then drops all terms in $\mathcal{M}_\mu^E$ which are explicitly independent of k, and thus obtains $\mathcal{M}_\mu^1$. Finally one adds to $\mathcal{M}_\mu^1$ a term $\mathcal{M}_\mu^2$ independent of k such that the sum of $\mathcal{M}_\mu^1$ and $\mathcal{M}_\mu^2$ is gauge invariant up to order k^0. Following this prescription, we can write down the bremsstrahlung amplitude without the derivatives of the T-matrices with respect to the off-shell quantites. In other words, cancellation of the off-shell amplitudes can be achieved through the use of the gauge invariance condition and the expansion of the amplitude through the order independent of k. For those terms of order k, however, the off-shell terms do not cancel out after enforcing gauge invariance upon the amplitude in nucleon-nucleon bremsstrahlung. We will estimate the effect of this order in the expansion of amplitude by suppresing the off-shell derivative terms and keeping the rest of the terms which are gauge invariant.

CHAPTER III. APPLICATION OF THE FESHBACH-YENNIE APPROXIMATION TO PROTON-CARBON BREMSSTRAHLUNG

It is well known that the bremsstrahlung amplitude in Low's theorem is evaluated at a fixed on-shell energy. This is not justified for a bremsstrahlung process with a rapid variation of the amplitude with respect to the energy in the corresponding elastic process (5). Feshbach and Yennie modified Low's theorem by evaluating the amplitudes at the incident and final energies. It has always been assumed that the modified theory, known as the Feshbach-Yennie approximation, can be used to describe the radiative resonant scattering processes. This assumption has never been thoroughly verified experimentaly and numerically, although some publications on the subject exist (20-22). Recently, we have made a more exact calculation (23) and compared with new experimental data obtained by the Brooklyn group (23). We describe the details of the calculation in section A, the results in section B, and the hybrid method of extraction time delay from data in section C.

A. THE FESHBACH-YENNIE APPROXIMATION FOR THE FERMION-BOSON CASE

The external amplitude, $\mathcal{M}_{\mu}^{E}$, can be written as (see Fig. II.1)

$$\mathcal{M}_{\mu}^{E} = \bar{u}(q_f, \nu_f)\Big[\Gamma_{\mu}\frac{\mathcal{Z}}{\not q_f + \not k - m}T_a + T_b\frac{\mathcal{Z}}{\not q_i - \not k - m}\Gamma_{\mu} + \frac{Z}{p_f\cdot k}p_{f\mu}T_c - \frac{Z}{p_i\cdot k}p_{i\mu}T_d\Big]u(q_i, \nu_i). \qquad \text{(III.1)}$$

Here T_a, T_b, T_c, and T_d are the half-off-shell T-matrices for fermion-boson collision, u's are Dirac spinors of fermions with the normalization $\bar{u}u = 1$, ν's are the spin quantum numbers, and $\mathcal{Z}$ (Z) is the charge of the fermion(boson). Note that we treat the nucleus as a particle, a boson, and adopt the convention: $\hbar = c = 1$. The off-shell-effect of the vertex function has been discussed by Nyman (28) and Fischer et al. (29). Since the contribution from the anomalous magnetic moment is usually small in the low energy $p^{12}C\gamma$ process, we neglect the off-mass-shell effect of the vertex function and write

$$\Gamma_{\mu} = \gamma_{\mu} - \frac{i}{2m}\lambda\sigma_{\mu\nu}k^{\nu}, \qquad \text{(III.2)}$$

where λ is the anomalous magnetic moment of fermion, and $\sigma_{\mu\nu} = \frac{i}{2}\left[\gamma_{\mu}, \gamma_{\nu}\right]$.

For $p^{12}C\gamma$ at 1.7-MeV, the contribution from those terms involving λ is of order k and small. These terms are therefore ignored in our calculation. Moreover, since $k \leq 250$ keV/c, $k/q_i \ll 1$, we may also make the following approximation:

$$\frac{1}{\not q_i - \not k - m}\gamma_\mu u(q_i,\nu_i) = \frac{q_{i\mu} + \gamma_\mu \not k/2}{-q_i\cdot k} u(q_i,\nu_i),$$

$$\approx -\frac{q_{i\mu}}{q_i\cdot k} u(q_i,\nu_i). \qquad \text{(III.3)}$$

With the help of these approximations, we obtain the external amplitude

$$\mathcal{M}^E_\mu = \bar u(q_f,\nu_f) M^E_\mu u(q_i,\nu_i), \qquad \text{(III.4)}$$

where $$M^E_\mu = \frac{\not q_{f\mu}}{q_f\cdot k} T_a - T_b \frac{\not q_{i\mu}}{q_i\cdot k} + \frac{\not p_{f\mu}}{p_f\cdot k} T_c - T_d \frac{\not p_{i\mu}}{p_i\cdot k}.$$

The half-off-shell T-matrices, T_j, j = a, b, c, d, require three Lorentz invariants which can be chosen to be center-of-mass energy squared, s_j, momentum transfered squared, t_j and off-shell-quantity, Δ_j, for the diagram j, j = a, b, c, d, in Fig. II.1. The definitions of these invariants are given in chapter II. To have the most important feature of the Feshbach-Yennie theory, we define the initial (final) center-of-mass energy squared s_i (s_f) as

$$s_i = s_a = s_c = (q_i+p_i)^2 = (m+M)^2 + 2ME_i,$$

$$s_f = s_b = s_d = (q_f+p_f)^2$$

$$= (m+M)^2 + 2M(E_i-k) + 2\vec q_i\cdot\vec k - 2k(E_i+m)$$

$$\approx (m+M)^2 + 2M(E_i-k). \qquad \text{(III.5)}$$

Thus we may evaluate $T_j(s_j, t_j, \Delta_j)$ at initial (j = a,c) or final (j = b, d) energy and expand it about the elastic point ($\Delta_j = 0$). With all theses approximations, the external amplitude becomes

$$M^E_\mu = \left(\frac{z q_{f\mu}}{q_f\cdot k} + \frac{Z p_{f\mu}}{p_f\cdot k}\right) T(s_i,t) - \left(\frac{z q_{i\mu}}{q_i\cdot k} + \frac{Z p_{i\mu}}{p_i\cdot k}\right) T(s_f,t)$$

$$-2(\bar p_f - p_i)\cdot(R+k)\left(\frac{z q_{f\mu}}{q_f\cdot k}\frac{\partial T(s_i,t)}{\partial t} - \frac{z q_{i\mu}}{q_i\cdot k}\frac{\partial T(s_f,t)}{\partial t}\right)$$

$$+2(\bar q_f - q_i)\cdot R\left(\frac{Z p_{f\mu}}{p_f\cdot k}\frac{\partial T(s_i,t)}{\partial t} - \frac{Z p_{i\mu}}{p_i\cdot k}\frac{\partial T(s_f,t)}{\partial t}\right)$$

$$+2z\bar q_{f\mu}\frac{\partial T(s_i,t,\Delta_a)}{\partial \Delta_a} + 2z q_{i\mu}\frac{\partial T(s_f,t,\Delta_b)}{\partial \Delta_b}$$

$$+2Z\bar p_{f\mu}\frac{\partial T(s_i,t,\Delta_c)}{\partial \Delta_c} + 2Z p_{i\mu}\frac{\partial T(s_f,t,\Delta_d)}{\partial \Delta_d} \quad . \qquad \text{(III.6)}$$

The internal amplitude can be obtained from the gauge invariance condition, $k^\mu \mathcal{M}^I_\mu = -k^\mu \mathcal{M}^E_\mu$, up to order k^0. Then the combination of $\mathcal{M}^E_\mu$ and $\mathcal{M}^I_\mu$ gives a total bremsstrahlung amplitude $\mathcal{M}_\mu$, to order k^0,

$$\mathcal{M}_\mu = \bar u(q_f, V_f)\left\{\left(\frac{z q_{f\mu}}{q_f\cdot k} + \frac{Z p_{f\mu}}{p_f\cdot k} - \frac{(z+Z)(q_f+p_f)_\mu}{(q_f+p_f)\cdot k}\right) T(s_i,t)\right.$$

$$\left. -\left(\frac{z q_{i\mu}}{q_i\cdot k} + \frac{Z p_{i\mu}}{p_i\cdot k} - \frac{(z+Z)(q_i+p_i)_\mu}{(q_i+p_i)\cdot k}\right) T(s_f,t) + \right.$$

$$+\frac{\partial T(s_i,t)}{\partial t}\left[\frac{2(\bar{q}_f-q_i)\cdot R}{p_f\cdot k}\,Z p_{f\mu}-\frac{2(\bar{p}_f-p_i)\cdot(R+k)}{q_f\cdot k}\,Z q_{f\mu}\right.$$

$$\left.+2\left((\bar{p}_f-p_i)Z-(\bar{q}_f-q_i)Z\right)\cdot N_R\,\bar{p}_{f\mu}+2Z(\bar{p}_f-p_i)_\mu\right]$$

$$-\frac{\partial T(s_f,t)}{\partial t}\left[\frac{2(\bar{q}_f-q_i)\cdot R}{p_i\cdot k}\,Z p_{i\mu}-\frac{2(\bar{p}_f-p_i)\cdot(R+k)}{q_i\cdot k}\,Z q_{i\mu}\right.$$

$$\left.\left.+2\left((\bar{p}_f-p_i)Z-(\bar{q}_f-q_i)Z\right)\cdot N_R\,\bar{p}_{f\mu}+2Z(\bar{p}_f-p_i)_\mu\right]\right\}u(q_i,\nu_i). \quad \text{(III.7)}$$

In this amplitude, the first two terms, which are of order k^{-1}, contribute to the principal term of the bremsstrahlung cross section. The derivative terms obtained here are slightly different from that originally derived by Feshbach and Yennie. Those terms with $T(s_i,t)$ are due to the radiation from the initial particles and those with $T(s_f,t)$ from final particles. If a further expansion of T about an on-shell point were made, we would have obtained a soft-photon approximation. EED-type calculations for $p^{12}C\gamma$ process can be obtained by neglecting the derivative terms and replacing s_f and s_i by their average or replacing s_f by s_i. Different choices of the point for the evaluation of the scattering amplitude give quite different results if the elastic amplitude varies rapidly with respect to energy. Furthermore, the sensitivity of the variation of the elastic amplitude with respect to scattering angle is a measure of the importance of the correction terms. These features can be seen from our results for the $p^{12}C\gamma$ calculations which are based upon Eq. III.7. Some results of our $p^{12}C\gamma$ calcu-

lations are shown in the following section.

B. CALCULATION OF THE PROTON-CARBON BREMSSTRAHLUNG CROSS SECTION

We have applied Eq. III.7 to calculate the cross section for the scattering of protons by ^{12}C near the 1.7-MeV resonance. The bremsstrahlung cross section for the scattering of an unpolarized beam from an unpolarized target can be written as

$$\sigma(\Omega_q, \Omega_\gamma, k) = \frac{1}{2} \sum_{pol,spin} |\mathcal{M}|^2 \mathcal{N} F , \qquad \text{(III.8)}$$

where the factor $\mathcal{N}$ is given by

$$\mathcal{N} = \frac{1}{2} m^2 \left[(q_i \cdot p_i)^2 - (mM)^2 \right]^{-\frac{1}{2}} . \qquad \text{(III.9)}$$

In practice, we have used the elastic p-^{12}C amplitude, $f_{\nu'\nu}$, to calculate $\sigma(\Omega_q, \Omega_\gamma, k)$ and the elastic scattering cross section,

$$\sigma^{el}(\Omega) = \frac{1}{2} \sum_{\nu'\nu} |f_{\nu'\nu}|^2 . \qquad \text{(III.10)}$$

The amplitude $f_{\nu'\nu}$, which is a function of elastic phase shifts and resonance parameters, can be found in Ref. 27.

Recently, Perng et al. used the principal term to analyze the Bologna data. They found it difficult to generate any set of resonance parameters which would fit both the p ^{12}C elastic data of Ref. 27 and the p ^{12}C γ data of the

Bologna group. This difficulty led them to conclude that either the bremsstrahlung data at 1.795-MeV was inconsistent with elastic data or the theoretical approximation was not accurate enough. To resolve this difficulty, we have improved the calculations of the Bologna group and Jan et al. by including the correction terms and have compared our result with the new data obtained by the Brooklyn group. We have also calculated the elastic scattering cross sections to see whether these calculations are in good agreement with the elastic data. A comparsion of our calculated elastic cross sections with the elastic data of Ref. 27 is shown in Fig.III.1. The solid curve represents the result obtained by using the resonance parameters of Armstrong et al. and the dotted curve using Maroni set (Table III.1).

TABLE III.1
The resonant parameters for the scattering of protons from carbon

Level	J^{π}	$\frac{1}{2}^+$	$\frac{3}{2}^-$	$\frac{5}{2}^+$
Armstrong et al.	E_λ (MeV)	0.951	3.510	3.609
	(10^{-13} MeV/cm)	7.580	0.515	3.550
Maroni et al.	E_λ (MeV)	0.951	3.540	3.606
	(10^{-13} MeV/cm)	7.580	0.550	3.179

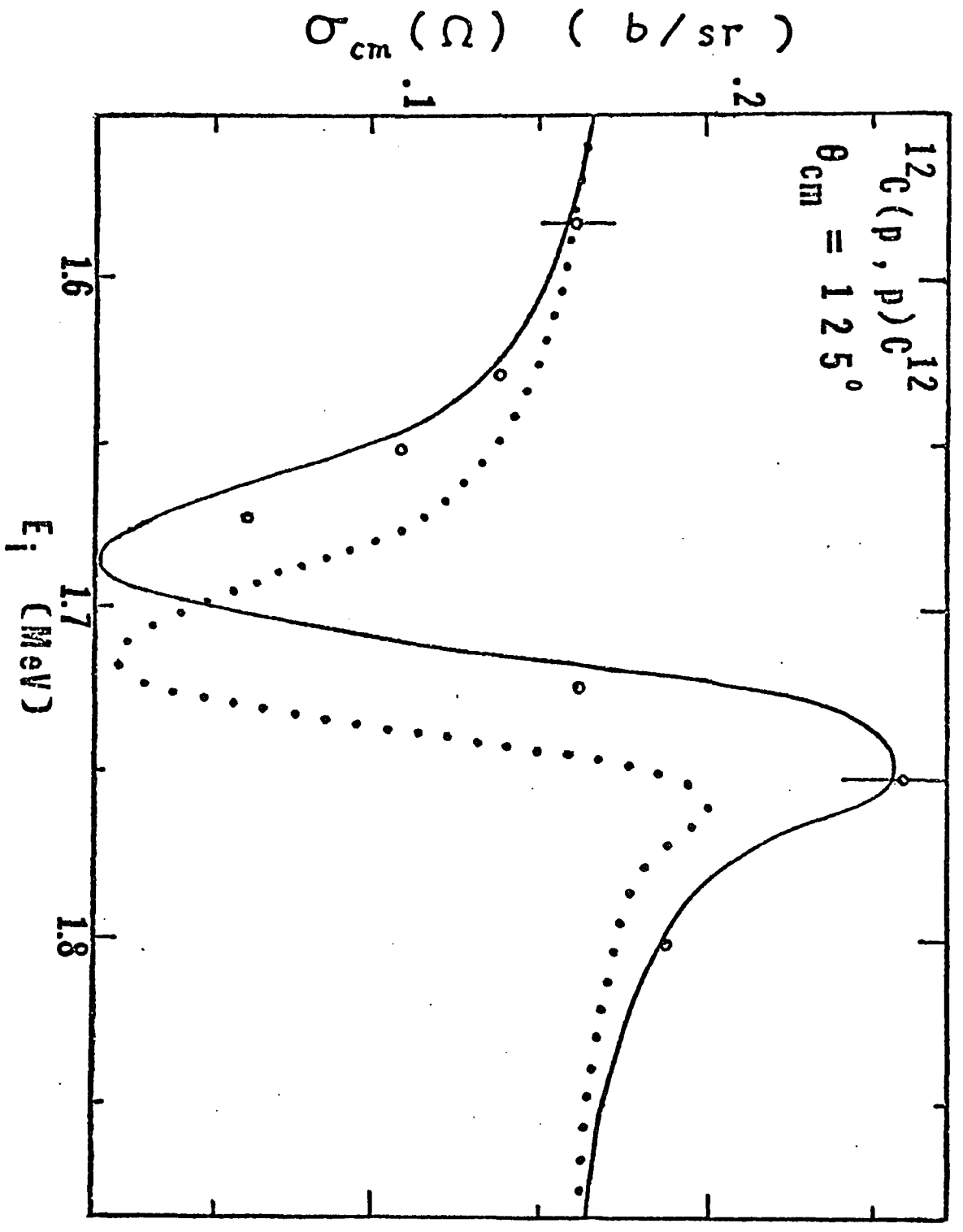

Fig. III.1 The elastic $p\,^{12}C$ cross sections as a function of the incident proton energy. The solid (dotted) curve is the result of the calculation using the resonance parameters of Armstrong et al. (Maroni et al.). The small circle represents the experimental data of Armstrong et al. (27).

The study of this figure indicates that Armstrong's parameters give the best fit to the elastic data. Therefore, we have used this set of parameters for our $p^{12}C\,\gamma$ calculations. In Figs. III.2-III.4, the bremsstrahlung spectra from the Bologna group are compared with three calculations in the laboratory system. The solid curves represent the results of our complete Feshbach-Yennie calculation, i.e., both the principal term and the correction terms are included. The dashed curves represent the calculations which include only the principal term, i.e., the results obtained in Ref. 22. The dotted curves represent the result of the soft-photon approximation as calculated in Ref. 22, i.e., with only the leading term. Inclusion of the correction terms does provide better agreement between the theoretical bremsstrahlung spectra and the experimental data at 1.765-MeV, as shown in Fig. III.2. Here, the structure due to the resonance is expected to appear near 20-keV for photon energy, k. At 1.895 MeV (Fig.III.4), the bump in the bremsstrahlung spectrum is expected to appear near 160 keV for k. All three calculations give similar results which are in agreement with the experimental data. However, in Fig. III.3, we have a puzzling case at 1.795 MeV. Since this is the only case which gives very poor agreement between theory and experiment, we would support the conclusion reached by Perng et al. that this set of bremsstrahlung data is inconsistent with the elastic data of Ref. 27.

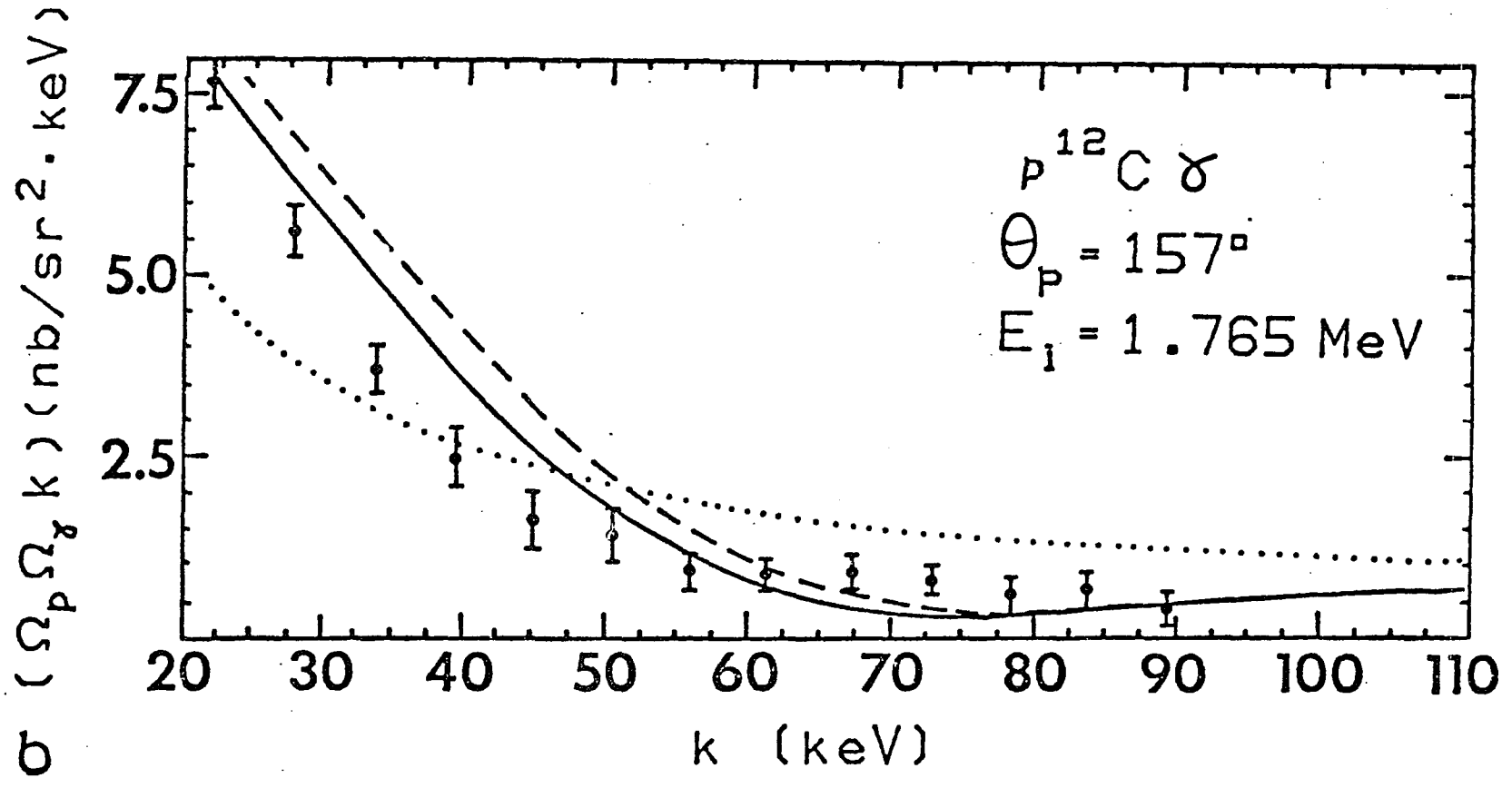

Fig. III.2 The pCγ cross sections in the laboratory system as a function of photon energy at an incident proton energy of 1765 keV. The dashed(solid) curve represents the result of our calculations using the principal term (principal and correction terms) of the Feshbach-Yennie approximation. The dotted curve represents the calculation using the leading term of the soft-photon approximation. The experimental data are from Ref. 21.

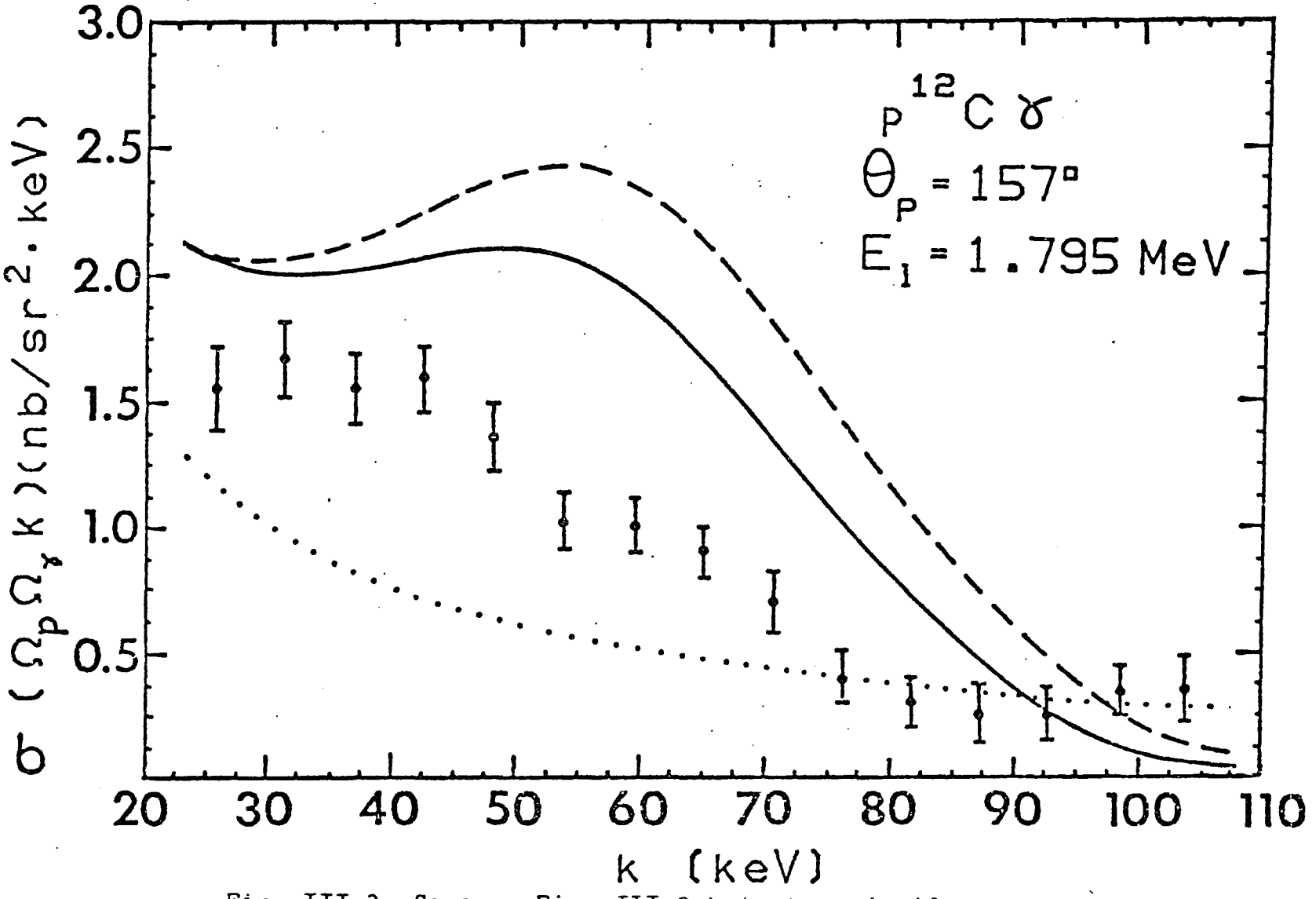

Fig. III.3 Same as Fig. III.2 but at an incident proton energy of 1795 keV.

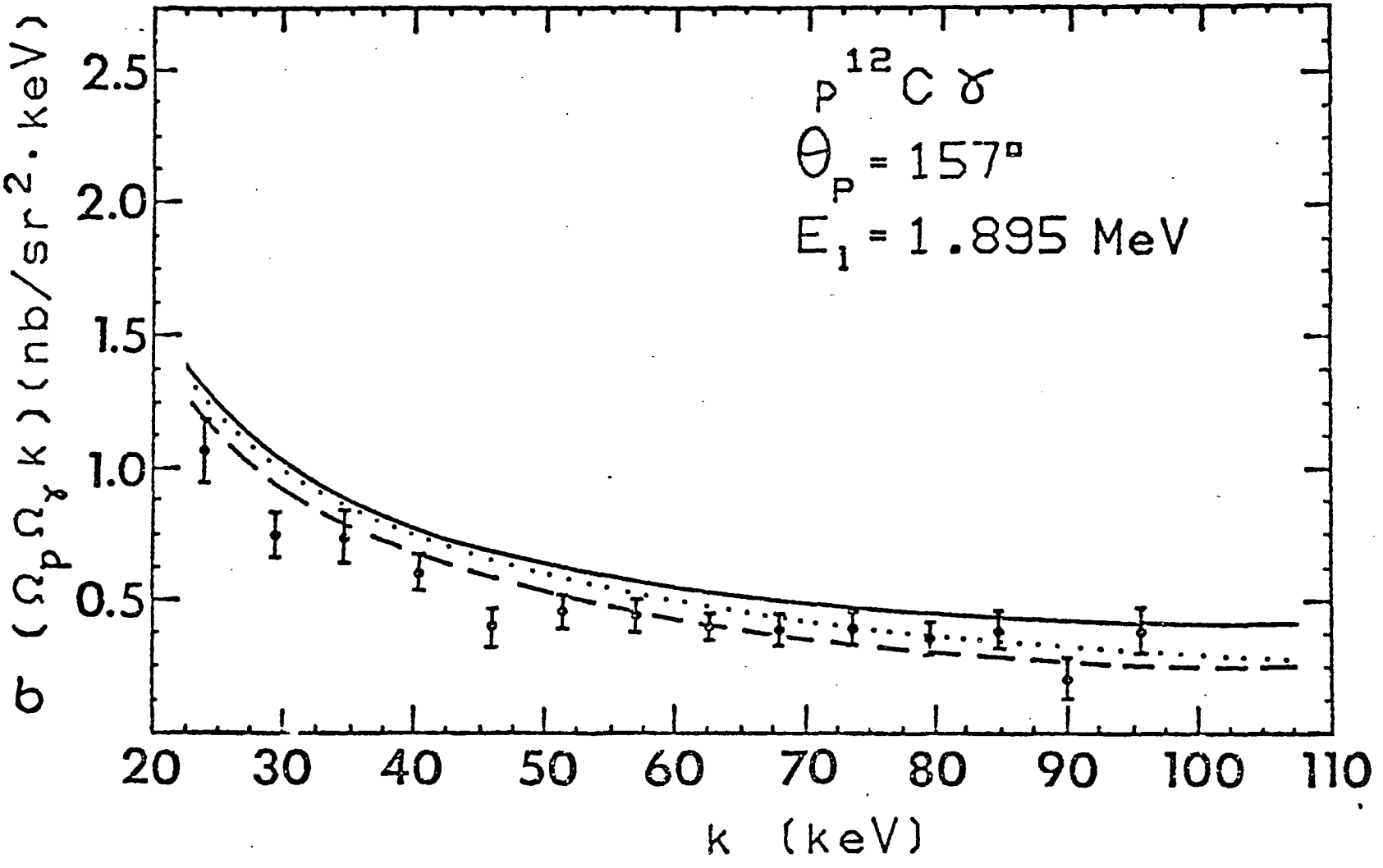

Fig. III.4 Same as Fig. III.2 but at an incident proton energy of 1895 keV.

The Brooklyn group have measured the relative bremsstrahlung cross section

$$\sigma_{rel} = \sigma(\Omega_q, \Omega_\gamma, k) / \sigma^{el}(\Omega). \qquad \text{(III.11)}$$

In Figs. III.5-III.7, we have compared the Brooklyn data with three different calculations. The solid and dashed curves represent, respectively, the calculations of the Feshbach-Yennie approximation with and without the correction terms, and the dotted curves represent the soft-photon approximation of Ref. 22. These results have been averaged over the finite size of the photon detector. At 1.594-MeV, there is no resonance structure in the range of k and all three calculations are in good agreement with data, as shown in Fig. III.5. In Figs.III.6 and III.7, we show experimental spectra at 1.81-MeV and 1.88-MeV. Structure due to the resonance is clearly observed in these cases. The agreement between the experiment and the soft-photon approximation is very poor. On the other hand, the results from the Feshbach-Yennie approximation do agree with data. Moreover, the contribution from the correction terms is not negligible in the region of resonance. It not only changes the magnitude of the cross section but also shifts the peak due to resonance effects.

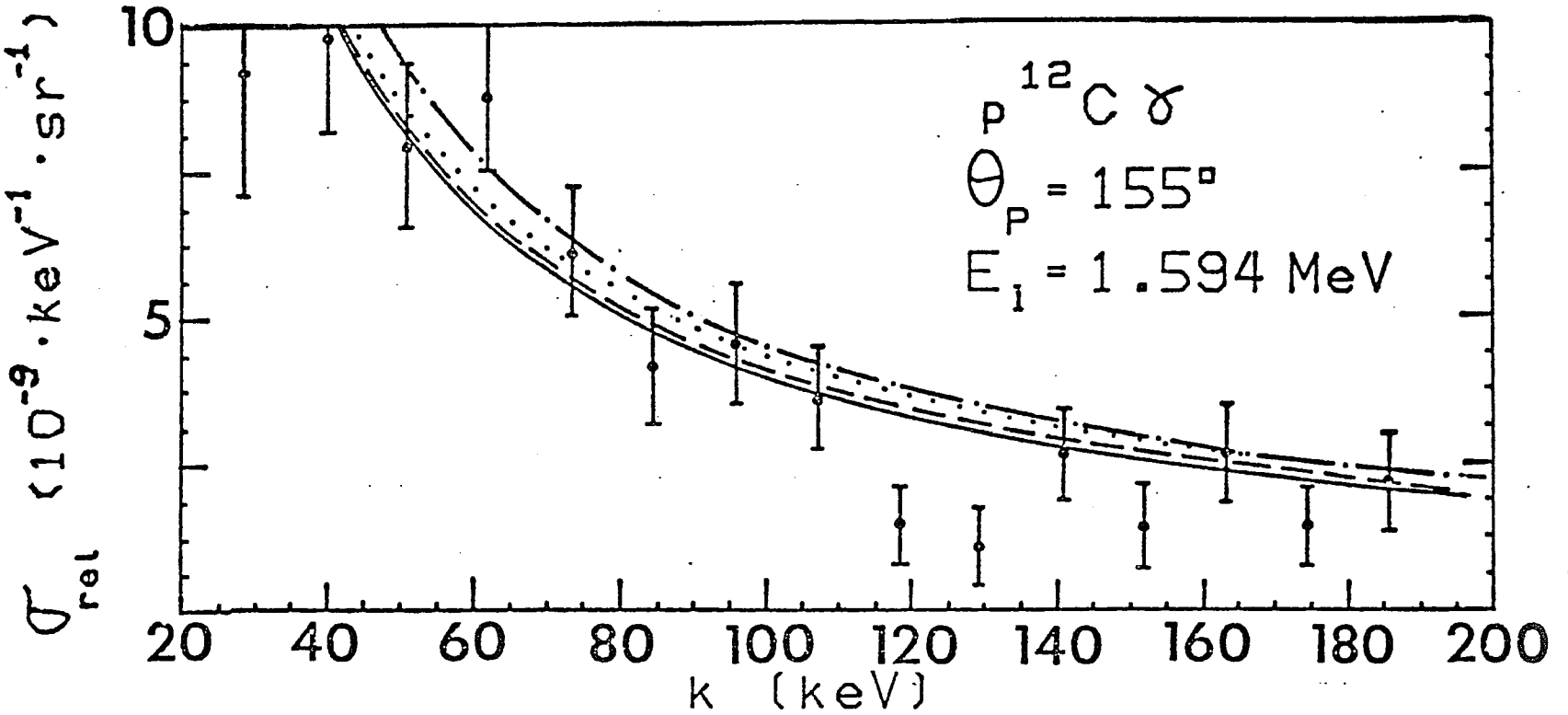

Fig. III.5 The pCγ bremsstrahlung cross section relative to the elastic scattering cross section as a function of photon energy at an incident proton energy of 1594 keV. The dashed (solid) curve represents our Feshbach-Yennie predictions calculated by using the principal term (principal and correction terms) , and averaged over the solid angle of photon detector. The dash-dotted curve represents our result calculated from the same approximation but without averaging over the finite size of photon detector. The dotted curve represents the result, averaged over the solid angle of photon detecotor, of the calculation using the leading term of soft-photon approximation. The experimental data are from Ref. 23.

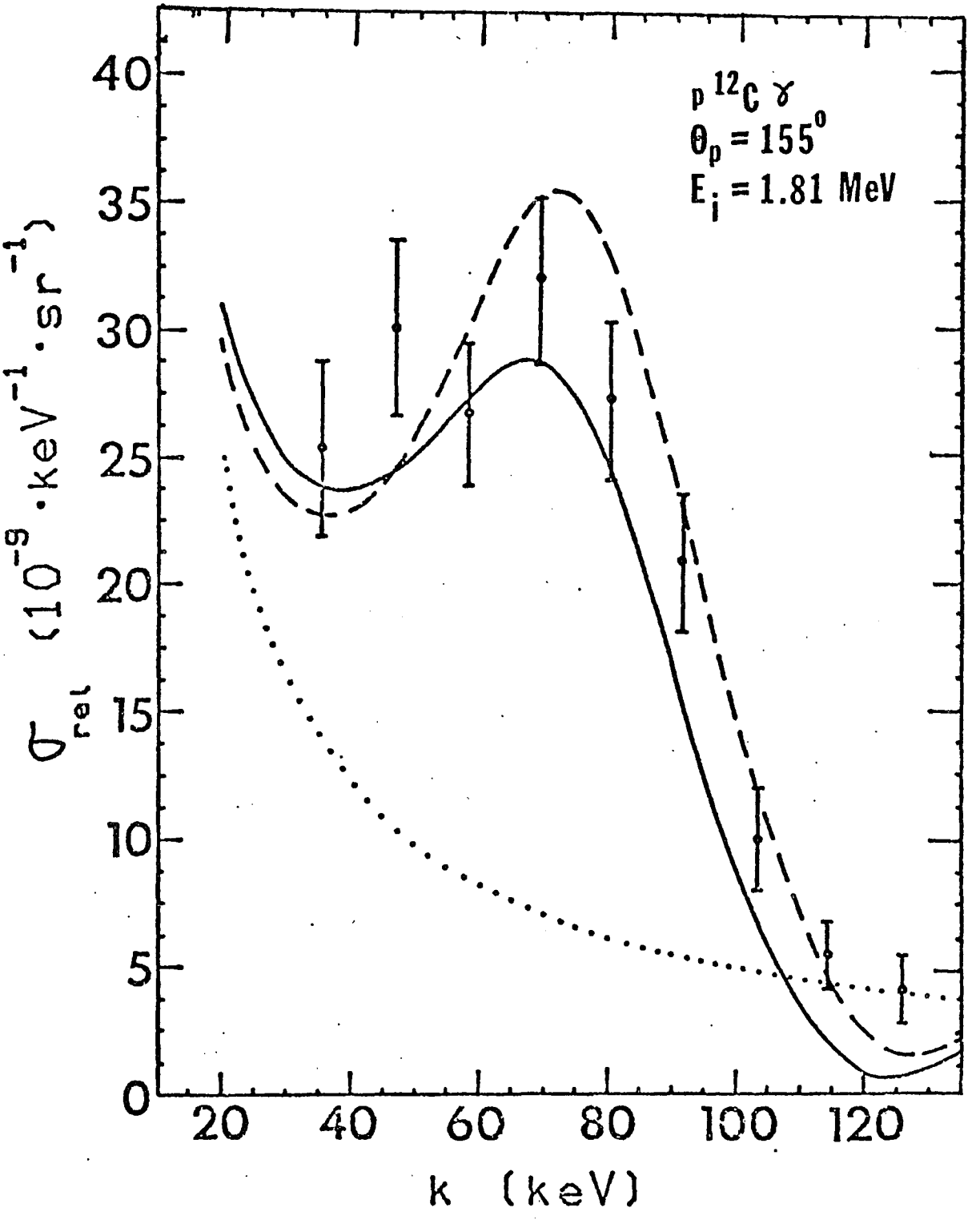

Fig. III.6 Same as Fig. III.5 but at an incident proton energy of 1810 keV. No dash-dotted curve is shown in this figure.

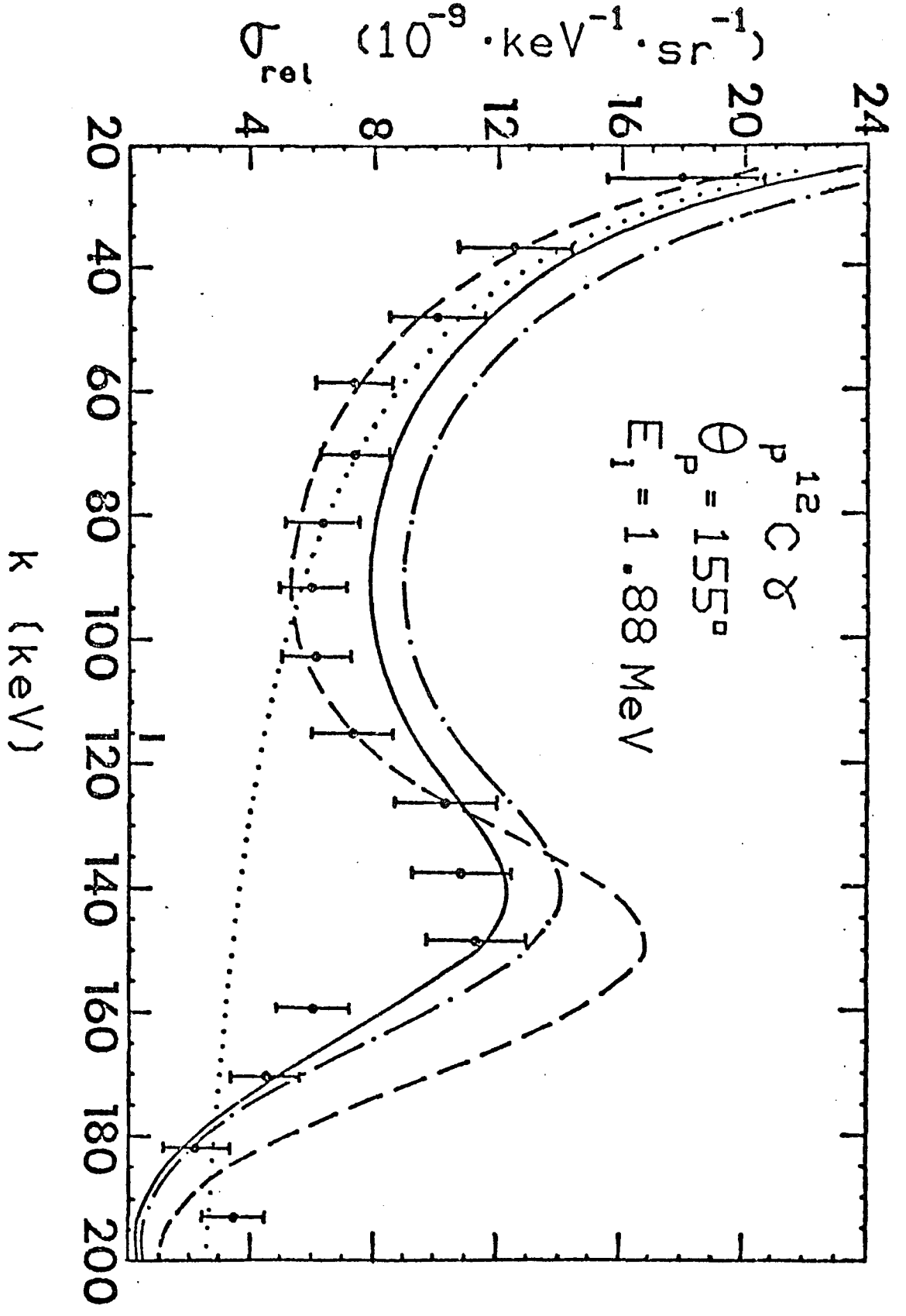

Fig. III.7 Same as Fig. III.5 but at an incident proton energy of 1880 keV.

C. EXTRACTION OF TIME DELAY IN THE p-^{12}C REACTION FROM DATA

The nucleon-nucleus bremsstrahlung process has been suggested (4,5) for the measurement of short time delay in nuclear reactions. The time delay is the elasped time between the arrival of the incident nucleon (t = 0) and the departure of the outgoing nucleon (t = τ), i,e, the lifetime of the compound nucleus formed in the collision which is too short to be measured by conventional methods. According to the Feshbach-Yennie approximation, the off-shell T-matrices may be evaluated at the incident energy, E_i, or at the final energy, E_f. This leads to the evaluation of one amplitude at the incident energy, $f_{\nu'\nu}(E_i)$, and a second amplitude at the final energy, $f_{\nu'\nu}(E_f)$. The phase difference, Φ, between these amplitudes is given, as in Ref. 3 and 4, by

$$\cos\omega\tau \approx \cos\Phi \equiv \frac{Re\left[\sum_{\nu'\nu} f^{*}_{\nu'\nu}(E_i)\ f_{\nu'\nu}(E_f)\right]}{\left[\sum_{\nu'\nu}\left|f_{\nu'\nu}(E_i)\right|^2\right]^{1/2}\left[\sum_{\nu'\nu}\left|f_{\nu'\nu}(E_f)\right|^2\right]^{1/2}} \quad , \qquad \text{(III.12)}$$

where $\hbar\omega = E_i - E_f$.

Maroni et al. reported the first measurement of time delay in low energy p-^{12}C scattering. They used their measured bremsstrahlung γ-ray counting rate, N_γ, and elastic counting rate, N, to determine the time delay through the

relation,

$$\cos\Phi = \frac{A k N_\gamma - B N(E_i) - C N(E_f)}{\left[N(E_i)\ \ N(E_f)\right]^{1/2}}\ , \qquad \text{(III.13)}$$

where A, B, and C are kinematical factors including the charges of proton and carbon.

Only the leading term is considered in deriving Eq. III.13. However, since the correction terms are not negligible in the region of the resonance, we should take into account the correction terms in the extraction of the time delay from data. Let us first derive an expression similar to Eq. III.13. Writing the leading term of the bremsstrahlung amplitude in Eq. III.7 as

$$\mathcal{M}_\mu = \bar{u} M_\mu u\ , \quad \epsilon^\mu M_\mu = e\epsilon\cdot\left[a_f T(E_i) - a_i T(E_f)\right]\ , \qquad \text{(III.14)}$$

we obtain the relation for the phase difference Φ ,

$$y \equiv \cos\Phi = f(\sigma_{rel}) + g(\sigma_i, \sigma_f) \qquad \text{(III.15)}$$

$$= \frac{1}{a_i\cdot a_f}\left[\frac{16\pi^3}{e^2 J k}\sigma_{rel} + a_f\cdot a_f + a_i\cdot a_i\frac{\sigma_i}{\sigma_f}\right]$$

where J is the Jacobian which relates the center-of-mass cross section to the laboratory one, and σ_i (σ_f) is the elastic cross section at the energy E_i (E_f). In principle, if the full bremsstrahlung amplitude of Eq. III.7 were used in the derivation of Eq. III.15, one would obtain a first order differential equation of the form

$$C\frac{dy}{dt} + y = f'(\sigma_{rel}) + g'(\sigma_i, \sigma_f) + \frac{d}{dt}h(\sigma_i, \sigma_f). \qquad \text{(III.16)}$$

In practice, however, an explicit expression of the Eq. III.16 is very difficult to obtain. We therefore propose a hybrid method for the determination of the time delay. In this method, the derivatives of $\cos\Phi$ with respect to t in the expression for the bremsstrahlung cross section, which is equivalent to $\frac{dy}{dt}$ of Eq. III.16, will be calculated from Eq. III.12 and the rest (equivalent to the right-hand side of Eq. III.16) will be calculated from the experimental data. The results of these calculations are then used to determine $\cos\Phi$ (which is y in the Eq. III.16).

Using the hybrid method described above, we have calculated first the values of $\cos\Phi$ for the incident proton energies of 1.88-MeV, 1.81-MeV and 1.594-MeV and then the time delay $\tau = \Phi/\omega$. These results are compared with the results of the theoretical calculation using Eq. III.12. These are shown in Fig. III.8 for an incident proton energy of 1.88 MeV, in Fig. III.9 for 1.81-MeV, and in Fig. III.10 for 1.594-MeV. The solid curves are the results of theoretical calculations using Eq. III.12. From Fig. III.8 and III.9, it is clear that the theoretical values for τ exhibit a bump of 1×10^{-20} second around 100-keV of photon energy. The extracted values of τ from the experimental data around k=100 keV have also about the same order of

10^{-20} second. However, for photon energy below 40-keV, the extracted values for τ from the experiment are higher than the theoretical values. This discrepancy may arise from the experimental uncertainty in the very soft photon region. At the incident energy of 1.594 MeV, which is below the 1.7-MeV resonance, the value of τ is expected to be zero since there is no bump in the bremsstrahlung spectrum implying that there is no interference bwtween the amplitudes $f_{\nu\nu}(E_i)$ and $f_{\nu'\nu}(E_f)$. This is shown in Fig. III.10.

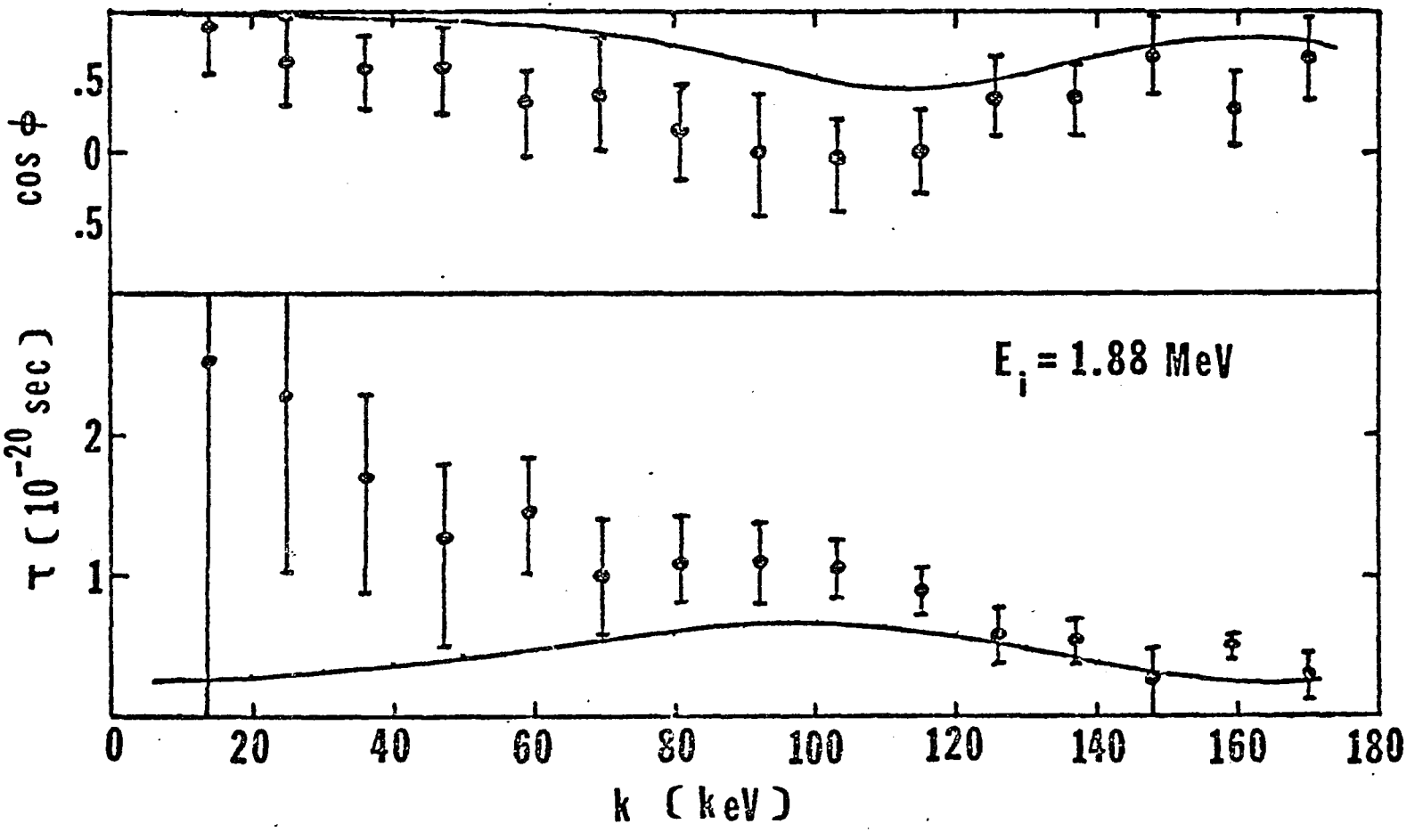

Fig. III.8 cos ϕ (see text for the definition of ϕ) and time delay extracted from the 1.88 MeV p ^{12}C γ data. The solid curves are the results of our calculations using Eq. III.12.

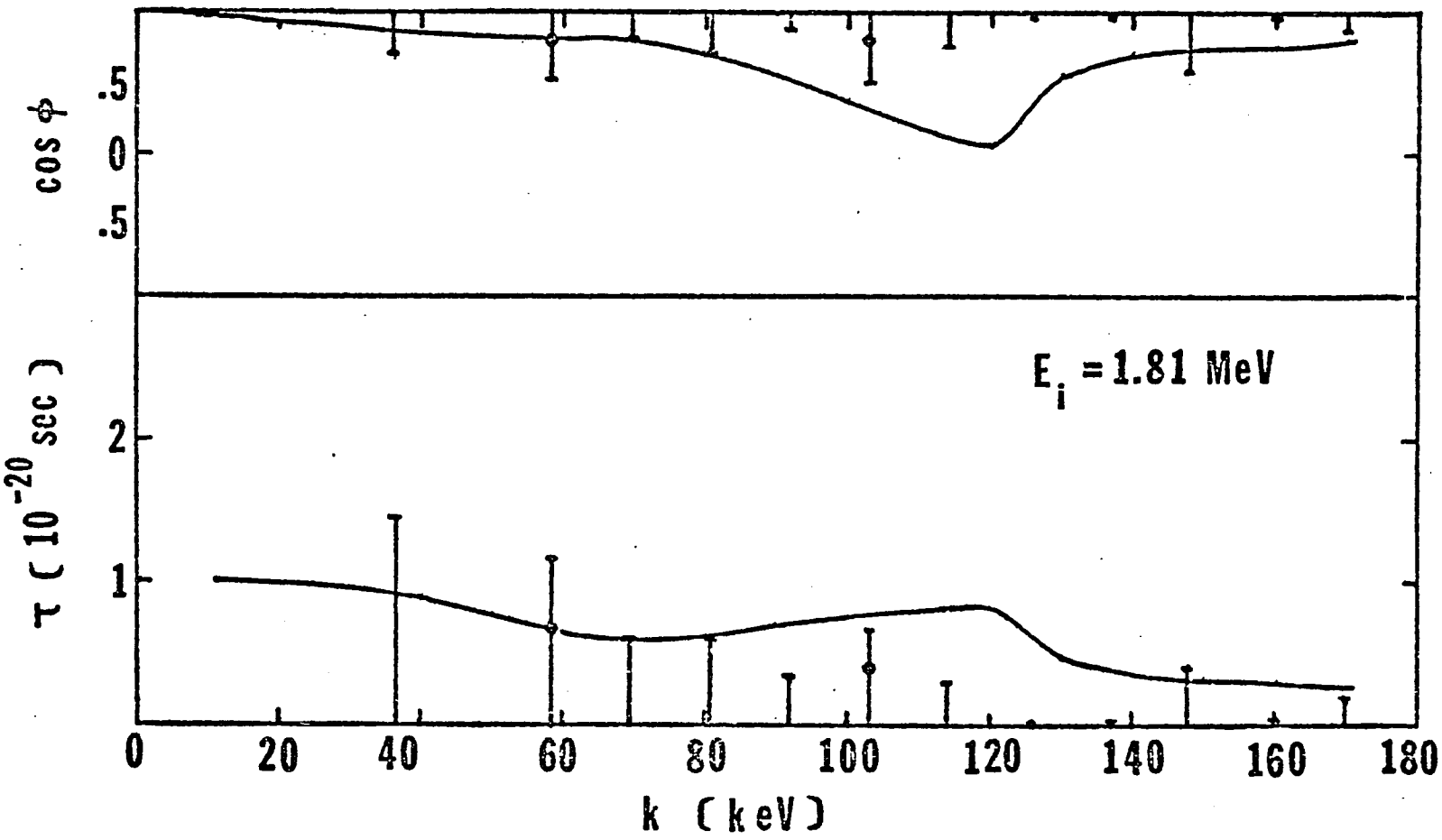

Fig. III.9 Same as Fig. III.8 but from the 1.81 MeV data.

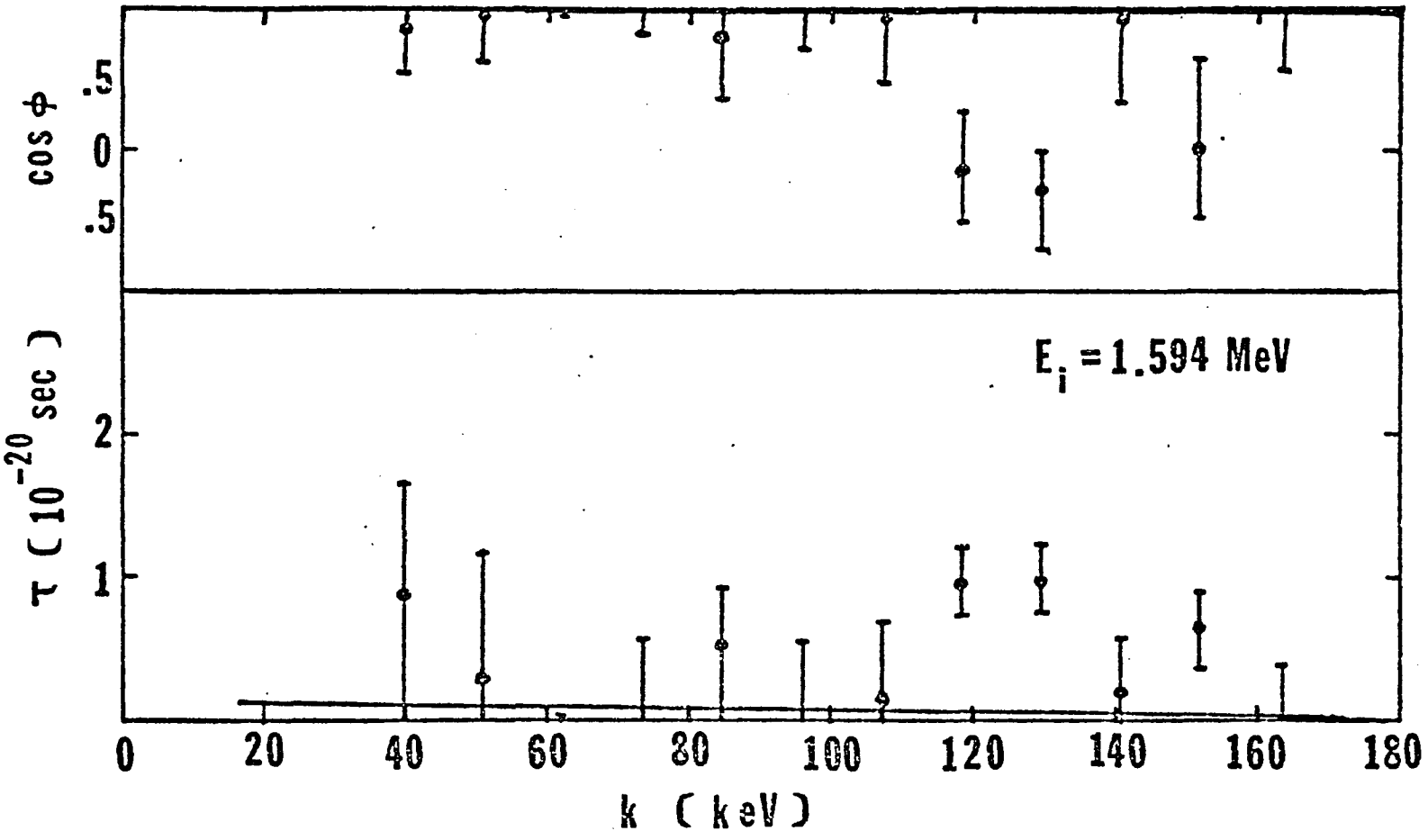

Fig. III.10 Same as Fig. III.8 but from the 1.594 MeV data.

CHAPTER IV. STUDY OF PION-PROTON BREMSSTRAHLUNG

The main interest in the study of the pion-proton bremsstrahlung processes has been the investigation of resonance effects and off-shell effects. For these purposes, many model dependent calculations and various model-independent calculations have been performed. Some calculations (19) predicted structure in the region of the Δ-resonance, but no structure was clearly observed in the experimental bremsstrahlung spectra (17-19). Furthermore, there exists a discrepancy among the model-independent approximations based upon the soft-photon theorem. The structure which appeared in the usual soft-photon approximation disapears in the calculation of EED (15,17-19) in which only the leading term of Low's result is included. The questionable second term in the expansion of T-matrices was correctly treated by Liou and Nutt who used a complete expansion in their calculation of the $\pi^{\pm}p\gamma$ coplanar case. This method is, essentially, based upon the expansion of all arguments of the half-off-shell T-matrices about values with zero photon energy, $k = 0$. It is different from other approximations which do not treat the expansion of the kinematics and dynamics consistently.

Traditionally, most calculations are carried out under coplanar conditions because of their simplicity. But noncoplanar events are important, and most of the UCLA data are

noncoplanar cases. Therefore, it is necessary to extend the soft-photon approximation of LN to include the noncoplanar case. Fortunately, almost all equations used in LN are in covariant form and this make our work (25) easy. From this work, we have found that the soft-photon approximation of LN works not only for the coplanar case but also for the noncoplanar case except for some cases in which the resonance effects seem to be important.

In addition to the calculation of the cross section using the soft-photon approximation of LN, we have also applied the Feshbach-Yennie approximation to analyze the $\pi^{\pm}p\gamma$ data of UCLA. This calculation always predicts a bump in the bremsstrahlung spectrum. The bump is small for most photon counters but large for a few counters.

A. APPLICATION OF THE SOFT-PHOTON APPROXIMATION OF LN TO THE NONCOPLANAR FERMION-BOSON CASE

To apply the soft-photon approximation of LN, we first briefly sketch the main steps for the derivation of the bremsstrahlung cross section. We wish to calculate an R-type cross section in the soft-photon expansion. The reason for this choice was discussed in chapter II. We first expand q_f^μ and p_f^μ in powers of k. To the first order in k^μ, we obtain Eq. II.6. These expansions are then used to expand s, t, and Δ consistently. Next we follow Low's

prescription to expand the half-off-shell T-matrices. When these expansions are introduced in the external bremsstrahlung amplitude, $\mathcal{M}_\mu^E$, we obtain the expansion of $\mathcal{M}_\mu^E$ in powers of k. By imposing the gauge invariance condition, $k^\mu \mathcal{M}_\mu^I = -k^\mu \mathcal{M}_\mu^E$, we obtain the internal amplitude, $\mathcal{M}_\mu^I$. The total amplitude, $\mathcal{M}_\mu$, is then obtained by the sum of $\mathcal{M}_\mu^E$ and $\mathcal{M}_\mu^I$. At this point, the off-shell derivatives cancel out up to order k^0. For consistancy, we also expand the phase space factor in the form of $F = F^{(0)} + F^{(1)} + \cdots$ (details of this expansion can be found in LN) and the proton projection operators which result from spin-summations. Finally, the bremsstrahlung differential cross section can be written as

$$\sigma(\Omega_q, \Omega_\gamma, k) = \sigma_{-1}/k + \sigma_0 , \qquad \text{(IV.1)}$$

where σ_{-1} and σ_0 depend on the elastic scattering amplitude and/or its derivatives, but not on k. Any difference between this cross section and experiment indicates a contribution from off-shell effects, resonance effects, or higher order on-shell terms. Small deviation implys a small contribution. Unfortunately, it is hard to tell the magnitude of individual effects from this difference.

For noncoplanar events, some modifications should be made. Let A and B in Eq. II.1 represent the incident pion and the target proton, respectively. Then the five four-momenta for the process are defined by Eq. II.2 and the

energy-momentum conservation is given by Eq. II.3. These equations of the energy-momentum conservation for the bremsstrahlung process reduce to those for elastic process, denoted by the same variables with a bar on each variable, in the limit of zero photon energy. Thus, the depenent variables $\bar{q}_f$, $\bar{p}_f$, $\bar{\theta}_p$, and $\bar{\phi}_p$ can be solved for. The quantity R_μ in LN is then calculated from these solutions. Although LN is derived for coplanar events, the expression for R_μ holds for noncoplanar events too. The bremsstrahlung amplitude in LN is also valid for noncoplanar cases:

$$\mathcal{M}_\mu = \bar{u}(p_f)\left[\mathcal{M}_\mu^X + \mathcal{M}_\mu^Y\right] u(p_i) , \qquad \text{(IV.2)}$$

where $\mathcal{M}_\mu^X$ and $\mathcal{M}_\mu^Y$ are from Eq. 22 of LN. The phase space factor F given by Eq. 28 of LN must be modified. For noncoplanar cases it becomes

$$F = q_f^2 \Big/ \left\{ \left| E_p q_f - E_q p_f \left[\cos\theta_p \cos\theta_\pi + \sin\theta_p \sin\theta_\pi \cos(\phi_\pi - \phi_p) \right] \right| \right\} . \qquad \text{(IV.3)}$$

However, the expressions for $F^{(0)}$ and $F^{(1)}$ given by Eq. 35 of LN can still be used since they are very general. Here, again the new solutions for $\bar{q}_f$ and $\bar{p}_f$ must be used in calculating $F^{(0)}$ and $F^{(1)}$. Once tnese modifications are made, the bremsstrahlung cross section can be calculated from the following expression:

$$\sigma(\Omega_q, \Omega_\gamma, k) = \frac{e^2 M^2 k F}{8\left[(q_i \cdot p_i)^2 - (mM)^2\right]^{1/2}} \left(\frac{1}{2\pi}\right)^5 \frac{1}{2} \sum_{pol,\,spin} \left| \epsilon^\mu \mathcal{M}_\mu \right|^2 . \qquad \text{(IV.4)}$$

B. APPLICATION OF THE FESHBACH-YENNIE APPROXIMATION TO THE PION-PROTON BREMSSTRAHLUNG PROCESS

In Chapt. III, we have applied the Feshbach-Yennie approximation to calculate the proton-carbon bremsstrahlung cross section. This approximation can also be used for the $\pi^{\pm}p\gamma$ process. In this approximation, the T-matrix for the elastic pion-proton scattering is to be evaluated at both the initial and final energies, which is a characteristic feature of the Feshbach-Yennie approximation.

Following the same notations used in Chapt. III, the T-matrix for the elastic $\pi^{\pm}p$ scattering has the form

$$T(s,t) = -A(s,t) + \frac{1}{2}(\not{k}_i + \not{k}_f) B(s,t). \qquad \text{(IV.5)}$$

In the soft-photon approximation, the half-off-shell T-matrices $T_j(s_j, t_j, \Delta_j)$, j = a, b, c, and d, are to be expanded about an on-shell point. One may take k = 0 as the on-shell point and expand T_j about it for each j as in the soft-photon approximation of LN. In this case, the "only" on-shell amplitude we need in the calculation of the bremsstrahlung amplitude is

$$T_i \equiv T(s_i, t) = -A(s_i, t) + \frac{1}{2}(\not{k}_i + \not{k}_f) B(s_i, t). \qquad \text{(IV.6)}$$

On the other hand, in the Feshbach-Yennie approximation, two different on-shell amplitudes are needed. In other words, the half-off-shell T-matrices are expanded about two on-

shell points, (s_i,t) for diagrams II.1a and II.1c, and (s_f,t) for diagrams II.1b and II.1d. Thus, two elastic T-matrices needed for our calculation are $T_i = T(s_i,t)$ and $T_f = T(s_f,t)$. To evaluate T_f we have to, apart from the replacement of s by s_f in A(s,t) and B(s,t), calculate $(\not{q}_i' + \not{q}_f)$. This may be done by considering an elastic process with final pion of four-momentum q_f^μ and final proton of four-momentum p_f^μ. Let us consider the energy momentum conservation

$$q_i'^\mu + p_i'^\mu = q_f^\mu + p_f^\mu , \qquad \text{(IV.7)}$$

and the requirements

$$s_f = (q_f + p_f)^2 , \qquad \text{(IV.8)}$$

$$t_0 = (q_f - q_i')^2 = (p_f - p_i')^2 , \qquad \text{(IV.9)}$$

so that the elastic amplitude T_f is given by

$$T_f = T(s_f,t) = -A(s_f,t) + \tfrac{1}{2}(\not{q}_i' + \not{q}_f) B(s_f,t). \qquad \text{(IV.10)}$$

These conditions give the following six equations

$$2m^2 - t_0 \equiv H = 2\, q_f \cdot q_i' ,$$

$$q_x + p_f \sin\theta_{p_f} \cos\phi_{p_f} \equiv B = q_i' \sin\theta_{q_i'} \cos\phi_{q_i'} + p_i' \sin\theta_{p_i'} \cos\phi_{p_i'} ,$$

$$q_y + p_f \sin\theta_{p_f} \sin\phi_{p_f} \equiv C = q_i' \sin\theta_{q_i'} \sin\phi_{q_i'} + p_i' \sin\theta_{p_i'} \sin\phi_{p_i'} ,$$

$$q_z + p_f \cos\theta_{p_f} \equiv D = q_i' \cos\theta_{q_i'} + p_i' \cos\theta_{p_i'} ,$$

$$(\vec{q}_f^{\,2}+m^2)^{1/2}+(\vec{p}_f^{\,2}+M^2)^{1/2}\equiv A = (q_i'^2+m^2)+(p_i'^2+M^2),$$

$$S_f = m^2+M^2+2q_i'\cdot p_i', \qquad \text{(IV.11)}$$

where q_x, q_y, and q_z are the x, y, and z components of $\vec{q}_f$, respectively,

and $$q_i'^{\mu}=\left(\left[\vec{q}_i'^{\,2}+m^2\right]^{1/2},\ \vec{q}_i'\right), \qquad p_i'^{\mu}=\left(\left[\vec{p}_i'^{\,2}+M^2\right]^{1/2},\ \vec{p}_i'\right).$$

If we introduce

$$x=\sin\theta_{q_i'}\cos\phi_{q_i'}, \quad y=\sin\theta_{q_i'}\sin\phi_{q_i'}, \quad z=\cos\theta_{q_i'}. \qquad \text{(IV.12)}$$

Then we have seven unknowns with an additional condition

$$x^2+y^2+z^2=1. \qquad \text{(IV.13)}$$

Using these seven equations we can simplify them and it is easy to show that the last two equations in Eq. IV.11 are equivalent. After simplification, we obtain Eq. IV.13 and the following three equations with five unknowns (q_i', p_i', x, y, z):

$$p_i'^{\,2}=(B-xq_i')^2+(C-yq_i')^2+(D-zq_i')^2,$$

$$E = 2A(\vec{q}_i'^{\,2}+m^2)^{1/2}-2m^2-2q_i'(Bx+Cy+Dz), \qquad \text{(IV.14)}$$

$$z = -xq_x-yq_y+\left[2(\vec{q}_f^{\,2}+m^2)^{1/2}(\vec{q}_i'^{\,2}+m^2)^{1/2}-H\right]/(2q_i'q_z).$$

In the laboratory system, we have $q_i >> 0$. It would be instructive to choose an additional condition which will force $q_i'^{\mu}$ to be close to q_i^{μ}. Thus we choose $\theta_{q_i'} = 0$ and obtain

$$q_i' = \left\{ \left[\frac{E - DH/q_z + m^2}{2A - (2D/q_z)(\vec{q}_f^{\,2} + m^2)^{1/2}} \right]^2 - m^2 \right\}^{1/2} . \qquad \text{(IV.15)}$$

Next, we consider the contribution from the anomalous magnetic moment by using Eq. V.5 instead of Eq.III.3. This change introduces additional terms of order k° into the bremsstrahlung amplitude. With these additional terms and Eq. III.7, we write the total bremsstrahlung amplitude to order k so that we can see the contribution from each order. The final results are, up to order k°,

$$\mathcal{M} = \epsilon_\mu M^\mu = \epsilon_\mu \bar{u}_{p_f} \Gamma^\mu u_{p_i} , \qquad \Gamma^\mu = \Gamma^\mu(\tfrac{1}{k}) + \Gamma^\mu(k^\circ),$$

$$\Gamma^\mu(\tfrac{1}{k}) = \left[\frac{z q_f^\mu}{q_f \cdot k} - \frac{z(q_f + p_f)^\mu}{(q_f + p_f)\cdot k} \right] T_i + \left[\frac{Z p_f^\mu}{p_f \cdot k} - \frac{Z(q_f + p_f)^\mu}{(q_f + p_f)\cdot k} \right] T_i$$

$$- \left[\frac{z q_i^\mu}{q_i \cdot k} - \frac{z(q_i + p_i)^\mu}{(q_i + p_i)\cdot k} \right] T_f - \left[\frac{Z p_i^\mu}{p_i \cdot k} - \frac{Z(q_i + p_i)^\mu}{(q_i + p_i)\cdot k} \right] T_f ,$$

$$\Gamma^\mu(k^\circ) = C_o^\mu T_i + T_f D_o^\mu - 2(\bar{p}_f - p_i)\cdot(R + k) \left[\frac{z q_f^\mu}{q_f \cdot k} \frac{\partial T_i}{\partial t} - \frac{z q_i^\mu}{q_i \cdot k} \frac{\partial T_f}{\partial t} \right]$$

$$+ 2z \left[(\bar{p}_f - p_i)^\mu + 2(\bar{p}_f - p_i)\cdot N_R \bar{p}_f^{\,\mu} \right] \left[\frac{\partial T_i}{\partial t} - \frac{\partial T_f}{\partial t} \right]$$

$$+2(\bar{q}_f - q_i)\cdot R\left\{\frac{Z p_f^\mu}{p_f\cdot k}\frac{\partial T_i}{\partial t} - \frac{Z p_i^\mu}{p_i\cdot k}\frac{\partial T_f}{\partial t}\right\}$$

$$+2Z(\bar{q}_f - q_i)\cdot N_R\,\bar{p}_f^\mu\left\{\frac{\partial T_f}{\partial t} - \frac{\partial T_i}{\partial t}\right\},$$

$$C_o^\mu = \frac{Z\gamma^\mu k}{2p_f\cdot k} + \frac{\lambda}{2m}\left\{\gamma^\mu - \frac{p_f^\mu k}{p_f\cdot k}\right\} + \frac{\lambda}{2}\frac{\gamma^\mu k}{p_f\cdot k},$$

$$D_o^\mu = -\frac{Z\gamma^\mu k}{2p_i\cdot k} + \frac{\lambda}{2m}\left\{\gamma^\mu - \frac{p_i^\mu k}{p_i\cdot k}\right\} - \frac{\lambda}{2}\frac{\gamma^\mu k}{p_i\cdot k}. \qquad \text{(IV.16)}$$

Using this amplitude, the bremsstrahlung cross section can be calculated as

$$\sigma = -\frac{1}{2}\mathcal{N}\,F\,Tr\left(\Lambda_{p_i}\gamma^0\Upsilon^{\mu+}\gamma^0\Lambda_{p_f}\Upsilon_\mu\right), \qquad \text{(IV.17)}$$

where the factor $\mathcal{N}$ is given by Eq. III.9, the "full" phase space factor F is given by Eq. IV.3, and the "full" projection operators Λ_{p_i} and Λ_{p_f} are

$$\Lambda_{p_i} = (\not{p}_i + M)/2M, \quad \Lambda_{p_f} = (\not{p}_f + M)/2M. \qquad \text{(IV.18)}$$

C. RESULTS AND DISCUSSION

We have used Eq. IV.4 with the elastic phase shifts of Barnes et al. (34) to calculate $\pi^\pm p\gamma$ cross sections in the laboratory system as a function of k for various photon counters G_i (i = 1, 2, ..., 19) (Table IV.1 and Fig. IV.1c)

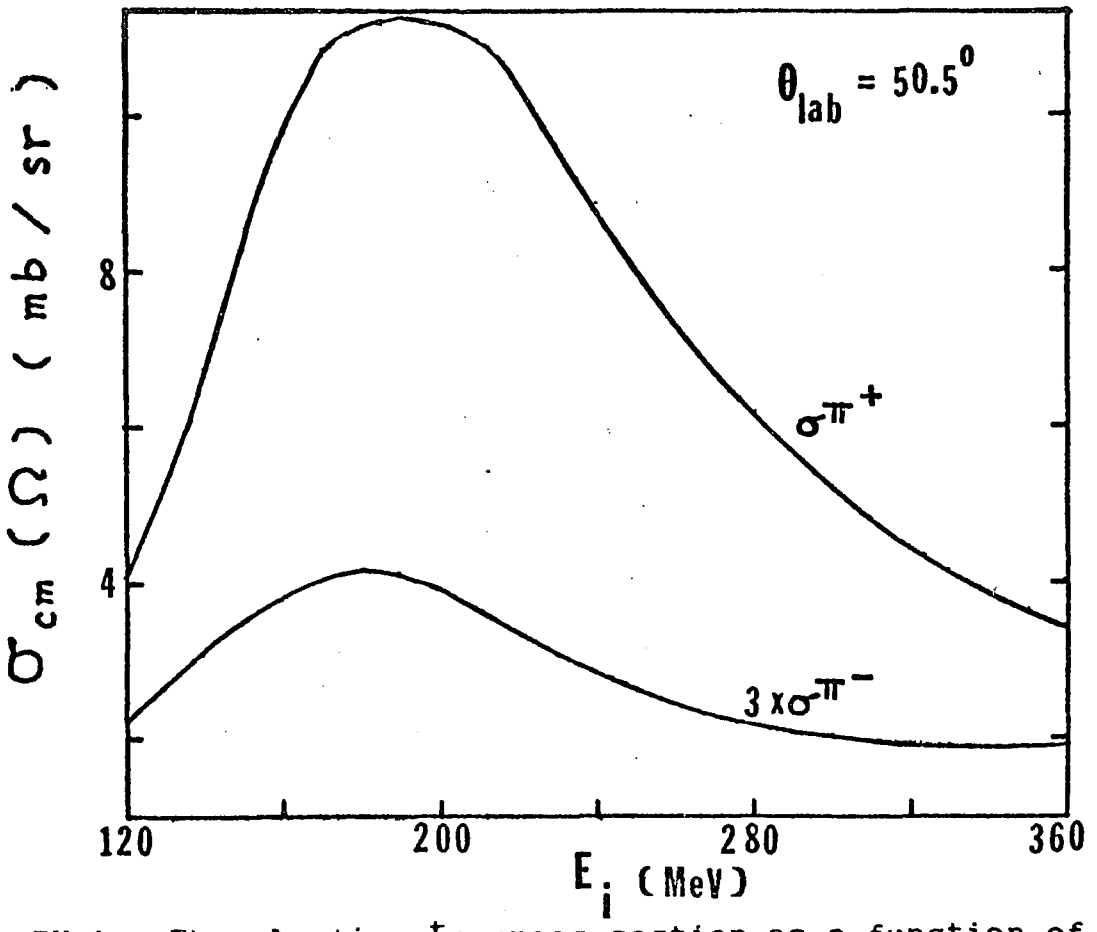

Fig. IV.1a The elastic $\pi^{\pm}p$ cross section as a function of the incident pion energy.

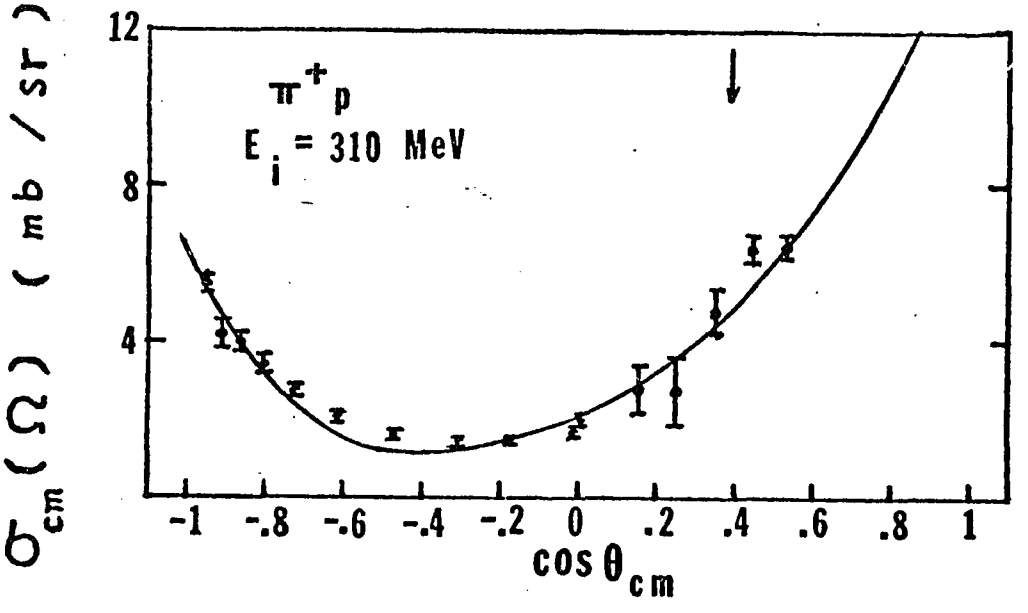

Fig. IV.1b The angular distribution of the π^+p elastic scattering cross sections at 310 MeV. The experimental data are from Ref. 68.

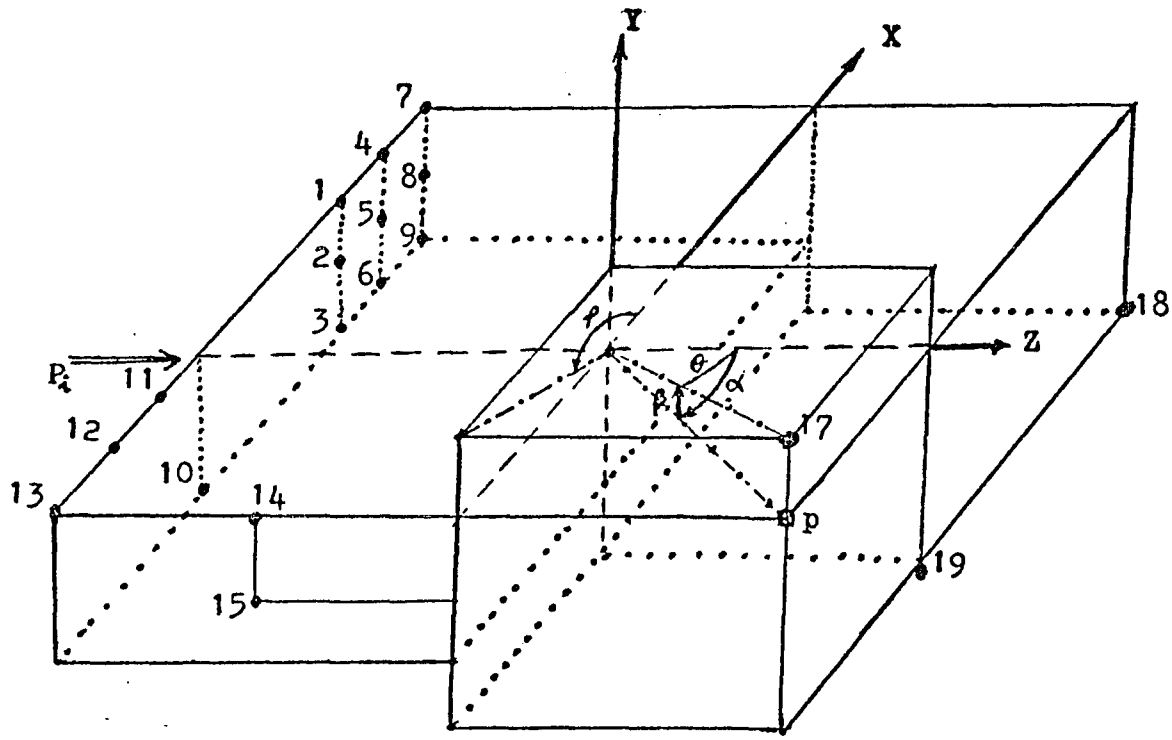

IV.1c The coordinate system and relative locations of the photon counters used in the UCLA $\pi^{\pm} p\gamma$ experiment.

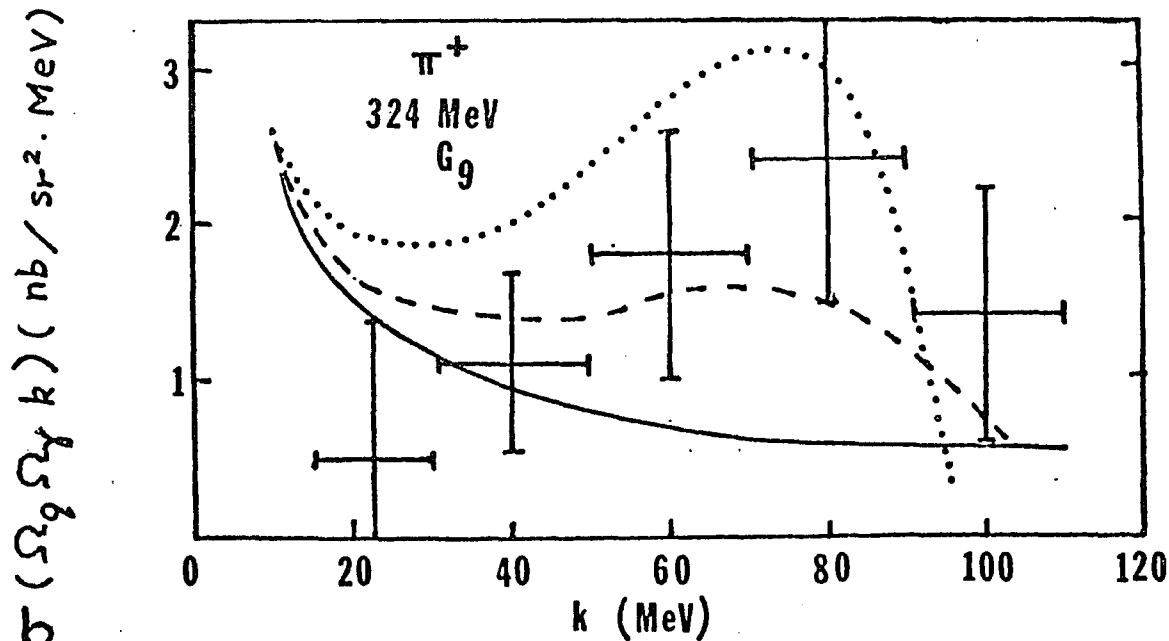

Fig. IV.3b $\pi^+ p\gamma$ bremsstrahlung spectra for the counter G9 at an incident pion energy of 324 MeV. The solid curve is the result obtained by using the soft-photon approximation of LN. The dashed (dotted) curve is the result obtained by using the σ_{-1}/k and σ_0 terms (σ_{-1}/k, σ_0 and $\sigma_1 k$) of the Feshbach-Yennie approximation.

TABLE IV.1
Locations of detectors used in the UCLA $\pi^{\pm}p\gamma$ experiment

Counter	α (deg)	β (deg)	θ (deg)	ϕ (deg)	d (cm) (to target)
G1	200.	0.	160.	0.	61.1
G2	200.	-18.	153.34	316.47	56.
G3	200.	-36.	139.48	295.11	56.
G4	220.	0.	140.	0.	56.
G5	220.	-18.	136.77	333.16	56.
G6	220.	-36.	128.30	311.50	56.
G7	240.	0.	120.	0.	56.
G8	240.	-18.	118.39	339.43	56.
G9	240.	-36.	113.86	320.01	56.
G10	180.	-36.	144.	270.	56.
G11	160.	0.	160.	180.	63.
G12	140.	0.	140.	180.	63.
G13	120.	0.	120.	180.	63.
G14	103.	0.	103.	180.	63.
G15	103.	-20.	102.20	200.48	63.
G17	50.	4.	50.12	174.78	300.
G18	320.	-56.	64.64	293.44	63.
G19	0.	-59.	59.	270.	63.
pion	50.5±7.	-10±24	50.5	180.	73.8[a]
proton	323±27	-26±26	0. (upper limit)	0. (upper limit)	92.1[b]

α = horizontal projection of the angle measured clockwise from the beam line.
β = the angle of elevation measured upwords from the horizontal plane.
[a] distance to first pion spark chamber.
[b] distance to first plane of counters.

at three incident kinetic energies for each of the $\pi^+ p\gamma$ and $\pi^- p\gamma$ cases. As usual, we have checked the elastic amplitude used in the bremsstrahlung calculation by comparing the elastic cross section with the experimental data in Figs. IV.1a and IV.1b. We have also used Eq. IV.16, with the derivatives of $T(s, t)$ with respect to t approximated by

$$\frac{\partial T(s,t)}{\partial t} = -\frac{\partial A(s,t)}{\partial t} + \frac{1}{2}(\not{k}_i + \not{k}_f)\frac{\partial B(s,t)}{\partial t} \qquad \text{(IV.19)}$$

to calculate bremsstrahlung cross sections in the Feshbach-Yennie approximation. In all these calculations, the pion scattering angle is fixed at 50.5°. The results are shown in Figs. IV.2-IV.14. We have presented two bremsstrahlung spectra at each incident pion energy for each photon counter. Here, we have chosen one incident energy for each photon counter since in most cases the other two incident energies give almost similar results. The calculation of the soft-photon approximation of LN always predicts bremsstrahlung spectra with typical 1/k dependence and agrees well with most of the UCLA data. The Feshbach-Yennie approximation always predicts a bump in the bremsstrahlung spectrum. In most cases, the bumps are small and the difference between this prediction and the soft-photon approximation of LN is of the size of the error bar. But for some counters, for instance, counters G3, G6, and G9 for the $\pi^+ p\gamma$ process at 269-MeV, this difference is large and indicates the importance of resonance effect and other contributions if our approximations are accurate enough.

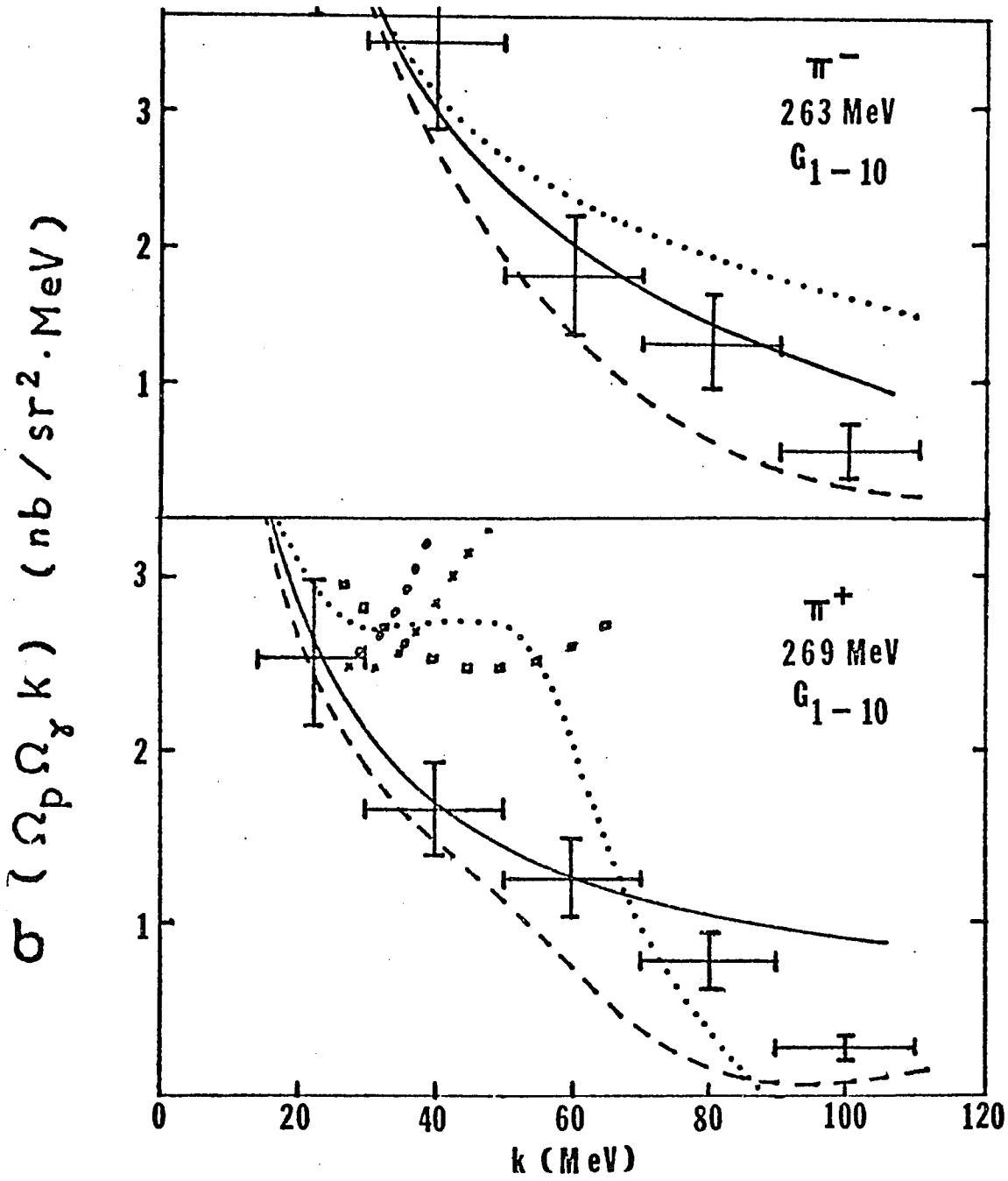

Fig. IV.2 The $\pi^{\pm}p\gamma$ cross sections averaged over the photon counters G1-G10 are compared with the experimental data of Ref. 19 at 263 MeV ($\pi^{-}p\gamma$) and 269 MeV ($\pi^{+}p\gamma$). The solid curve represents our results for the soft-photon approximation. The dashed (dotted) curve represents our results for the Feshbach-Yennie approximation using σ_{-1}/k and σ_0 terms (σ_{-1}/k, σ_0 and $\sigma_1 k$ terms). The "$\circ$", "$\times$" and "$\square$" are obtained from the curves "KP0", "KP2", and "SPA", respectively, of Ref. 19.

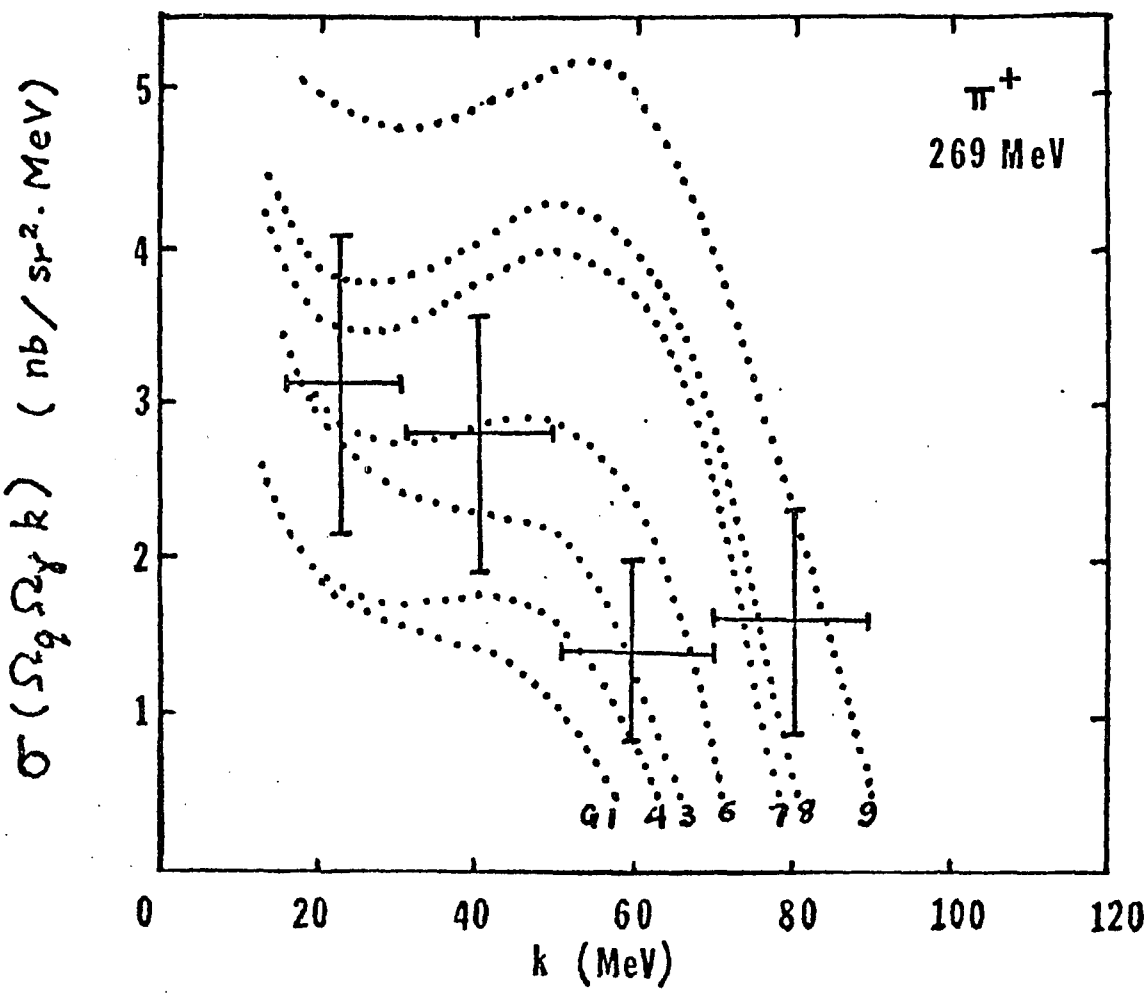

Fig. IV.3a The $\pi^+ p\gamma$ bremsstrahlung spectra for photon counters G1, G3, G4, G6, G7, G8, and G9 at the incident pion energy of 269 MeV. The dotted curve is our result obtained by using the first three terms of the cross section of the Feshbach-Yennie approximation. The experimental data which are for the counter G9 are from Ref. 19.

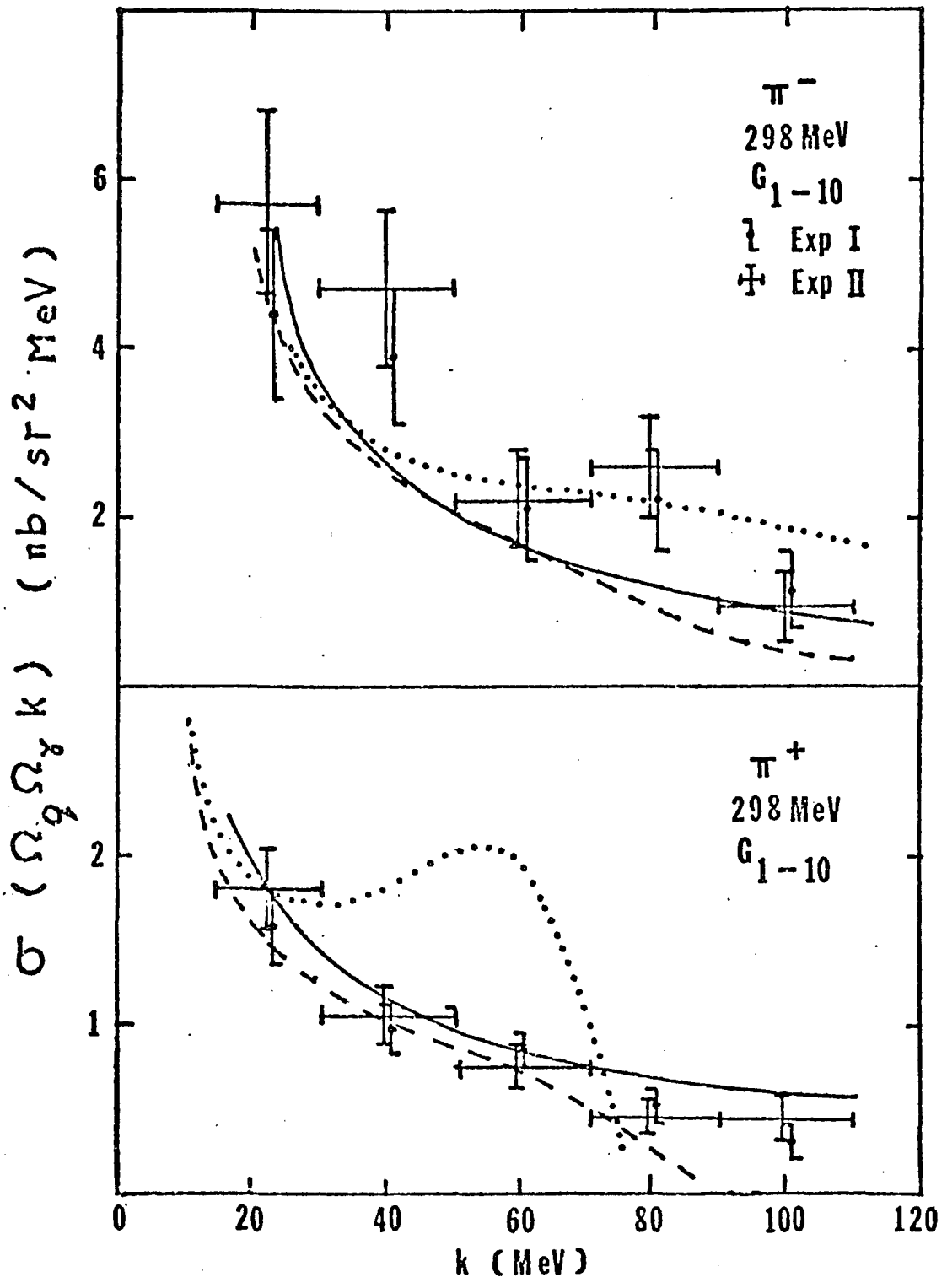

Fig. IV.4 Same as Fig. IV.2 but at an incident pion energy of 298 MeV.

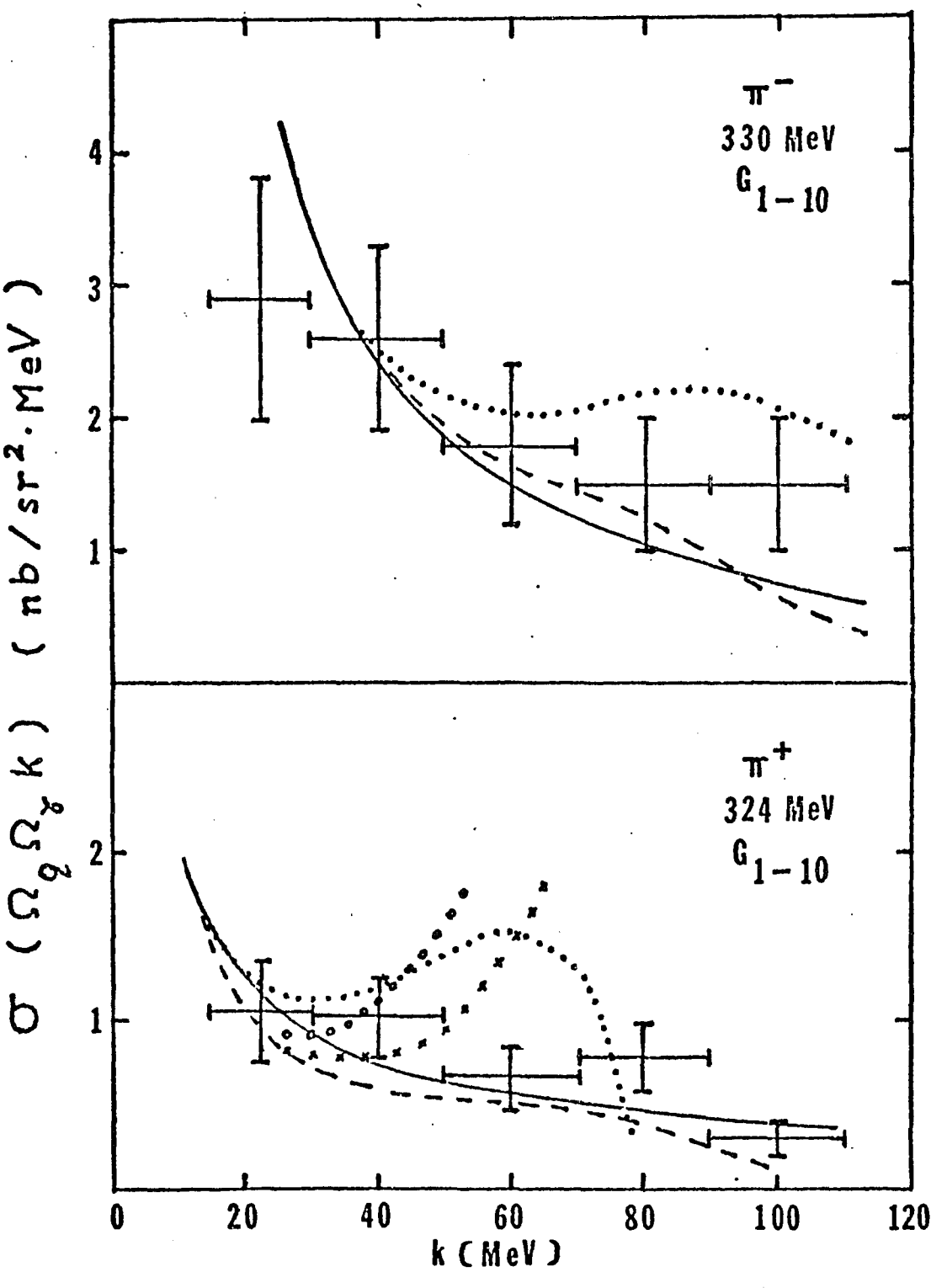

Fig. IV.5 Same as Fig. IV.2 but at an incident pion energies of 324 MeV ($\pi^+ p\gamma$) and 330 MeV ($\pi^- p\gamma$).

In order to see the general feature of the agreement between our calculations and the UCLA data for counters G1 through G10, we have averaged the calculated bremsstrahlung cross sections over the photon counters G1 - G10 and have compared these averaged cross sections with the UCLA data. In Fig.IV.2, the averaged cross sections are plotted against photon energy, k, for the $\pi^- p\gamma$ process at 263-MeV (top) and for the $\pi^+ p\gamma$ process at 269-MeV (bottom). The solid curves represent our calculations of the soft-photon approximation of LN and the dotted (dashed) curves represent the results of our Feshbach-Yennie predictions calculated by using the first three (two) terms in the cross sections. The experimental data are from the Refs. 17-19. The bump appearing around 50 MeV photon energy for the $\pi^+ p\gamma$ case is mainly due to the bump appearing in the spectra for counters G3-G9 as shown in Fig. IV.3a. However, this bump is not observed in the experimental data. This may be an indication that other contributions such as higher order terms in our expansion or other effects might not be small, so that the resonance effect is cancelled out. In Fig.IV.4, we present similar plots at 298-MeV for the $\pi^- p\gamma$ case (top) and the $\pi^+ p\gamma$ case (bottom). In Fig. IV.5, similar plots are shown for $\pi^- p\gamma$ at 330-MeV (top) and for $\pi^+ p\gamma$ at 324-MeV (bottom). For $\pi^+ p\gamma$ at 324-MeV, the bump is mainly due to the bumps from counters G6 - G8. It is interesting to note that, for counter G9 at this incident pion energy, the experimental data for the $\pi^+ p\gamma$ can only be described by

the Feshbach-Yennie approximation, as shown in Fig. IV.3b.

Moreover, we have compared our theoretical calculations with the UCLA data for individual photon counters G11 through G19. We present here only one incident energy for each photon counters. Comparisons between theory and experiment are made in Fig. IV.6 for photon counters G11, in Figs. IV.7-IV.10 for photon counters G12-G15, and in Figs. IV.11-IV.13 for counters G17-G19. In Fig. IV.14, a plot of the $\pi^+ p\gamma$ cross section versus photon angles α are shown for photon energies of 22.5-MeV (bottom) and 40-MeV (top). The experimental data (circles for k=22.5-MeV and squares for k=40-MeV) are the UCLA data. The solid (dotted) curves with "Δ" (#) are the results of the calculation using the soft-photon approximation of LN (the Feshbach-Yennie approximation). From these figures, the following conclusions may be drawn: (i) The Feshbach-Yennie approximation gives better agreement with the $\pi^- p\gamma$ data for counters G13 through G15 at 263-MeV than the soft-photon approximation of LN. (ii) In the $\pi^+ p\gamma$ case, the bumps predicted by the Feshbach-Yennie approximation are small for these counters and hence the agreement between our prediction and the UCLA data is good.

Note that it was argued by the UCLA group that although the pion spectrometer was centered at 50.5° to the beam, the effective average scattering angle was about 52° because of

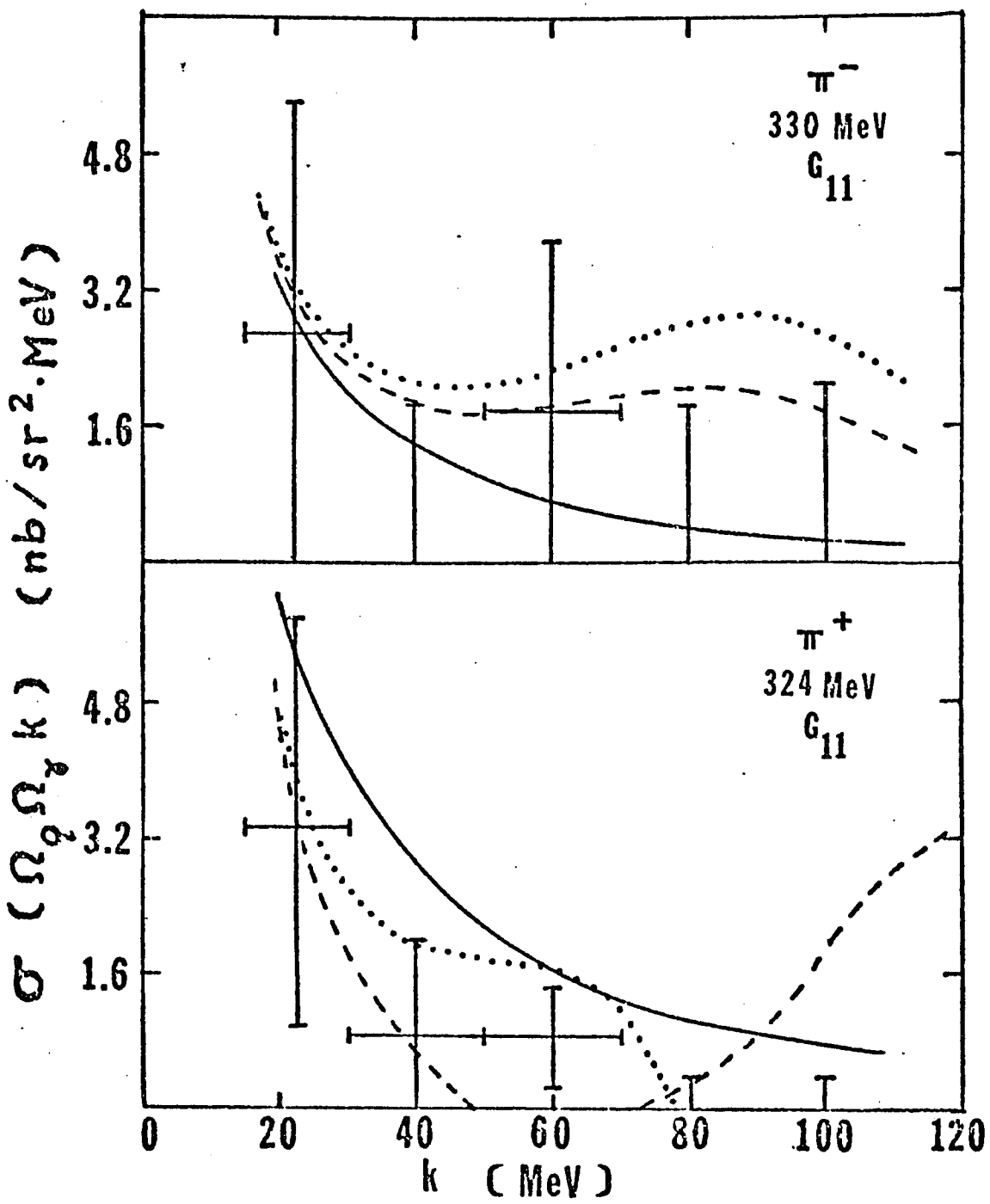

Fig. IV.6 Same as Fig. IV.3b, but for photon counter G11 at the incident pion energy of 324 (330) MeV for $\pi^+ p \gamma$ ($\pi^- p \gamma$).

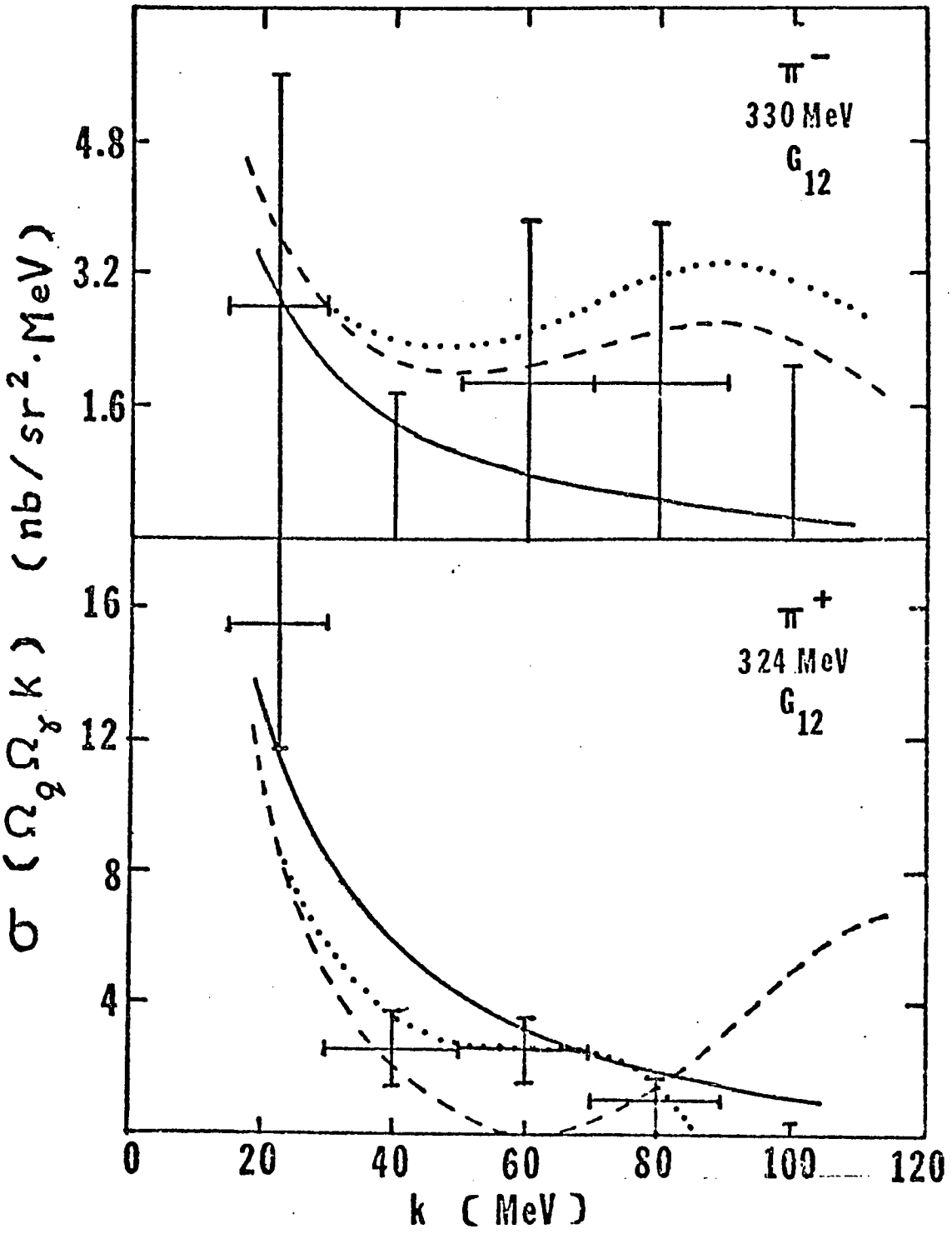

Fig. IV.7 Same as Fig. IV.6 but for counter G12.

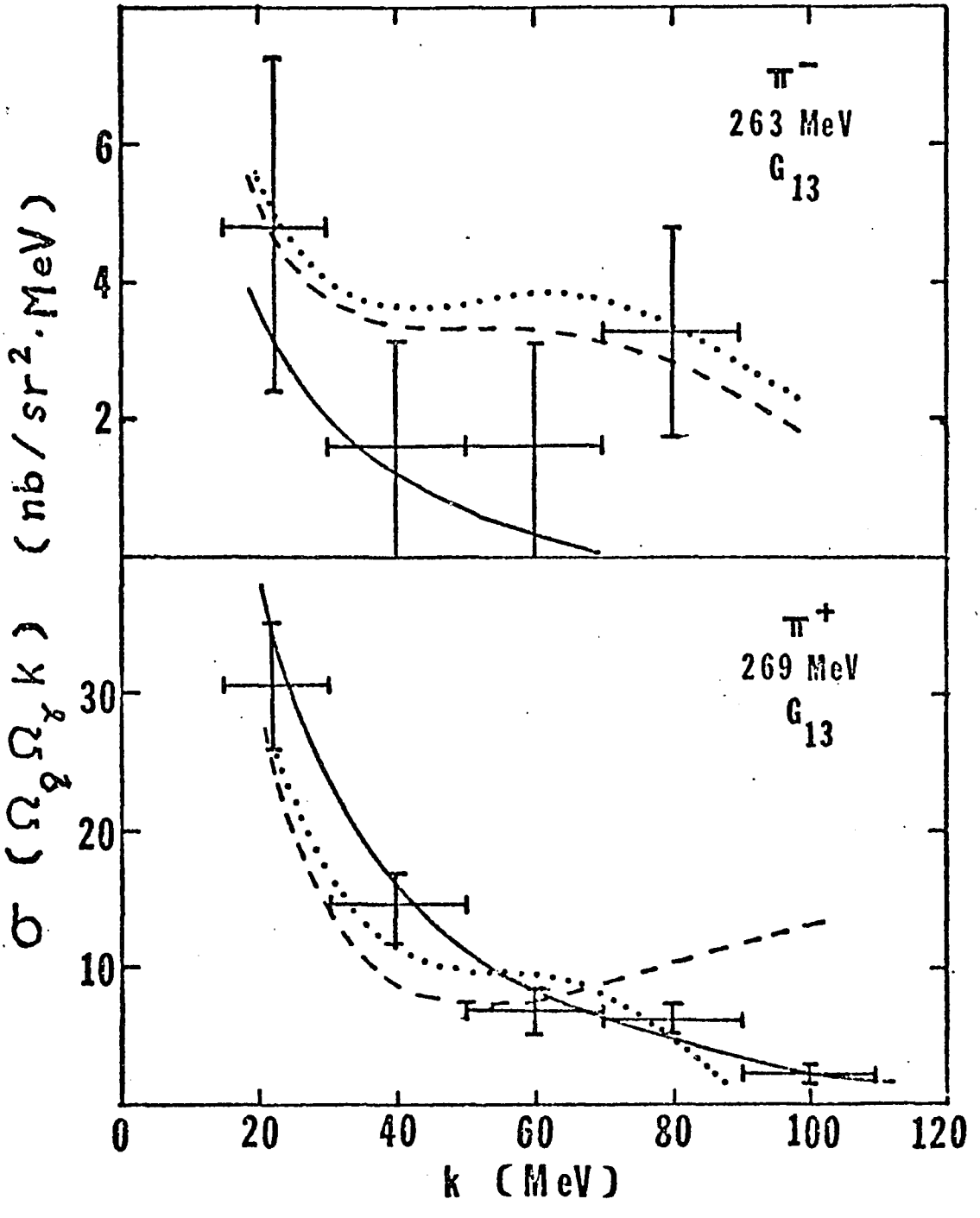

Fig. IV.8 Same as Fig. IV.3b but for counter G13 at the incident pion energy of 269 (263) MeV for $\pi^+ p\gamma$ ($\pi^- p\gamma$).

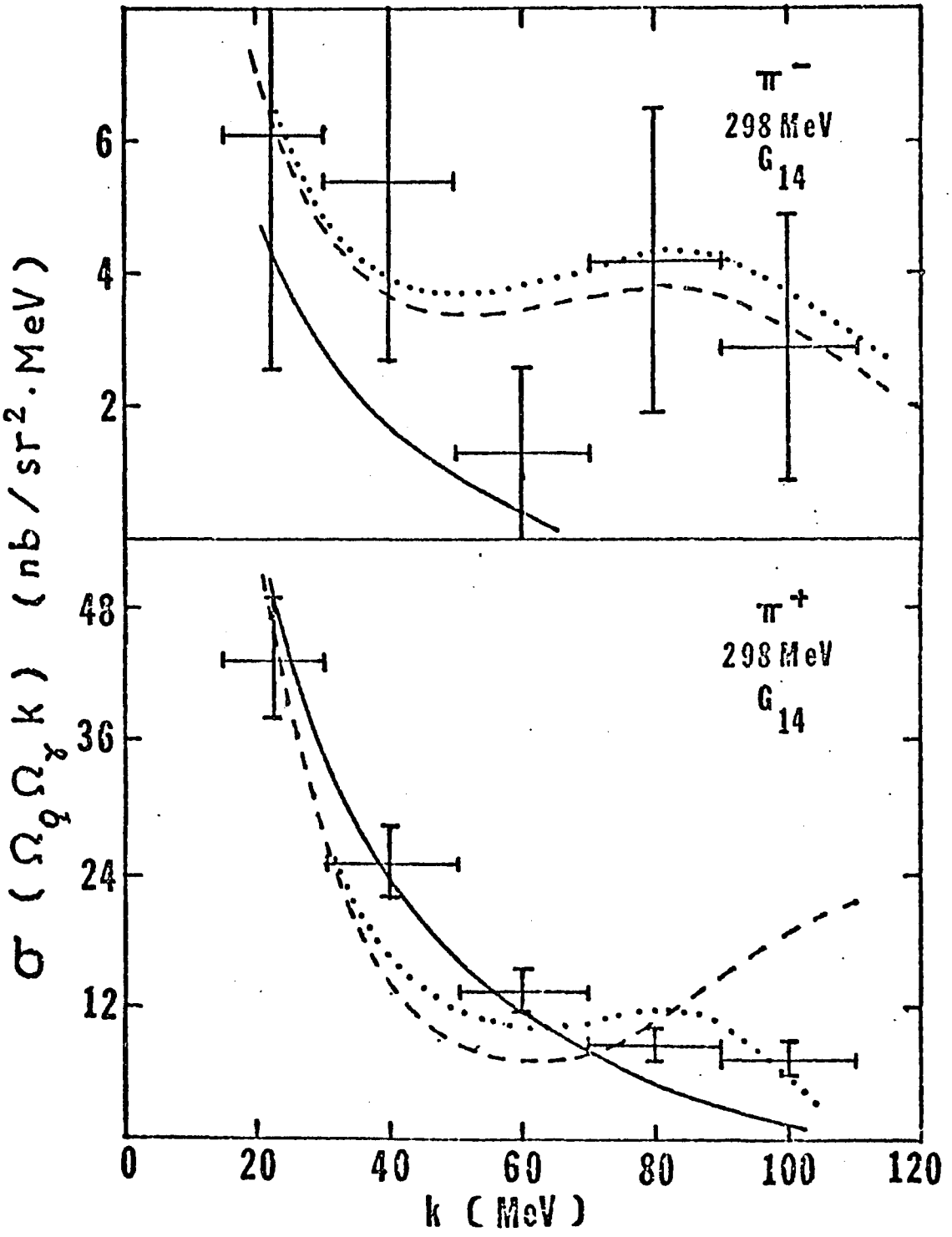

Fig. IV.9 Same as Fig. IV.3b but for counter G14 at an incident energy of 298 MeV.

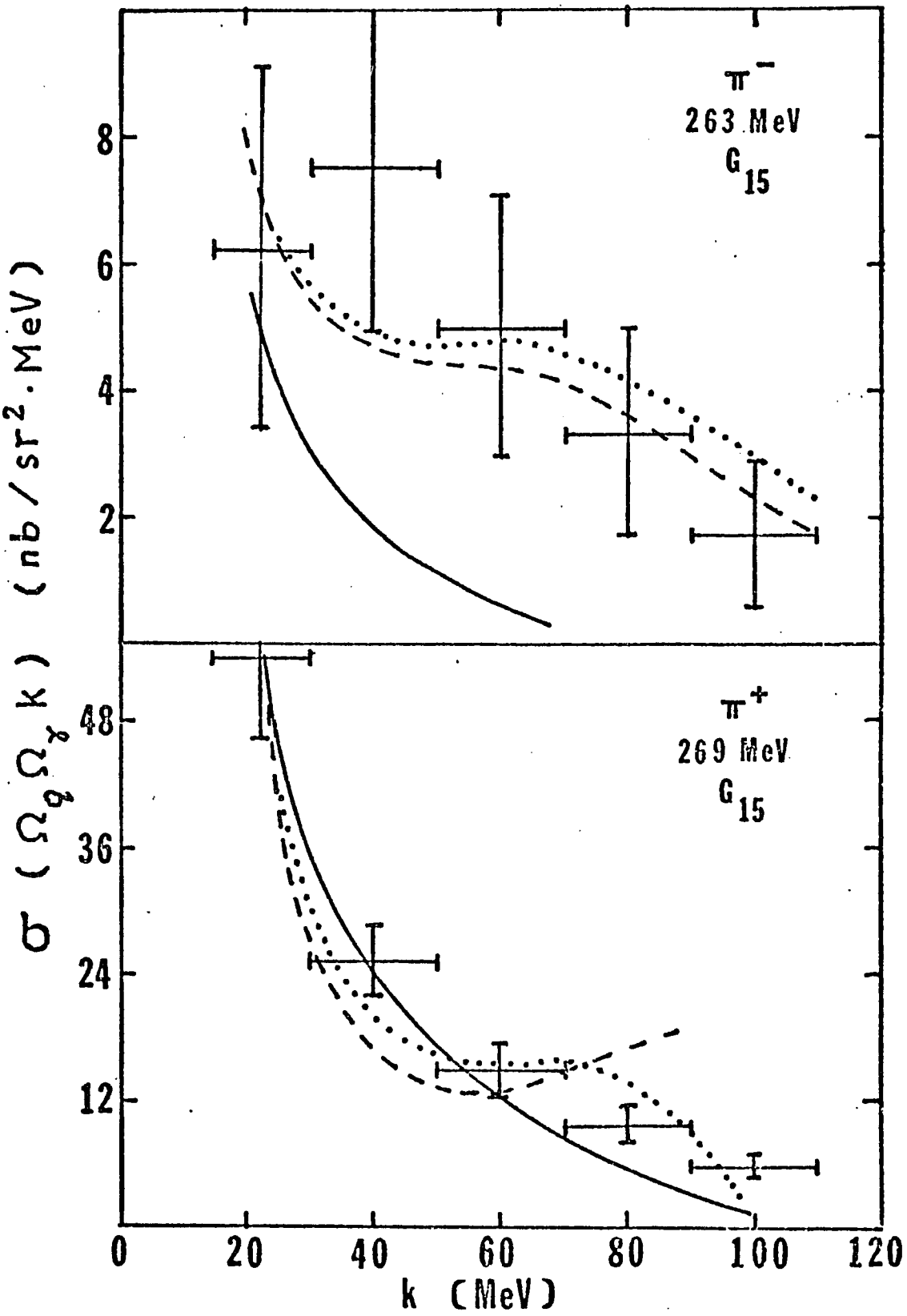

Fig. IV.10 Same as Fig.IV.8 but for counter G15.

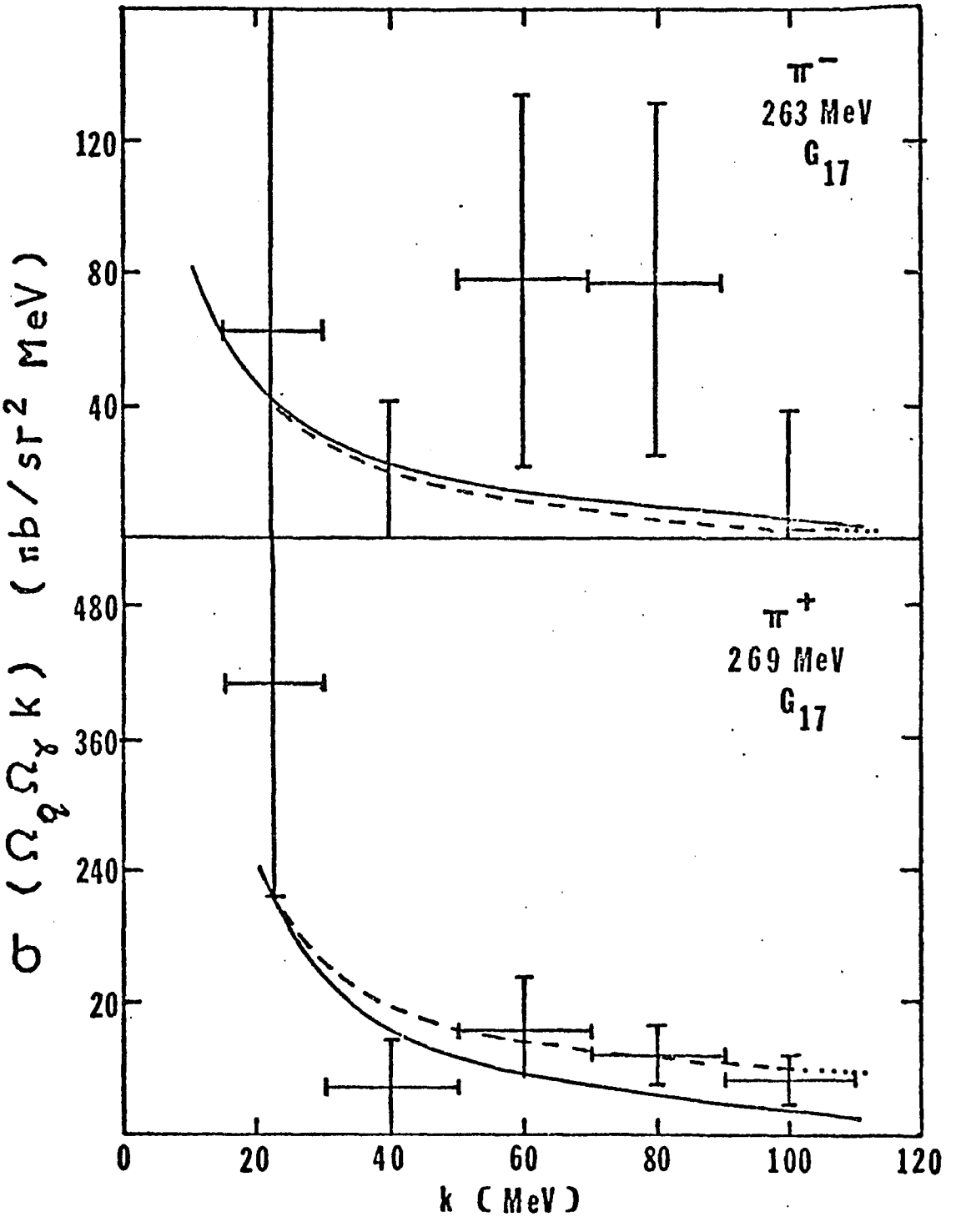

Fig. IV.11 Same as Fig. IV.8 but for counter G17.

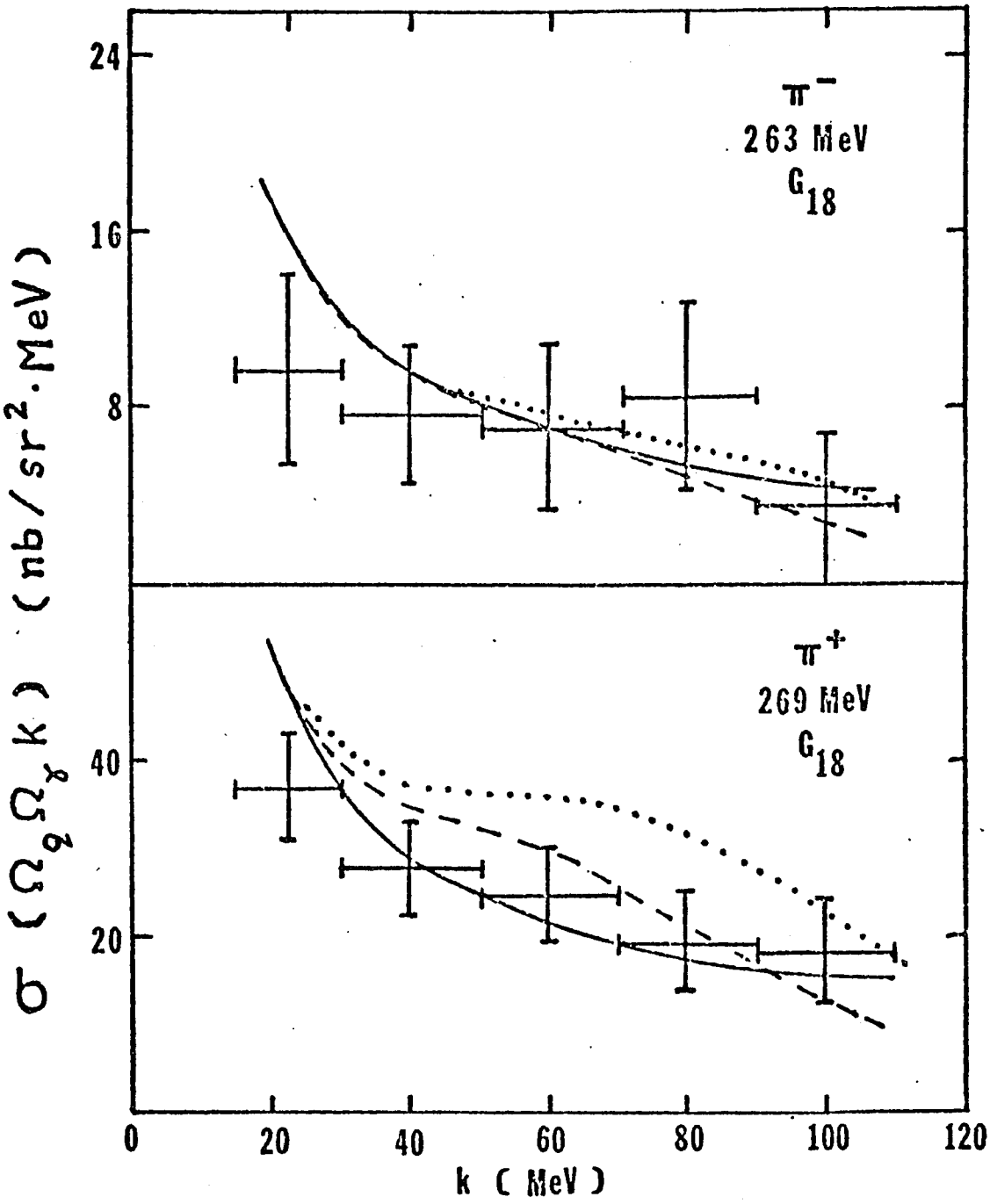

Fig. IV.12 Same as Fig. IV.8, but for counter G18.

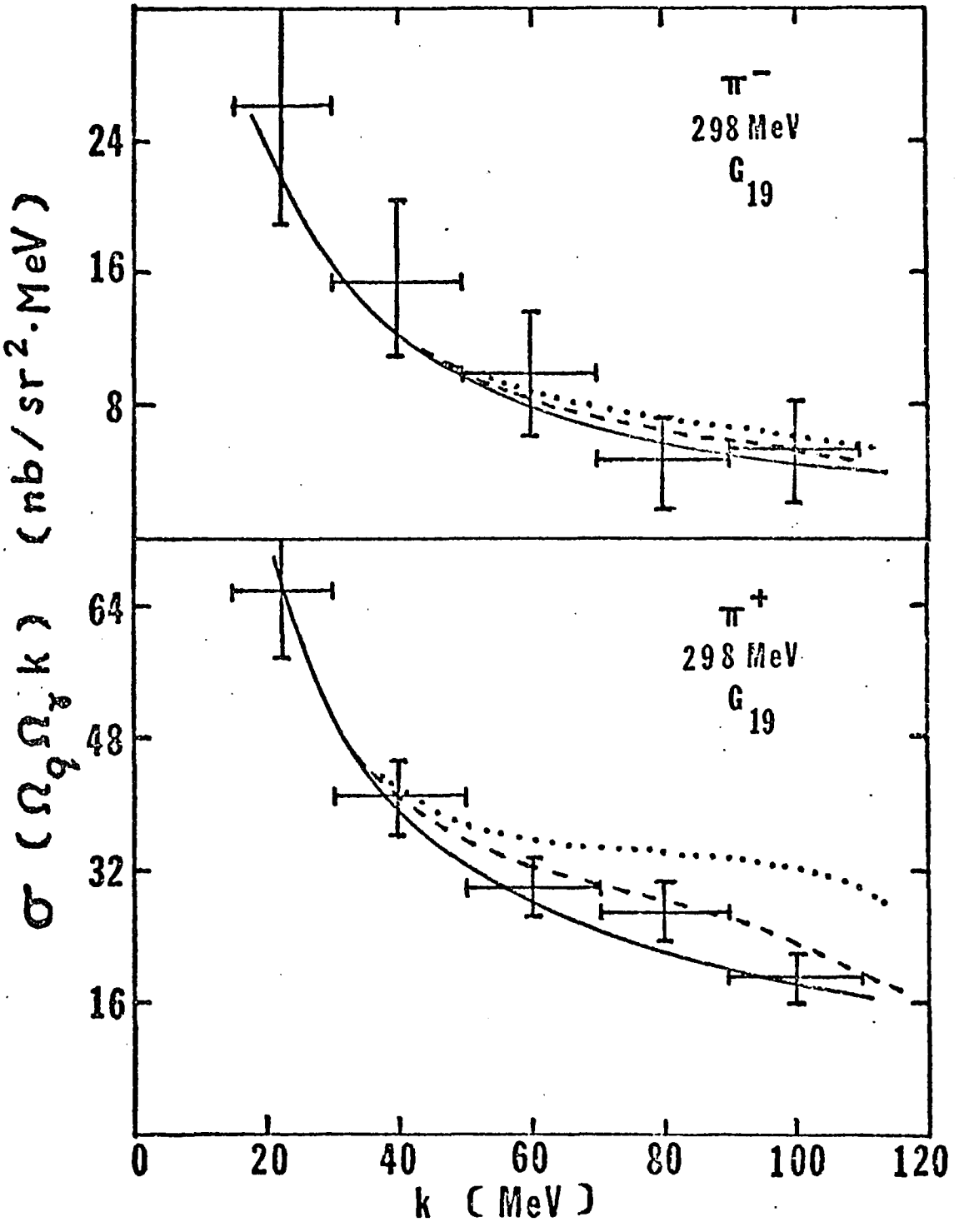

Fig. IV.13 Same as Fig. IV.9 but for counter G19.

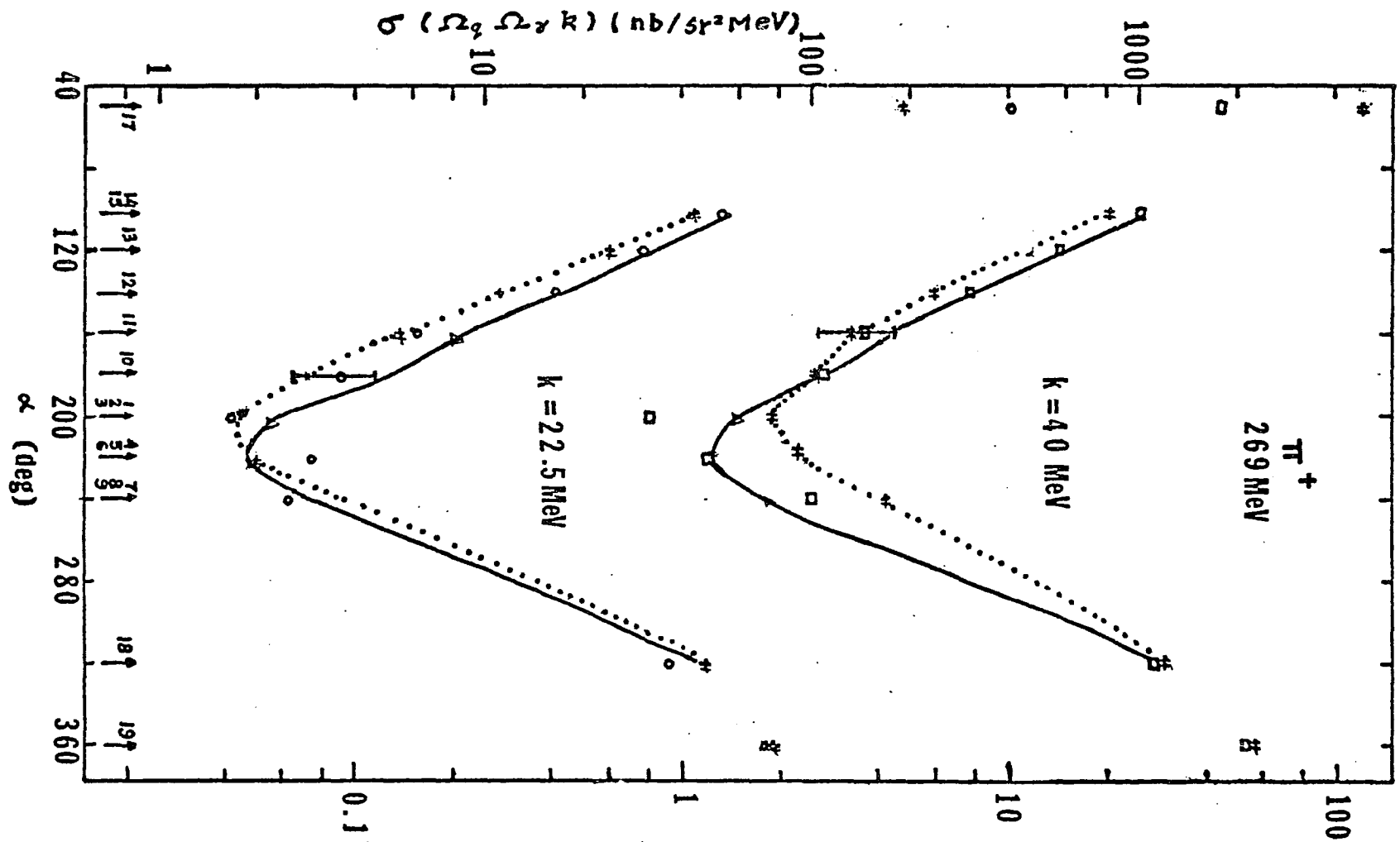

Fig. IV.14 The angular distribution of $\pi^+ p\gamma$ cross section as a function of α (the horizontal angle measured clockwise from the beam line) for the photon energy of 40 MeV. and 25 MeV. The dotted curve and "+" (solid curve and "△") are our Feshbach-Yennie (soft-photon) predictions. The experimental data (o,□) are from Ref. 19.

the large vertical acceptance of the spectrometer. We have carried out some calculations at 298-MeV using 52° rather than 50.5° and found that the effect of this change on our results is generally small (less than 5%) except for G17 (about 17% for $\pi^- p \gamma$). Since G17 has the worst statistical accuracy, the effect on the over-all agreement between the UCLA data and the calculations based on 50.5° is therefore small.

In conclusion, we have extended the soft-photon approximation of LN to the noncoplanar case. Generally speaking, our calculated cross sections for the $\pi^{\pm} p \gamma$ process are in good agreement with the UCLA data. This agreement shows that the soft-photon approximation works well for the $\pi^{\pm} p \gamma$ processes and indicates that the O(k) terms in the expansion of the cross section contribute very little to the cross section in most of the kinematic regions studied. On the other hand, the Feshbach-Yennie approximation predicts a bump in the bremsstrahlung spectrum. This bump is small in most cases and thus leaves the result of our calculation in good agreement with UCLA data. However, the bumps predicted for some counters are too high and thus indicate that other contributions, such as the higher order terms, resonance effects, and off-shell effects might be important in achieving certain cancellations in the cross section.

CHAPTER V STUDY OF NUCLEON-NUCLEON BREMSSTRAHLUNG

A. BACKGROUND

Most of the nucleon-nucleon bremsstrahlung calculations are model-dependent ppγ calculations. Sobel and Cromer (35) introduced "quasiphase parameters", which can be calculated from various phenomenological potentials, for their potential model ppγ calculations and they found that the difference between the cross sections calculated from the Yale and Hamada-Johnston potentials is small. Brown (36) reached the same conclusion for the Bryan-Scott and Hamada-Johnston potentials. Dreschsel and Maximon (37) also found small differences between the Reid (soft core) and Hamada-Johnston potentials. McGuire (38), Liou and Sobel (39) found that the relativistic correction was small in the center of mass frame. Heller and Rich (41) showed that the Coulomb effect was small except for an incident energy near 150-MeV at angles less than 10°.

Although the small difference between ppγ cross sections calculated from two different potentials may be discouraging, it is still interesting to investigate the off-shell behavior of the nucleon-nucleon interaction. The soft-photon theorem can be used to build up a good foundation for the extraction of off-shell effects from bremsstrahlung processes. Nyman (12) formulated the soft-photon

theorem in a covariant form for the ppγ process and found agreement between his calculations and experimental data at 158-MeV. The contributions of individual terms in the bremsstrahlung amplitude have been investigated by Fearing (43) who found a large difference between the calculation in the soft-photon approximation and the calculation using the Hamada-Johnston potentials at 200-MeV for $\theta_1 = \theta_2 = 12^\circ$ and $\theta_\gamma = 0^\circ$ and 180°. Recently, high energy data at 730-MeV have been reported and compared with two model-independent calculations by Nefkens et al. (44,45). In the latest publication (45), it is concluded that there exists large discrepancy at high photon energies, apart from a conflict at low photon energy between the experimental data and their calculations for one counter. To make a further study for these processes, we have applied the soft-photon approximation of LN and the Feshbach-Yennie approximation to the fermion-fermion case and these calculations will be discussed in sections B and C, respectively. We have obtained, in general, good agreement between the experimental data and our predicted cross sections for the ppγ process. But the discrepancy at large k for some kinematical regions still exists, indicating that the contribution from the higher order terms of the soft-photon expansion or the isobar effects (63-65) may be important at 730-MeV. Further dicussions together with numerical results are presented in section D.

B. THE SOFT-PHOTON APPROXIMATION OF LN FOR THE FERMION-FERMION CASE

The elatic scattering amplitude plays an important role in the construction of the bremsstrahlung amplitude. Before deriving the bremsstrahlung amplitude, let us first write the elastic scattering amplitude in a form suitable for our application. The amplitude for elastic nucleon-nucleon scattering has been well established (40). Following Nyman (12) and Goldberger et al. (46), we choose the Feynman amplitude used in GGMW because of its easy extension to the bremsstrahlung situation. With the conventions (47) $\bar{u}u = 1$ and $\hbar = c = 1$, we rewrite the Feynman amplitude $\mathcal{M}(s,t)$ in the following form

$$\mathcal{M}(s,t) = \sum_{\alpha=1}^{5} \mathcal{F}_\alpha^e(s,t)\, G_\alpha \ , \qquad \text{(V.1)}$$

where the two Lorentz scalars, s and t, are given in chapter II and

$$G_\alpha = \bar{u}_{q_f} g_\alpha u_{q_i}\ \bar{u}_{p_f} g^\alpha u_{p_i} \ ,$$

$$(g_1, g_2, g_3, g_4, g_5) = (1, \sigma_{\mu\nu}/\sqrt{2}, i\gamma_5\gamma_\mu, \gamma_\mu, \gamma_5), \qquad \text{(V.2a)}$$

$$\begin{pmatrix} \mathcal{F}_1^e \\ \mathcal{F}_2^e \\ \mathcal{F}_3^e \\ \mathcal{F}_4^e \\ \mathcal{F}_5^e \end{pmatrix} = \frac{1}{4} \begin{bmatrix} 3 & 6 & -4 & 4 & -1 \\ -1 & 2 & 0 & 0 & -1 \\ -1 & 0 & 6 & 2 & 1 \\ -1 & 0 & -2 & 2 & 1 \\ -1 & 6 & 4 & -4 & 3 \end{bmatrix} \begin{pmatrix} F_1 \\ F_2 \\ F_3 \\ F_4 \\ F_5 \end{pmatrix} . \qquad \text{(V.2b)}$$

The five invariant functions , $\{F_\alpha\}$, $\alpha = 1, 2, 3, 4, 5$, can be put into linear combinations of helicity amplitudes, $\{\phi_\alpha\}$, $\alpha = 1, 2, 3, 4, 5$,which are explicit functions of phase shifts. In Appendix A, We have derived F_α for proton-proton scattering from GGMW. The expressions obtained have a different appearance from those derived by Nyman and are simpler for numerical calculation, especially in the calculation of the Coulomb contribution which is treated exactly. Moreover, we have taken into account all of the inelasticity parameters so that our result can be used for processes above the pion-production threshold. The antisymmetrization of the scattering amplitude has also been considered in App. A. For the scattering of an unpolarized proton beam from an unpolarized proton target, the differential cross section in the center of mass system can be written as

$$\sigma(\Omega_{cm}) = \frac{1}{64}\frac{1}{\pi^2}\frac{m^4}{E^2} \qquad \text{(V.3a)}$$

$$= \sum_{\alpha=1}^{5}\sum_{\beta=1}^{5} Tr(\Lambda_{p_i}\bar{g}_\alpha \Lambda_{p_f} g_\beta)\, Tr(\Lambda_{q_i}\bar{g}^\alpha \Lambda_{q_f} g^\beta)$$

where $\bar{g}_\alpha = \gamma^\circ g_\alpha^+ \gamma^\circ$, and Λ_p are the energy projection operators,

$$\Lambda_p = \frac{\not{p}+M}{2M} \text{ , with } p = p_i,\ p_f,\ q_i, \text{ and } q_f . \qquad \text{(V.3b)}$$

Let us now construct the bremsstrahlung amplitude in the soft-photon approximation of LN for the nucleon-nucleon bremsstrahlung process. As usual, we write the bremsstrahlung amplitude, $\mathcal{M}$, as the sum of the external amplitude, M_μ^E, and the internal amplitude, M_μ^I,

$$\mathcal{M} = e \sum_\mu \epsilon^\mu M_\mu , \tag{V.4}$$

where

$$M_\mu = M_\mu^E + M_\mu^I .$$

Unlike the elastic scattering amplitude in which only two Lorentz invariants are needed, three Lorentz invariants are required for the bremsstrahlung amplitude since one of the two interacting nucleons is off its mass shell. We denote these three scalars by s_j, t_j, and Δ_j, as defined in chapter II, for the invariant functions, $\mathcal{J}_\alpha^j$, j = a,b ,c ,d. Looking at Fig. II.1, we notice that each of these diagrams, from a through d, contributes to the external amplitude. There, the complete expression for the external amplitude can be obtained from these diagrams. We have

$$M_\mu^E = \sum_{j=a,b,c,d} M_{j\mu}(s_j, t_j, \Delta_j),$$

$$M_j^\mu = \sum_{\alpha=1}^{5} \mathcal{F}_\alpha^j(s_j, t_j, \Delta_j)\, G_\alpha^{j\mu}, \tag{V.5}$$

where

$$G_\alpha^{a\mu} = \bar{u}_{q_f} \Gamma_\partial^\mu \frac{1}{\not{q}_f + \not{k} - m} g_\alpha u_{q_i}\ \bar{u}_{p_f} g^\alpha u_{p_i} ,$$

$$G_\alpha^{b\mu} = \bar{u}_{q_f} g_\alpha \frac{1}{\not{q}_i - \not{k} - m} \Gamma_3^\mu u_{q_i} \bar{u}_{p_f} g^\alpha u_{p_i} ,$$

$$G_\alpha^{c\mu} = \bar{u}_{q_f} g_\alpha u_{q_i} \bar{u}_{p_f} \Gamma_2^\mu \frac{1}{\not{p}_f + \not{k} - M} g^\alpha u_{p_i} ,$$

$$G_\alpha^{d\mu} = \bar{u}_{q_f} g_\alpha u_{q_i} \bar{u}_{p_f} g^\alpha \frac{1}{\not{p}_i + \not{k} - M} \Gamma_2^\mu u_{p_i} ,$$

and Γ_3^μ (Γ_2^μ) is the electromagnetic vertex function for nucleon.

Up to this point, everything is exact. It is worth while to discuss the origin of the off-shell contributions. Of course, the invariant functions $\{\mathcal{F}_\alpha^j\}$ and the electromagnetic vertex function may contribute. That is, the off-shell contributions may come from the electromagnetic vertices and the T_j (j=a$\sim$e) in Fig. II.1. The off-mass-shell effect of the electromagnetic vertex functions has been studied by Nyman (28) and Fischer and Minkowski (29). It was estimated that the anomalous moment would change the proton-proton bremsstrahlung cross section significantly in the "hard" photon region (28). A numerical calculation of the off-shell effects in the vertex has been initiated by Nyman. However, since the problem can not be treated without some ambiguity, these effects will be neglected in our work. The off-shell effcts of the invariant functions may be studied by soft-photon approximations. In our approximation, we take into account the off-shell contribution from both the explicit k-dependence and the implicit k-dependence of the bremsstrahlung amplitude.

Neglecting the off-shell effects from the electromagnetic vertices, we use the on-shell expression of the vertex functions

$$\Gamma_{\mathcal{Z}}^{\mu} = \mathcal{Z}\gamma^{\mu} - \frac{\lambda_{\mathcal{Z}}}{2m} i\sigma^{\mu\nu}k_{\nu}\,, \qquad \text{(V.6)}$$

$$\Gamma_{Z}^{\mu} = \Gamma_{\mathcal{Z}}^{\mu}\,(\text{with}\quad \mathcal{Z}\to Z\,,\ m\to M)\,,$$

where $\mathcal{Z}$ (Z) represents the charge of projectile (target). With the help of Dirac equation and γ-algebra such as $\{\gamma_{\mu}, \not{p}\} = 2p_{\mu}$, we can simplify the products of the propagator, the vertex function and the spinor as

$$\frac{1}{\not{p}_i - \not{k} - M}\Gamma_{Z}^{\mu} u_{p_i} = \left[-\frac{Z p_i^{\mu}}{p_i\cdot k} - \frac{Z\gamma^{\mu}\not{k}}{2p_i\cdot k} + \frac{\lambda_Z\gamma^{\mu}}{2M} - \frac{\lambda_Z p_i^{\mu}\not{k}}{2Mp_i\cdot k} - \frac{\lambda_Z\gamma^{\mu}\not{k}}{2p_i\cdot k}\right]u_{p_i},$$

$$\bar{u}_{p_f}\Gamma_{Z}^{\mu}\frac{1}{\not{p}_f + \not{k} - M} = \bar{u}_{p_f}\left[\frac{Z p_f^{\mu}}{p_f\cdot k} + \frac{Z\gamma^{\mu}\not{k}}{2p_f\cdot k} + \frac{\lambda_Z\gamma^{\mu}}{2M} - \frac{\lambda_Z p_f^{\mu}\not{k}}{2Mp_f\cdot k} + \frac{\lambda_Z\gamma^{\mu}\not{k}}{2p_f\cdot k}\right],$$

$$\bar{u}_{q_f}\Gamma_{\mathcal{Z}}^{\mu}\frac{1}{\not{q}_f + \not{k} - m} = \bar{u}_{q_f}\left[\frac{\mathcal{Z} q_f^{\mu}}{q_f\cdot k} + \frac{\mathcal{Z}\gamma^{\mu}\not{k}}{2q_f\cdot k} + \frac{\lambda_{\mathcal{Z}}\gamma^{\mu}}{2m} - \frac{\lambda_{\mathcal{Z}} q_f^{\mu}\not{k}}{2mq_f\cdot k} + \frac{\lambda_{\mathcal{Z}}\gamma^{\mu}\not{k}}{2q_f\cdot k}\right],$$

$$\frac{1}{\not{q}_i - \not{k} - m}\Gamma_{\mathcal{Z}}^{\mu} u_{q_i} = \left[-\frac{\mathcal{Z} q_i^{\mu}}{q_i\cdot k} - \frac{\mathcal{Z}\gamma^{\mu}\not{k}}{2q_i\cdot k} + \frac{\lambda_{\mathcal{Z}}\gamma^{\mu}}{2m} - \frac{\lambda_{\mathcal{Z}} q_i^{\mu}\not{k}}{2mq_i\cdot k} - \frac{\lambda_{\mathcal{Z}}\gamma^{\mu}\not{k}}{2q_i\cdot k}\right]u_{q_i}\,. \qquad \text{(V.7)}$$

The first two terms in each expression result from charge radiation and the rest from the magnetic moment contribution. To make a complete expansion, we apply the method of LN to expand the external amplitude about the on-shell point, k = 0. By employing the expressions in Eq. II.6, we obtain the following expansions

$$\frac{1}{q_f\cdot k} \approx \frac{1}{\bar{q}_f\cdot k} - \frac{k\cdot R}{(\bar{q}_f\cdot k)^2} + \frac{(k\cdot R)^2}{(\bar{q}_f\cdot k)^3}\,, \qquad \text{(V.8a)}$$

$$\frac{1}{p_f\cdot k} \approx \frac{1}{\bar{p}_f\cdot k} + \frac{k\cdot R}{(\bar{p}_f\cdot k)^2} + \frac{(k\cdot R)^2}{(\bar{p}_f\cdot k)^3} \quad . \qquad \text{(V.8b)}$$

Since the invariant functions $\mathcal{F}_\alpha^j(s_j, t_j, \Delta_j)$ are off-shell dependent, we use a Taylor expansion about k = 0 and obtain

$$\begin{aligned}
\mathcal{F}_\alpha^a(s_a,t_a,\Delta_a) &\approx \mathcal{F}_\alpha^e(s,t) - \left[2(\bar{p}_f - p_i)\cdot(R+k) - (R+k)^2\right]\frac{\partial \mathcal{F}_\alpha^a}{\partial t} \\
&\quad + 2(\bar{q}_f + R)\cdot k\,\frac{\partial \mathcal{F}_\alpha^a}{\partial \Delta_a} \quad , \\
\mathcal{F}_\alpha^b(s_b,t_b,\Delta_b) &\approx \mathcal{F}_\alpha^e(s,t) - 2(\bar{q}_f + \bar{p}_f)\cdot k\,\frac{\partial \mathcal{F}_\alpha^b}{\partial s} - 2q_i\cdot k\,\frac{\partial \mathcal{F}_\alpha^b}{\partial \Delta_b} \\
&\quad - \left[2(\bar{p}_f - p_i)\cdot(R+k) - (R+k)^2\right]\frac{\partial \mathcal{F}_\alpha}{\partial t} \quad , \\
\mathcal{F}_\alpha^c(s_c,t_c,\Delta_c) &\approx \mathcal{F}_\alpha^e(s,t) + \left[2(\bar{q}_f - q_i)\cdot R + R^2\right]\frac{\partial \mathcal{F}_\alpha^c}{\partial t} \\
&\quad + 2(\bar{p}_f - R)\cdot k\,\frac{\partial \mathcal{F}_\alpha^c}{\partial \Delta_c} \quad , \\
\mathcal{F}_\alpha^d(s_d,t_d,\Delta_d) &\approx \mathcal{F}_\alpha^e(s,t) - 2(\bar{q}_f + \bar{p}_f)\cdot k\,\frac{\partial \mathcal{F}_\alpha^d}{\partial s} - 2p_i\cdot k\,\frac{\partial \mathcal{F}_\alpha^d}{\partial \Delta_d} \\
&\quad + \left[2(\bar{q}_f - q_i)\cdot R + R^2\right]\frac{\partial \mathcal{F}_\alpha}{\partial t} \quad ,
\end{aligned} \qquad \text{(V.9)}$$

where all derivative terms are evaluated at zero photon energy. Note that Eqs. V.8a and V.8b are good approximations if $|k\cdot R| \ll |\bar{q}_f\cdot k|$ and $|k\cdot R| \ll |\bar{p}_f\cdot k|$. This might not be the case in some kinematical region, for instance, in the "hard" photon region and/or in the kinematical situation where one outgoing nucleon moves much faster than the other nucleon. Furthermore, the applicability of these approximations can be tested in the R-type cross sections since k is

an independent variable and we are allowed to make the expansion of bremsstrahlung amplitude about k = 0. In the H-type cross sections, however, k may not be an independent variable and the energy-momentum conservation law has to be violated if the bremsstrahlung amplitude is to be expanded about k= 0 (24). In fact, an ambiguity exists for an H-type cross section $\sigma(\Omega_1, \Omega_2, \gamma_\gamma)$ when one wants to determine the corresponding two-body elastic kinematics from given bremsstrahlung kinematics. To understand this ambiguity, we recall that the angles for the scattered nucleon and the recoil nucleon are fixed for the H-type cross section. Now, since the elastic two-body kinematics can be completely determined if the direction of either the scattered nucleon or the recoil nucleon is specified, one can choose one of the two sets of the elastic kinematics from a given three-body bremsstrahlung kinematics. These two sets of elastic kinematics are represented by $\Omega_1^e = \Omega_1$ and $\Omega_1^e = \Omega_2$, where Ω_1^e is the solid angle of the detected nucleon in the corresponding elastic process and Ω_1 (Ω_2) is the solid angle of the scattered (recoil) nucleon in the bremsstrahlung process. To avoid this ambiguity in our soft-photon approximation, we choose the R-type cross sections.

Combining Eqs. V.4 through V.9, together with Eq. II.6, we obtain the external amplitude, up to order k,

$$M_\mu^E = M_\mu^E(\tfrac{1}{k}) + M_\mu^E(k^0) + M_\mu^E(k), \qquad \text{(V.10)}$$

where $M_\mu^E(1/k)$, $M_\mu^E(k^0)$,and $M_\mu^E(k)$ are of order 1/k, order k^0, and order k, respectively. These expressions are given in App. C.

Following Low's prescription, we now apply the gauge invariance condition, $k^\mu M_\mu^I = -k^\mu M_\mu^E$, to obtain the internal amplitude. As a result, the off-shell derivatives in the external amplitude cancel precisely those in the internal amplitude (known as the off-shell cancellation). However, this does not hold for terms of O(k). Attempts have been made by Fischer et al. (29) and Haddock et al. (30) to include higher order terms. They introduced an approximation, the "Hard-photon theorem" as called by the latter authors, which has the following ambiguities (31): (i) This "theorem" is not unique due to the method of finite difference used. (ii) Some internal contribution of O(k) may be lost in the calculation because $k^\mu V_\mu(k) = 0$ does not imply $V_\mu(k) = 0$. Since we do not use the finite difference method here, the first ambiguity does not appear in our calculation. There seems no way to avoid the second ambiguity. However, it is interesting to see the contribution from the terms of order k which survive after imposing the gauage invariance condition. Our analysis shows that the amplitue $M_\mu^E(k) + M_\mu^E(k)$ is gauge invariant but still contains off-shell derivatives.

Finally, the total bremsstrahlung amplitude is

$$M^\mu = \sum_{\alpha=1}^{5} \left[\bar{u}_{q_f} X_\alpha^\mu u_{q_i} \; \bar{u}_{p_f} g^\alpha u_{p_i} + \bar{u}_{q_f} g_\alpha u_{q_i} \; \bar{u}_{p_f} Y^{\alpha\mu} u_{p_i} \right],$$

where

$$X_\alpha^\mu \equiv X_\alpha^\mu(\tfrac{1}{k}) + X_\alpha^\mu(k^\circ) + X_\alpha^\mu(k), \qquad \text{(V.11)}$$

$$Y_\alpha^\mu \equiv Y_\alpha^\mu(\tfrac{1}{k}) + Y_\alpha^\mu(k^\circ) + Y_\alpha^\mu(k),$$

$$X_\alpha^\mu(\tfrac{1}{k}) = \mathcal{F}_\alpha^e g_\alpha \left(\frac{\not{z}\, \bar{q}_f^\mu}{\bar{q}_f \cdot k} - \frac{\not{z}\, q_i^\mu}{q_i \cdot k} \right),$$

$$X_\alpha^\mu(k^\circ) = \mathcal{F}_\alpha^e \left[A_o^\mu g_\alpha + g_\alpha B_o^\mu \right] + \frac{\partial \mathcal{F}_\alpha}{\partial s} \left[2(\bar{q}_f + \bar{p}_f)\cdot k \frac{\not{z}\, q_i^\mu}{q_i \cdot k} - 2(\bar{q}_f + \bar{p}_f)^\mu \right] g_\alpha + \frac{\partial \mathcal{F}_\alpha}{\partial t} \left[2(\bar{p}_f - p_i)\cdot(R+k) \times \left(\frac{\not{z}\, q_i^\mu}{q_i \cdot k} - \frac{\not{z}\, \bar{q}_f^\mu}{\bar{q}_f \cdot k} \right) \right] g_\alpha ,$$

$$X_\alpha^\mu(k) = \mathcal{F}_\alpha^e A_1^\mu g_\alpha - \frac{\partial \mathcal{F}_\alpha}{\partial s} 2(\bar{q}_f + \bar{p}_f)\cdot k \; g_\alpha B_o^\mu + \frac{\partial \mathcal{F}_\alpha}{\partial t} \left[(R+k)^2 \left(\frac{\not{z}\, \bar{q}_f^\mu}{\bar{q}_f \cdot k} - \frac{\not{z}\, q_i^\mu}{q_i \cdot k} \right) g_\alpha - \left(A_o^\mu g_\alpha + g_\alpha B_o^\mu \right) 2(\bar{p}_f - p_i)\cdot(R+k) \right],$$

$$Y_\alpha^\mu = X_\alpha^\mu \left(\text{with } R \to -(R+k),\; \not{z} \to \not{Z},\; m \to M,\; q \to p,\; A \to C,\; B \to D. \right),$$

and A's, B's, C's and D's are given in App. C.

A comment on this amplitude is in order. These results contain not only the standard first two terms of the expan-

sion but also the term of order k. The contribution from this additional term of order k will be estimated in this work.

Having derived the bremsstrahlung amplitude, we next square the absolute bremsstrahlung amplitude and sum over final (initial) spins and sum over photon polarizations for the scattering of an unpolarized proton beam from an unpolarized proton target. The result is

$$
\begin{aligned}
Q &\equiv \sum_{pol}\sum_{spin}|\mathcal{M}|^2 \\
&= -\sum_{\alpha}\sum_{\beta}\sum_{\mu}\Big\{ \mathrm{Tr}\Big[\Lambda_{p_i}\bar{g}^{\alpha}\Lambda_{p_f}g^{\beta}\Big]\,\mathrm{Tr}\Big[\Lambda_{q_i}\bar{X}^{\mu}_{\alpha}\Lambda_{q_f}X_{\beta\mu}\Big] \\
&\quad + \mathrm{Tr}\Big[\Lambda_{p_i}\bar{g}_{\alpha}\Lambda_{p_f}Y^{\beta}_{\mu}\Big]\,\mathrm{Tr}\Big[\Lambda_{q_i}\bar{X}^{\mu}_{\alpha}\Lambda_{q_f}g_{\beta}\Big] \\
&\quad + \mathrm{Tr}\Big[\Lambda_{p_i}\bar{Y}^{\alpha\mu}\Lambda_{p_f}g^{\beta}\Big]\,\mathrm{Tr}\Big[\Lambda_{q_i}\bar{g}_{\alpha}\Lambda_{q_f}X_{\beta\mu}\Big] \\
&\quad + \mathrm{Tr}\Big[\Lambda_{p_i}\bar{Y}^{\alpha\mu}\Lambda_{p_f}Y^{\beta}_{\mu}\Big]\,\mathrm{Tr}\Big[\Lambda_{q_i}\bar{g}_{\alpha}\Lambda_{q_f}g_{\beta}\Big], \qquad \text{(V.12a)}
\end{aligned}
$$

where the energy projection operators, Λ_{p_f} and Λ_{q_f}, are given by

$$\Lambda_{p_f}\approx\Lambda_{p_f}(k^\circ)+\Lambda_{p_f}(k), \qquad \Lambda_{q_f}\approx\Lambda_{q_f}(k^\circ)+\Lambda_{q_f}(k),$$

with

$$
\begin{aligned}
&\Lambda_{p_f}(k^\circ)=\frac{\bar{p}_f+M}{2M}, \qquad \Lambda_{p_f}(k)=-\frac{\bar{K}+\bar{k}}{2M}, \\
&\Lambda_{q_f}(k^\circ)=\frac{\bar{q}_f+m}{2m}, \qquad \Lambda_{q_f}(k)=\frac{\bar{k}}{2m}, \qquad \text{(V.12b)}
\end{aligned}
$$

and

$$\bar{X}^{\mu}_{\alpha}=\gamma^\circ X^{\mu\dagger}_{\alpha}\gamma^\circ, \qquad \bar{Y}^{\mu}_{\alpha}=\gamma^\circ Y^{\mu\dagger}_{\alpha}\gamma^\circ.$$

It is not only lengthy but also difficult to write down an explicit expression for each coefficient of the expansion of the cross section in powers of k and give a meaningful interpretation for it. In order to expand the bremsstrahlung amplitude in powers of k and to study the contribution from each term of the expansion, we have to exapnd X and Λ in powers of k. The contribution from each term of the expansion of the amplitude can be made numerically by using a fast computer. For convenience, we denote the term of order k^{-2} in Q by Q_{-2}, the term of order k^{-1} by Q_{-1}, and the term of order k^{0} by Q_{0}. Then we have

$$Q = \sum_{pol} \sum_{spin} |\mathcal{M}|^2 \approx Q_{-2} + Q_{-1} + Q_0 \,. \qquad \text{(V.13)}$$

Using these expressions, we can calculate the diffrerential cross sections for the scattering of an unpolarized beam from an unpolarized target. The R-type cross section is

$$\sigma(\Omega_q, \Omega_\gamma, k) = \frac{e^2 m^2 M^2 k^2 F}{2\left[(q_i \cdot p_i)^2 - (mM)^2\right]^{1/2}} \left(\frac{1}{2\pi}\right)^5 \frac{1}{4}\, Q \qquad \text{(V.14)}$$

where the phase space factor F has the same form as in the $\pi^{\pm} p\gamma$ case. We will use first the full phase space factor and then the expanded form $F = F^{(0)} + F^{(1)} + F^{(2)}$ in our numerical calculation in order to see the effect of the expansion of F in powers of photon energy k. Following LN in which $F^{(0)}$ and $F^{(1)}$ are given, we have expanded F to one order higher in k as given in App. B. Therefore, two calculations may be performed, one of which is

$$\sigma(\Omega_q, \Omega_\gamma, k) = \frac{\sigma_{-1}}{k} + \sigma_0 + \sigma_1 k \ , \qquad (V.15)$$

where

$$\sigma_{-1} = k^2 C F^{(0)} Q_{-2} ,$$

$$\sigma_0 = KC(F^{(1)} Q_{-2} + F^{(0)} Q_{-1}) ,$$

$$\sigma_1 = C(F^{(0)} Q_0 + F^{(1)} Q_{-1} + F^{(2)} Q_{-2}) ,$$

with $C = - e^2 m^2 M^2 / (8((q_i \cdot p_i)^2 - m^2 M^2)(2\pi)^5)$, and $e^2 = 4\pi/137$.

The other calculation gives

$$\sigma'(\Omega_q, \Omega_\gamma, k) = \frac{\sigma'_{-1}}{k} + \sigma'_0 + \sigma'_1 k , \qquad (V.16)$$

where

$$\sigma'_{-1} = k^2 C F Q_{-2} ,$$

$$\sigma'_0 = kCFQ_{-1} ,$$

$$\sigma'_1 = CFQ_0 .$$

It is important to note that the phase space factor we used is valid only in the laboratory system. Therefore $\sigma(\Omega_\gamma, \Omega_q, k)$ and $\sigma'(\Omega_\gamma, \Omega_q, k)$ given above are laboratory cross sections if the F in Eq. B.1 is used.

Strictly speaking, the soft-photon approximation can not be made for the H-type cross section without violating the energy momentum conservation law as mentioned before. Therefore, the R-type cross section is to be prefered for our study. However, since most of the early experimental data have been reported in the form of H-type cross sec-

tions, we have to make the following approximations in order to compare our result with these data. If we assume that the violation of the energy momentum conservation due to the use of the expanded bremsstrahlung amplitude M_μ of Eq. V.11 is not serious, we may choose the direction of the outgoing nucleon with higher velocity as an input for the calculation of elastic kinematics which are then used to calculate the expanded bremsstrahlung amplitude M_μ. The H-type cross section has the form

$$\sigma(\Omega_1, \Omega_2, \psi_\gamma) = \frac{e^2 m^2 M^2 F'}{2\left[(p_i \cdot p_i)^2 - (mM)^2\right]^{1/2}} \left(\frac{1}{2\pi}\right)^5 \frac{1}{4} Q$$

$$= \frac{\sigma_{-1}^H}{k} + \sigma_0^H + \sigma_1^H k , \qquad (V.17)$$

where

$$\sigma_{-1}^H = kCF'Q_{-2} ,$$

$$\sigma_0^H = CF'Q_{-1} ,$$

$$\sigma_1^H = CF'Q_0/k .$$

The phase space factor F and the definition of ψ_γ are given in App. C. The choice made in this calculation is not unique. One may equally well choose the direction of the other outgoing nucleon as an input for the calculation. Usually, the photon energy is not small for most of the measured H-type cross sections. The choice will then depend upon the direction of the emitted photon as well as the incident proton energy. This ambiguity appears only in making the soft-photon expansion for the H-type cross section.

Further discussion about this can be found in section D.

C. APPLICATION OF THE FESHBACH-YENNIE APPROXIMATION TO NUCLEON-NUCLEON BREMSSTRAHLUNG

Feshbach-Yennie theory has been extended from the spin-0-spin-$\frac{1}{2}$ case to the spin-$\frac{1}{2}$-spin-$\frac{1}{2}$ case by Partovi (33) in a non-relativistic model and by Dahlblom and Green (67) in a simplified non-relativistic fashion. Here we try to make a more exact calculation by taking into account the correction term in a relativistic fashion. It should be noted that this approximation, being more or less arbitrary in the evaluation of the invariant functions, is not recommended for the extraction of off-shell effects.

A distinguishing chacteristic of the Feshbach-Yennie approximation is the evaluation of half-off-shell T-matrices at two different energies which make this approximation different from the soft-photon approximation. To derive the Feshbach-Yennie approximation for the spin-$\frac{1}{2}$-spin-$\frac{1}{2}$ case, we follow the procedures used in chapter III and employ certain expressions derived in this chapter. The products of the propagator and electromagnetic vertex function can be written as

$$G_\alpha^{a\mu} = \bar{u}_{q_f}\left[\frac{\mathfrak{z}\, q_f^\mu}{q_f\cdot k} - \frac{\lambda_{\mathfrak{z}}\gamma^\mu}{2m} - \frac{\lambda_{\mathfrak{z}}\, q_f^\mu \not{k}}{2m\, q_f\cdot k} - (\mathfrak{z}+\lambda_{\mathfrak{z}})\frac{\gamma^\mu \not{k}}{2\, q_f\cdot k}\right] g_\alpha\, u_{q_i}$$
$$\times \bar{u}_{p_f}\, g^\alpha\, u_{p_i}\ ,$$

$$G_\alpha^{b\mu} = \bar{u}_{q_f} g_\alpha \left[-\frac{\mathcal{Z} q_i^\mu}{q_i\cdot k} + \frac{\lambda_{\mathcal{Z}} \gamma^\mu}{2m} - \frac{\lambda_{\mathcal{Z}} q_i^\mu \not{k}}{2m\, q_i\cdot k} - \frac{(\mathcal{Z}+\lambda_{\mathcal{Z}})\gamma^\mu \not{k}}{2\, q_i\cdot k} \right] u_{q_i} \bar{u}_{p_f} g^\alpha u_{p_i},$$

$$G_\alpha^{c\mu} = \bar{u}_{q_f} g_\alpha u_{q_i} \bar{u}_{p_f} \left[\frac{\mathcal{Z} p_f^\mu}{p_f\cdot k} + \frac{\lambda_{\mathcal{Z}} \gamma^\mu}{2M} - \frac{\lambda_{\mathcal{Z}} p_f^\mu \not{k}}{2M\, p_f\cdot k} + \frac{(\mathcal{Z}+\lambda_{\mathcal{Z}})\gamma^\mu \not{k}}{2\, p_f\cdot k} \right] g^\alpha u_{p_i},$$

$$G_\alpha^{d\mu} = \bar{u}_{q_f} g_\alpha u_{q_i} \bar{u}_{p_f} g^\alpha \left[-\frac{\mathcal{Z} p_i^\mu}{p_i\cdot k} + \frac{\lambda_{\mathcal{Z}} \gamma^\mu}{2M} - \frac{\lambda_{\mathcal{Z}} p_i^\mu \not{k}}{2M\, p_i\cdot k} - \frac{(\mathcal{Z}+\lambda_{\mathcal{Z}})\gamma^\mu \not{k}}{2\, p_i\cdot k} \right] u_{p_i}.$$

(V.18)

No further expansion is needed for G_α^μ's. The important feature of the Feshbach-Yennie theory is incorporated through the use of Eq. III.5 and the following expansions of the invariant functions

$$\mathcal{F}_\alpha^a(s_a, t_a, \Delta_a) \approx \mathcal{F}_\alpha^e(s_i, t) - 2(\bar{p}_f - p_i)\cdot(R+k) \left[\frac{\partial \mathcal{F}_\alpha^a(s_i, t_a, \Delta_a)}{\partial t} \right]_{k=0} + 2\bar{q}_f \cdot k \left[\frac{\partial \mathcal{F}_\alpha^a(s_i, t_a, \Delta_a)}{\partial \Delta_a} \right]_{k=0},$$

$$\mathcal{F}_\alpha^b(s_b, t_b, \Delta_b) \approx \mathcal{F}_\alpha^e(s_f, t) - 2(\bar{p}_f - p_i)\cdot(R+k) \left[\frac{\partial \mathcal{F}_\alpha^b(s_f, t_b, \Delta_b)}{\partial t} \right]_{k=0} - 2 q_i \cdot k \left[\frac{\partial \mathcal{F}_\alpha^b(s_f, t_b, \Delta_b)}{\partial \Delta_b} \right]_{k=0},$$

$$\mathcal{F}_\alpha^c(s_c, t_c, \Delta_c) \approx \mathcal{F}_\alpha^e(s_i, t) + 2(\bar{q}_f - q_i)\cdot R \left[\frac{\partial \mathcal{F}_\alpha^c(s_i, t_c, \Delta_c)}{\partial t} \right]_{k=0} + 2\bar{p}_f \cdot k \left[\frac{\partial \mathcal{F}_\alpha^c(s_i, t_c, \Delta_c)}{\partial \Delta_c} \right]_{k=0},$$

$$\mathcal{F}_\alpha^d(s_d, t_d, \Delta_d) \approx \mathcal{F}_\alpha^e(s_f, t) + 2(\bar{q}_f - q_i)\cdot R \left[\frac{\partial \mathcal{F}_\alpha^d(s_f, t_d, \Delta_d)}{\partial t} \right]_{k=0} - 2 p_i \cdot k \left[\frac{\partial \mathcal{F}_\alpha^d(s_f, t_d, \Delta_d)}{\partial \Delta_d} \right]_{k=0}. \qquad (V.19)$$

The external bremsstrahlung amplitude is obtained from Eq. V.5 and the internal bremsstrahlung amplitude is then obtained through the use of gauge invariance condition. Summing over these two amplitudes, we have the total bremsstrahlung amplitude, up to order k^0,

$$M_\mu = \sum_{\alpha=1}^{5} \left[\bar{u}_{q_f} X_\alpha^\mu u_{q_i} \bar{u}_{p_f} g^\alpha u_{p_i} + \bar{u}_{q_f} g_\alpha u_{q_i} \bar{u}_{p_f} Y^{\alpha\mu} u_{p_i} \right] , \quad \text{(V.20a)}$$

where

$$X_\alpha^\mu \equiv X_\alpha^\mu(\tfrac{1}{k}) + X_\alpha^\mu(k^0) ,$$

$$Y_\alpha^\mu \equiv Y_\alpha^\mu(\tfrac{1}{k}) + Y_\alpha^\mu(k^0) ,$$

$$X_\alpha^\mu(\tfrac{1}{k}) = \left[\mathcal{F}_\alpha^e(s_i,t) \left(\frac{z q_f^\mu}{q_f\cdot k} - \frac{z(q_f+p_f)^\mu}{(q_f+p_f)\cdot k} \right) - \left(\frac{z q_i^\mu}{q_i\cdot k} - \frac{z(q_i+p_i)^\mu}{(q_i+p_i)\cdot k} \right) \times \mathcal{F}_\alpha^e(s_f,t) \right] g_\alpha ,$$

$$X_\alpha^\mu(k^0) = \left[\mathcal{F}_\alpha^e(s_i,t) A_0^\mu g_\alpha + g_\alpha B_0^\mu \mathcal{F}_\alpha^e(s_f,t) \right] - 2(\bar{p}_f - p_i)\cdot(R+k) \times \left[\frac{\partial \mathcal{F}_\alpha(s_i,t)}{\partial t} \frac{z q_f^\mu}{q_f\cdot k} - \frac{\partial \mathcal{F}_\alpha(s_f,t)}{\partial t} \frac{z q_i^\mu}{q_i\cdot k} \right] g_\alpha + 2z \left(\frac{\partial \mathcal{F}_\alpha(s_i,t)}{\partial t} - \frac{\partial \mathcal{F}_\alpha(s_f,t)}{\partial t} \right) g_\alpha \left[(\bar{p}_f - p_i)^\mu + (\bar{p}_f - p_i)\cdot N_R \bar{p}_f^\mu \right] .$$

$$Y_\alpha^\mu(\tfrac{1}{k}) = \left[\mathcal{F}_\alpha^e(s_i,t) \left(\frac{z p_f^\mu}{p_f\cdot k} - \frac{z(q_f+p_f)^\mu}{(q_f+p_f)\cdot k} \right) - \left(\frac{z p_i^\mu}{p_i\cdot k} - \frac{z(q_i+p_i)^\mu}{(q_i+p_i)\cdot k} \right) \times \mathcal{F}_\alpha^e(s_f,t) \right] g_\alpha ,$$

$$Y_\alpha^\mu(k^0) = \left[\mathcal{F}_\alpha^e(s_i,t) C_0^\mu g_\alpha + g_\alpha D_0^\mu \mathcal{F}_\alpha^e(s_f,t) \right] - 2(\bar{q}_f - q_i)\cdot R \times \left[\frac{\partial \mathcal{F}_\alpha(s_i,t)}{\partial t} \frac{z p_f^\mu}{p_f\cdot k} - \frac{\partial \mathcal{F}_\alpha(s_f,t)}{\partial t} \frac{z p_i^\mu}{p_i\cdot k} \right] g_\alpha - 2z(\bar{q}_f - q_i)\cdot N_R \left(\frac{\partial \mathcal{F}_\alpha(s_i,t)}{\partial t} - \frac{\partial \mathcal{F}_\alpha(s_f,t)}{\partial t} \right) .$$

$$A_0^\mu = \frac{\lambda_3 \gamma^\mu}{2m} - \frac{\lambda_3 q_f^\mu \not{k}}{2m q_f \cdot k} + \frac{(3+\lambda_3)\gamma^\mu \not{k}}{2 q_f \cdot k} ,$$

$$B_0^\mu = \frac{\lambda_3 \gamma^\mu}{2m} - \frac{\lambda_3 q_i^\mu \not{k}}{2m q_i \cdot k} - \frac{(3+\lambda_3)\gamma^\mu \not{k}}{2 q_i \cdot k} ,$$

$$C_0^\mu = \frac{\lambda_2 \gamma^\mu}{2M} - \frac{\lambda_2 P_f^\mu \not{k}}{2M P_f \cdot k} + \frac{(2+\lambda_2)\gamma^\mu \not{k}}{2 P_f \cdot k} ,$$

$$D_0^\mu = \frac{\lambda_2 \gamma^\mu}{2M} - \frac{\lambda_2 P_i^\mu \not{k}}{2M P_i \cdot k} - \frac{(2+\lambda_2)\gamma^\mu \not{k}}{2 P_i \cdot k} . \qquad \text{(V.20b)}$$

The bremsstrahlung cross section follows the same form as that in last section except that the energy projection operators Λ_{p_f} and Λ_{q_f} are not expanded in powers of k.

D. RESULTS AND DISCUSSION

We have employed Eqs. V.11 and V.12 to develop three computer codes for the calculations of ppγ cross sections. Two of them are for the R-type cross sections, one using the soft-photon approximation of LN and the other using the Feshbach-Yennie approximation. The third code is for H-type cross sections using the soft-photon approximation of LN. The computer code for the kinematics used in the third code is the same as that used in Ref. 40. In all these computations, the trace evaluation is done by using numerical representations for the γ-matrices and by grouping the terms of the same order in k in the bremsstrahlung amplitude. The numerical representation of spinors is not required in our computations since the energy projection operators have been used.

Due to the importance of the elastic scattering amplitude in our approximations, we have checked the elastic cross section for proton-proton scattering. For an incident proton energy below the threshold for pion-production, the phase shifts of Ref. 49 are used in our calculations. Above pion-production, we employ inelasticity parameters as mentioned in App. A and use the elastic phase shifts of Ref. 50. Including elastic phase shifts up to H-wave, we have obtained good agreement between the experimental data and our predicted cross sections for p-p scattering.

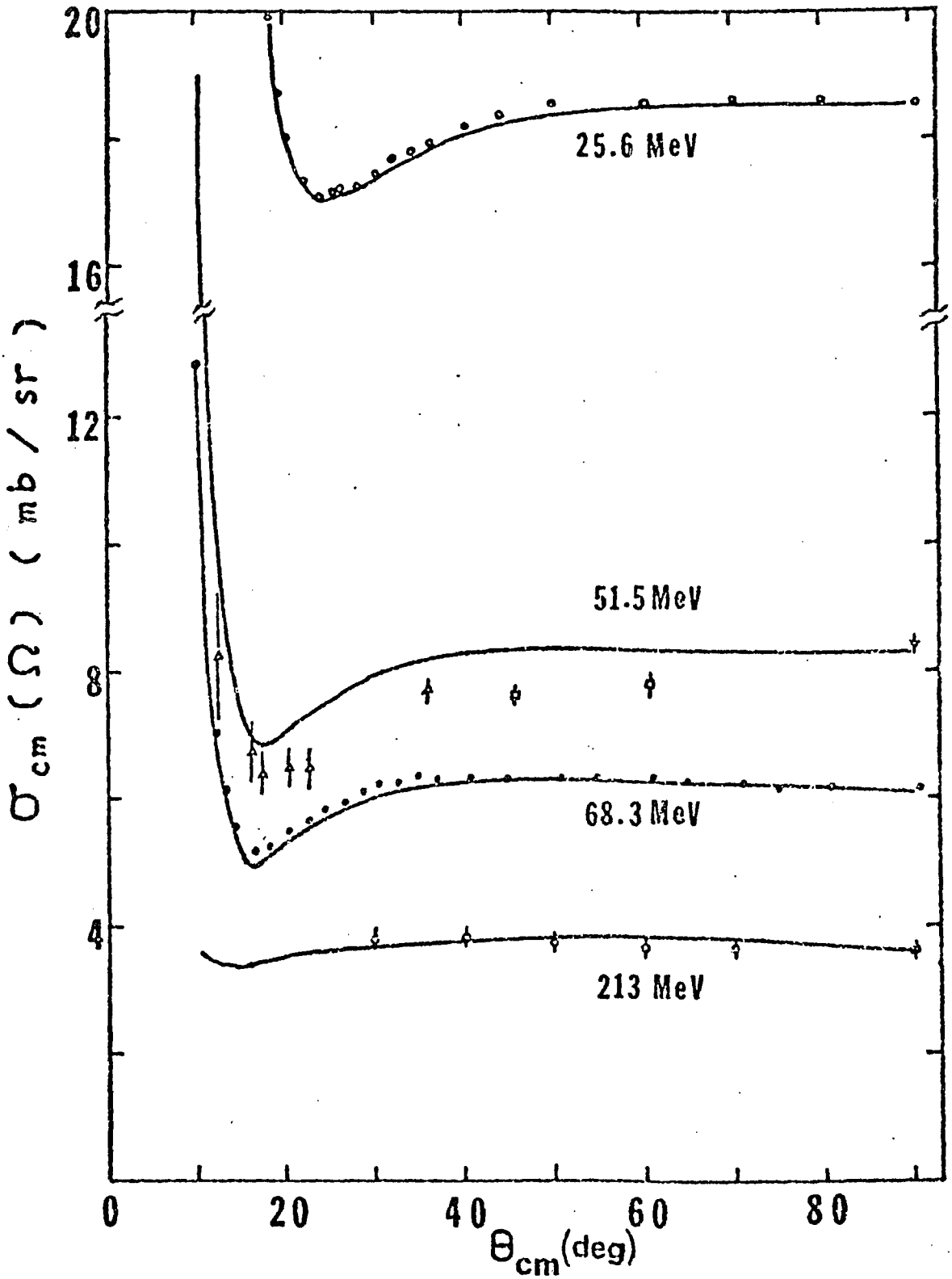

Fig. V.1 The p-p elastic scattering cross section in the cm system as a function of the scattering angle at the incident proton energies of 25.6 , 51.5, 68.3 and 213 MeV (lab.). The experiment data are from Refs. 51-54.

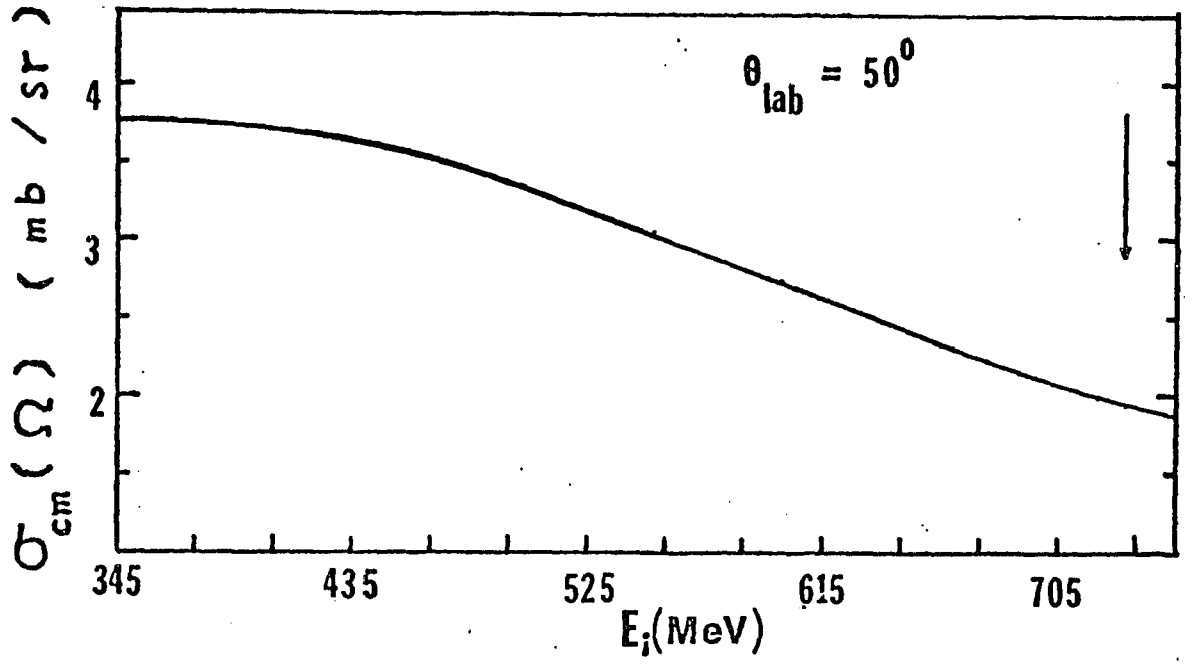

Fig. V.2a The p-p elastic scattering cross section as a function of the incident proton energy for the proton scattering angle of 50° (lab.).

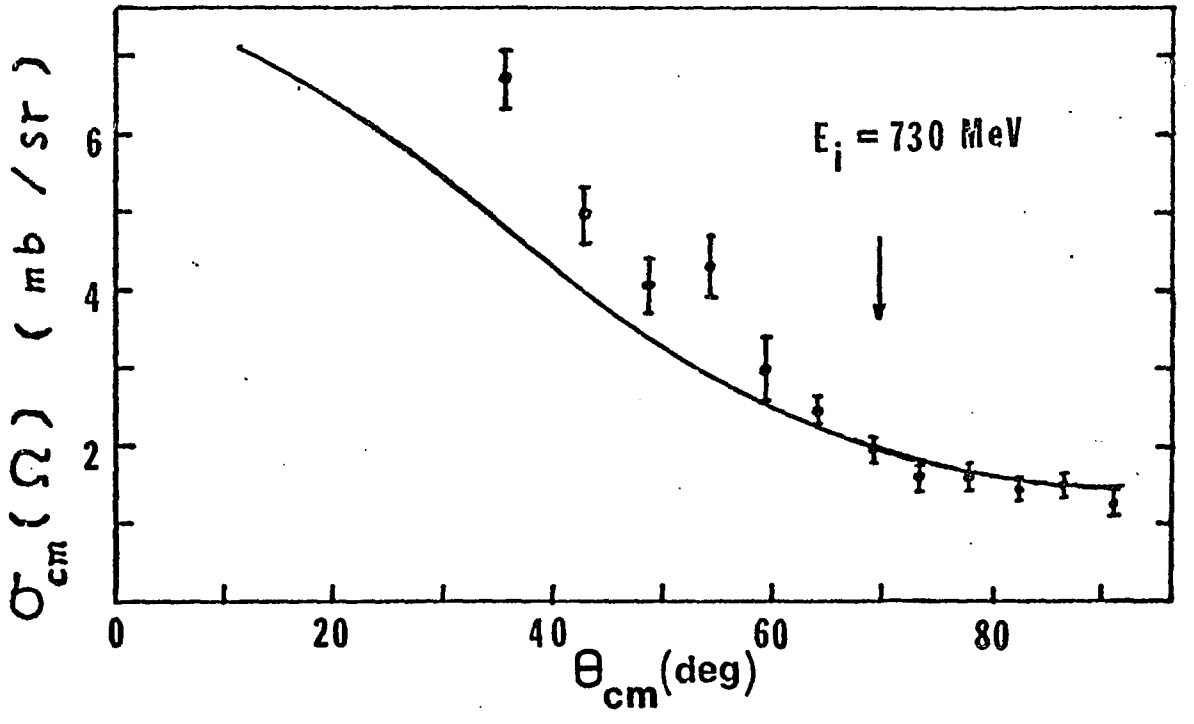

Fig. V.2b The angular distribution of the differential cross sections for the p-p elastic scattering at an incident proton energy of 730 MeV. The experimental data are from Ref. 55.

In Fig. V.1, the angular distributions of proton-proton differential cross sections in the cm system are shown for incident proton energies below 300-MeV. The experimental data are from Refs. 51-54. It is seen that our predicted cross sections agree well with the experimental data at 25.6 -MeV, 68.3-MeV and 213-MeV. At 51.5-MeV, our results are higher than experiment. Since most of our results are in very good agreement with the experimental data, the slight departure of our predicted values from the 51.5-MeV data should not be important. From these results,the Coulomb interference effect is clearly observed in the forward angles. As for an incident proton energy above the threshold for pion-production, we have compared the result of our calculation in the cm system at an incident proton energy of 730-MeV (lab.) with the experimental data of Ref. 55. In Fig. V.2b, our predicted cross section is higher then experiment for cm scattering angle below 50°, but the agreement is excellent for scattering angles above 60°. The angular range in which we are interested in this work, because of the existing bremsstrahlung experiments, is around 70° as shown by an arrow in this figure. Therefore, we believe that the elastic scattering amplitude used here should be accurate enough for our bremsstrahlung calculations.

Since the derivatives of the elastic amplitude with respect to energy or scattering angle are required in the Feshbach-Yennie approximation, we have also plotted, in

Fig. V.2a, the elastic p-p scattering cross section as a function of the incident proton energy at the laboratory scattering angle of 50°. Here, again, the arrow in the figure shows the region where our bremsstrahlung calculation is to be performed. Consider Figs. V.2a and V.2b, the smooth curves near the kinematical region of interest ensure the evaluation of the derivatives to be proper. In short, the p-p elastic scattering amplitude used in our bremsstrahlung calculation is accurate enough for our purposes. Applying this amplitude to bremsstrahlung calculations, we obtain the ppγ cross sections at the incident proton energies of 42-MeV, 48-MeV, 99-MeV, 157-MeV and 730-MeV. These results will be dicussed in two categories, one for an incident energy below 300-MeV (the threshold for pion-production) and the other for an incident energy above the threshold.

(a) Proton-proton Bremsstrahlung Below 300 MeV Incident Proton Energy.

A great number of the experimental proton-proton bremsstrahlung data have been reported during the past two decades. Most of these data are at incident proton energies below 300-MeV. From these data, only some have been chosen for our analysis because of the consideration of running time in computation. First, we present in Fig. V.3 the result of our calculation of $\sigma(\Omega_1, \Omega_2)$ at 157-MeV with a symmetric proton angle of 30° as a function of noncoplanar-

ity angles ($\bar{\phi}$). The cross section $\sigma(\Omega_1, \Omega_2)$ is the integrated cross section of $\sigma(\Omega_1, \Omega_2, \psi_\gamma)$ over ψ_γ, i.e.,

$$\sigma(\Omega_1, \Omega_2) = 2\int_0^\pi \sigma(\Omega_1, \Omega_2, \psi_\gamma)\, d\psi_\gamma ,$$

where a factor of 2 is introduced because we consider a symmetric case here and the range of ψ_γ is from 0° to 360°. The experimental data are from Ref. 56. The solid line is the result of our calculation using the soft-photon approximation of LN and the dotted line is from Liou and Sobel (39), which is a potential model calculation. It can be seen from this figure that the agreement between our result and the experimental data or the model calculation is good. To make a detailed comparison, we have plotted, in Fig. V.4, the angular distributions of $\sigma(\Omega_1, \Omega_2, \psi_\gamma)$ in the laboratory system as functions of ψ_γ at an incident energy of 157-MeV for two noncoplanarity angles $\bar{\phi} = 0.5^\circ$ and 1.5°. The outgoing protons have a polar angle of 35°. The solid curves represent our results obtained by using the choice $\Omega_1^e = \Omega_2$ so that one of the elastic proton moves along the direction of the outgoing proton which has a larger velocity than the other outgoing proton in the bremsstrahlung process. The dashed curves are obtained by using the choice $\Omega_1^e = \Omega_1$. These results are compared with the experimental data of Ref. 56 and the model calculation of Ref. 57 which is plotted as dotted curves here. The agreement between our results and the experimental data is good in general. How-

ever, for ψ_γ around 145°, solid curves appear to be lower than the experimental data or the result of the model calculation of Ref. 57. This pheonomenon can be explained by noting the expressions of Eqs. II.6, V.8 and V.9. As mensioned earlier, these expansions are good approximations if $|k\cdot R| \ll |\bar{q}_f\cdot k|$ and $|k\cdot R| \ll |\bar{p}_f\cdot k|$. Under the choice of $\Omega_1^e = \Omega_2$, we have the vector $\vec{R} = (\vec{q}_f - \vec{\bar{q}}_f)$ which is antiparallel to $\vec{q}_f$. For the case shown in Fig. V.4, the direction of $\vec{R}$ should be at $\theta = 145^\circ$ because the proton polar angle is 35°. Thus, the conditions on $|k\cdot R|$ do not hold around $\psi_\gamma = 145^\circ$. We would therefore expect that the higher order terms of the soft-photon expansion are not negligible in this particular case. On the other hand, if the choice of $\Omega_1^e = \Omega_1$ had been made, we might expect some contribution from the higher order terms in k around $\psi_\gamma = 35^\circ$ and negligible contribution around $\psi_\gamma = 145^\circ$. This is exactly the result we observe in Fig. V.4, although the difference between these two choices at $\psi_\gamma = 35^\circ$ is about the size of the experimental error bar. Furthermore, there is no good reason for us to disregard either of these two choices and it would be contradictory to the requirement of a consistent expansion if we took the average of these two results. This ambiguity in choosing the elastic kinematics for the soft-photon expansion exists only in the calculation of the H-type cross sections $\sigma(\Omega_1, \Omega_2, x)$, $x = \theta_\gamma$, k, q_f, E_q, p_f, E_p, ϕ_γ, or ψ_γ. In Fig. V.5, two similar results are shown. From this figure, we obtain again good agreement between our

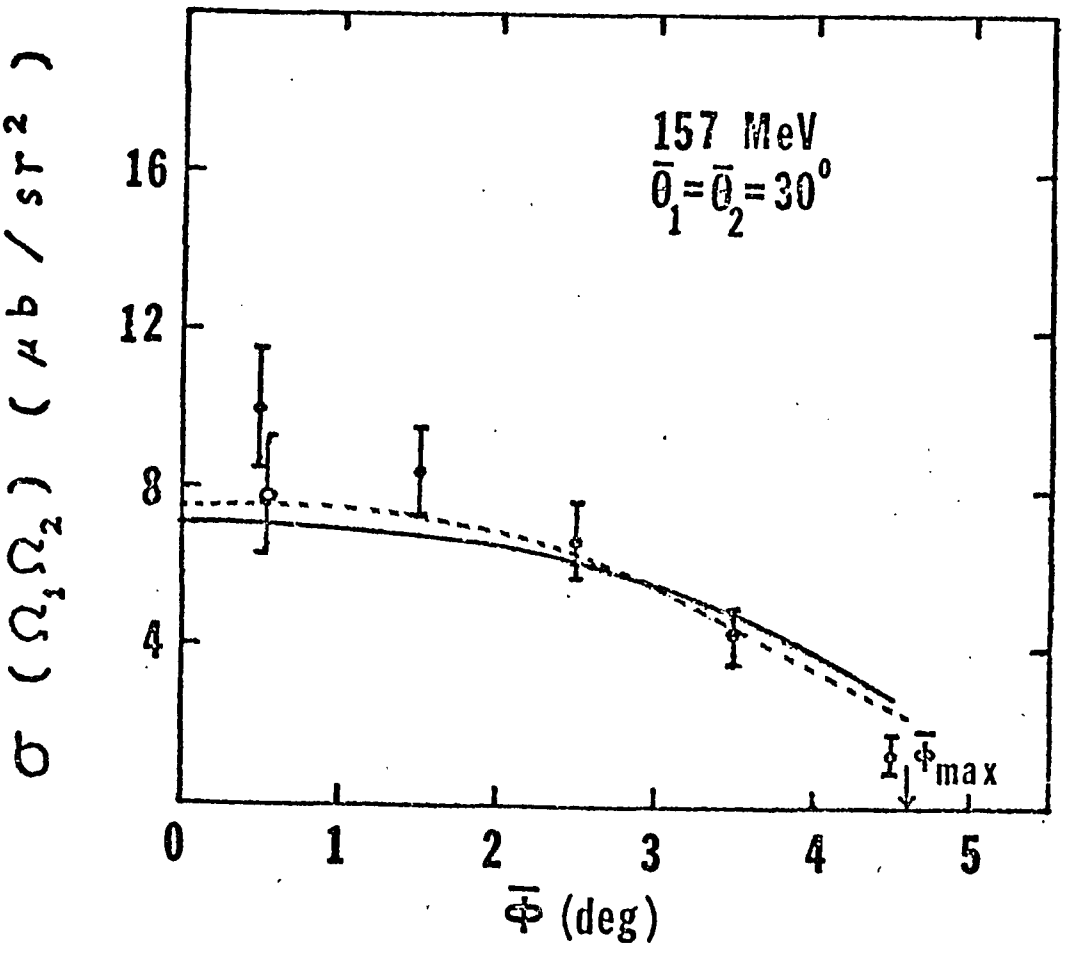

Fig. V.3 The ppγ cross section σ (Ω_1 , Ω_2) as a function of the noncoplanarity angle at an incident proton energy of 157 MeV. The proton polar angle is $\bar{\theta}_1 = \bar{\theta}_2 = 30^\circ$. The solid curve represents our result obtained by using the soft-photon approximation of LN. The dotted curve is the result of a model calculation of Ref. 57. The experiment data are from Ref. 56.

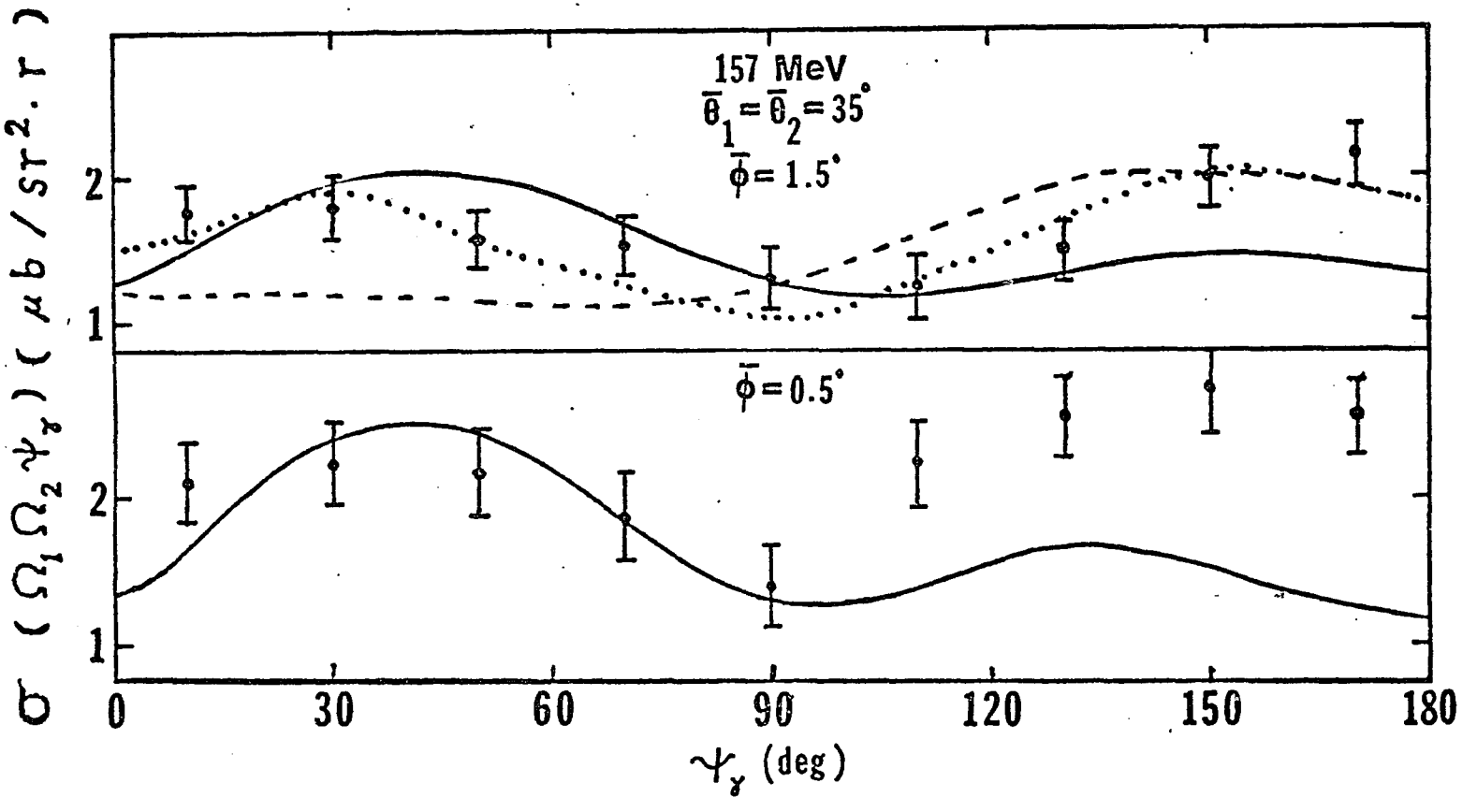

Fig. V.4 The comparison of our calculated ppγ cross sections with the experimental data of Ref. 56. The incident proton energy is 157 MeV and the proton polar angles are $\bar{\theta}_1 = \bar{\theta}_2 = 35^\circ$. The noncoplanarity angles are $\bar{\Phi} = 1.5^\circ$ (top) and 0.5° (bottom). The solid curve is our result calculated from the soft-photon approximation of LN with the choice of $\Omega_1^e = \Omega_2$ ($\Omega_1^e = \Omega_1$). The dotted curve is the result of a model calculation of Ref. 39.

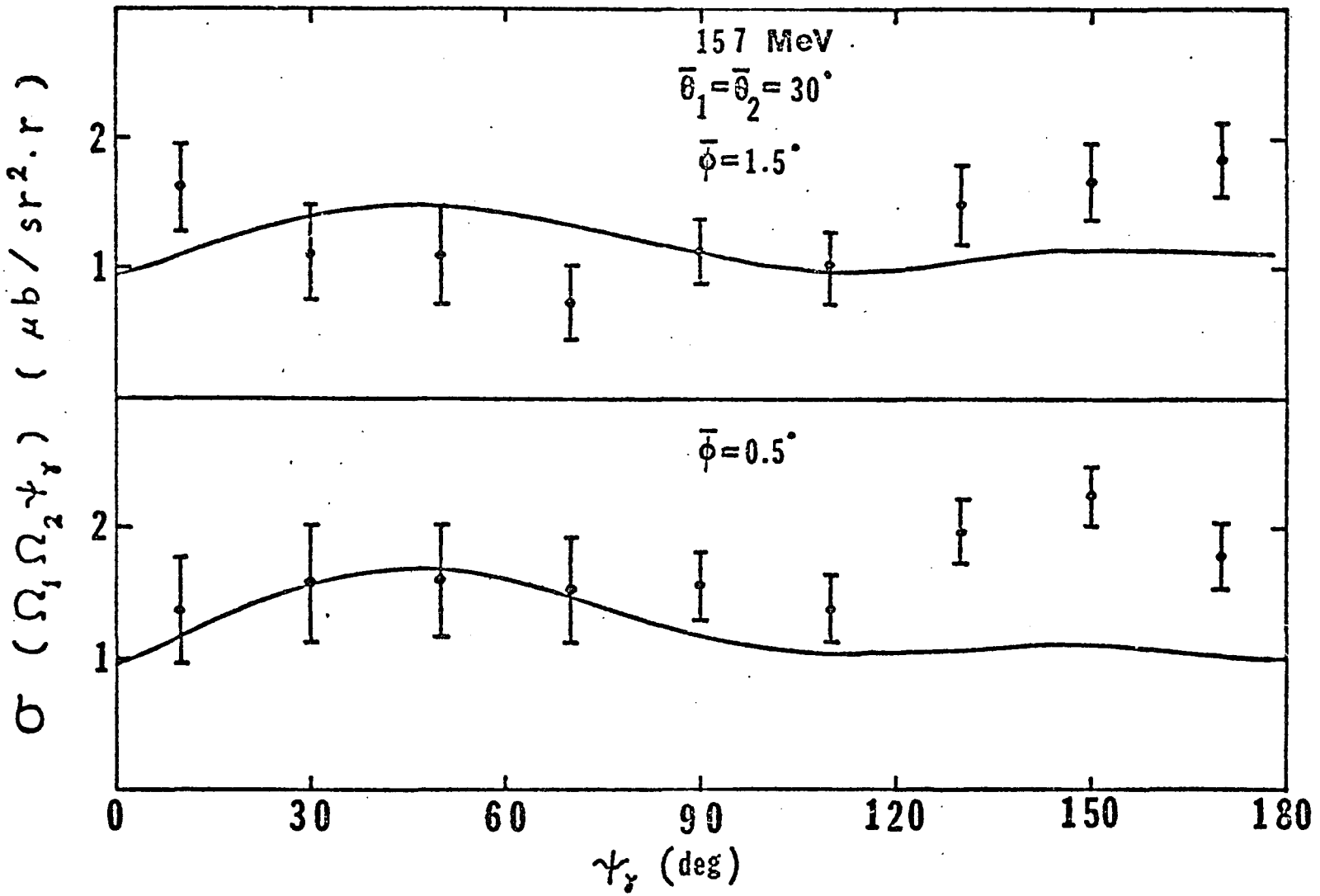

Fig. V.5 Same as Fig. V.4 but for the proton angles $\bar{\theta}_1 = \bar{\theta}_2 = 30^\circ$.

predicted cross sections and the experimental data for photons emitted away from the backward direction of Ω_1^e which is fixed in our expansion of the bremsstrahlung amplitude.

A plot of photon angular distributions $\sigma(\Omega_1, \Omega_2, \psi_\gamma)$ as functions of ψ_γ at an incident proton energy of 99-MeV with noncoplanarity angle of 0.1° is shown in Fig. V.6. The proton polar angles are $\bar{\theta}_1 = \bar{\theta}_2 = 35^\circ$. The experimental histogram is from Ref. 58. In order to test the ambiguity in the soft-photon expansion of the H-type cross section, two choices of Ω_1^e have been made separately in our calculations. Since the incident proton energy is low, the contribution from higher order terms in our expansion becomes negligible. Therefore, the difference between the results of the two different choices is small. Our predicted cross sections is shown by a solid curve and the model calculation of Ref. 56 by a dotted curve. The difference between our calculation and the model calculation is within the size of the experimental error and both of them give good agreement with experiment except in the region of large ψ_γ. Note that, for $\psi_\gamma > 130^\circ$, our results are always smaller than the experimental data and so is the model calculation of Ref.56.

The argument that little contribution comes from the higher order terms of our expansion of the bremsstrahlung amplitude for low energy scattering has also been confirmed.

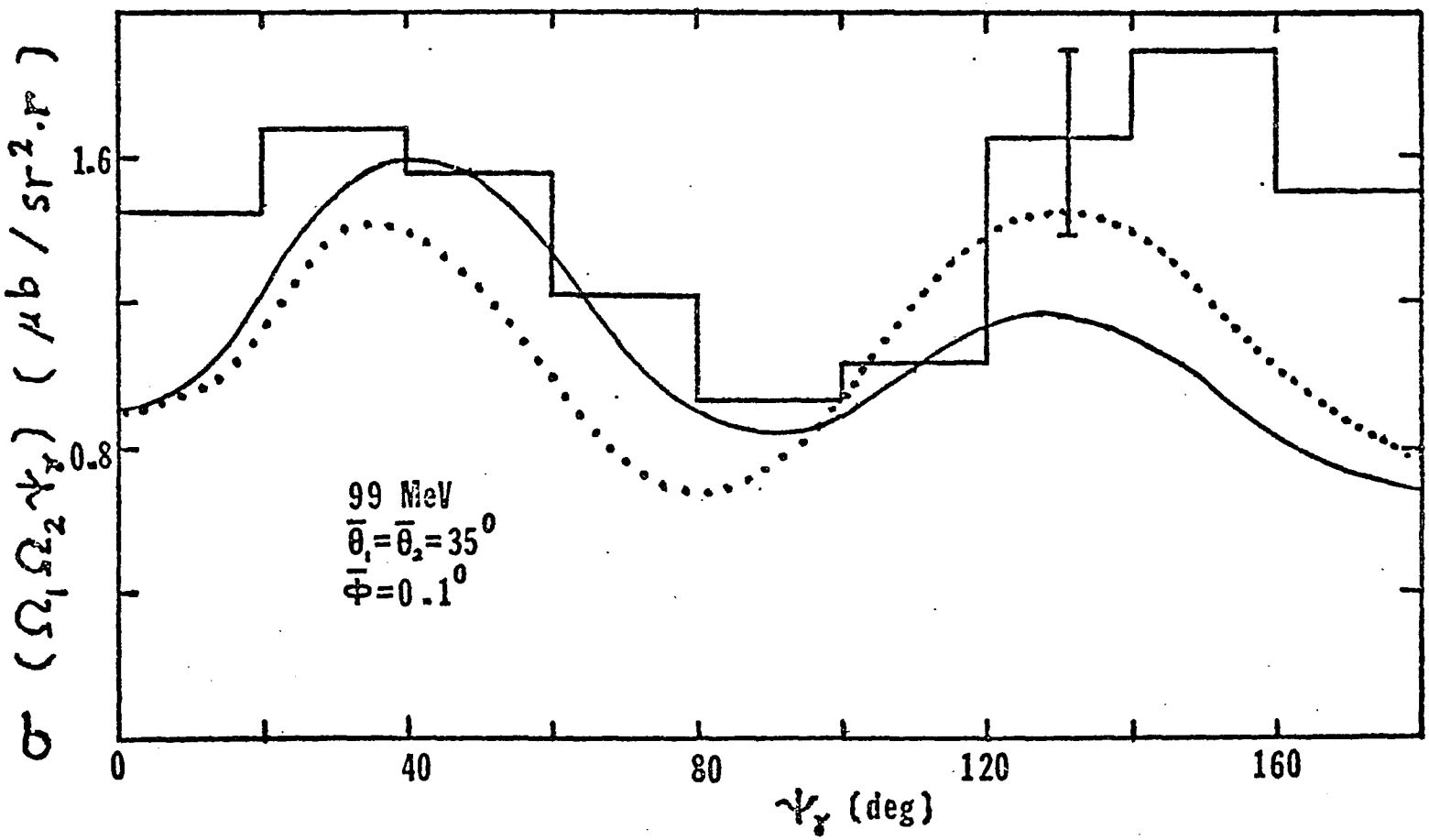

Fig. V.6 Same as Fig. V.4 but at an incident proton energy of 99 MeV for the nocoplanarity angle of 0.1°. The experimental data are from Ref. 58.

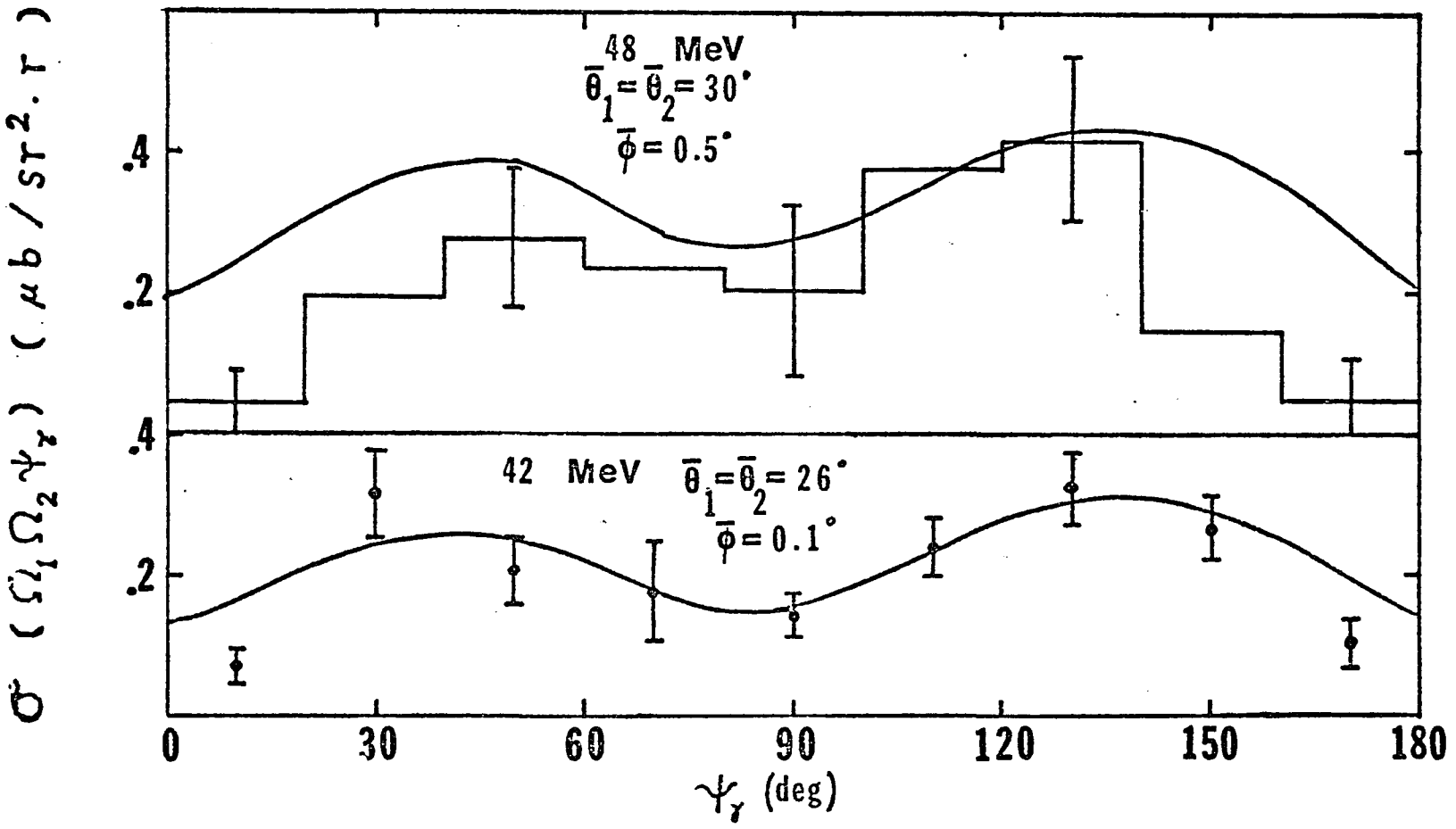

Fig. V.7 Same as Fig. V.4 but at the incident proton energies of 48 MeV (top) and 42 MeV (bottom). The proton polar angles are = =30 (top) and 26 (bottom) and the noncoplanarity angles are 0.5 (top) and 0.1 (bottom). The experiment data are from Refs, 59 and 60 for 48 MeV and 42 MeV, respectively.

In Fig. V.7, we have shown the results of our calculation for the incident energies of 48-MeV at proton angles $\bar{\theta}_1 = \bar{\theta}_2 = 30^\circ$ and 42-MeV at proton angles $\bar{\theta}_1 = \bar{\theta}_2 = 26^\circ$. The noncoplanarity angles are 0.5° and 0.1° for 48- and 42-MeV, respectively. Here, the choices of Ω_1^e do not affect our results since the incident proton energy is rather low, which makes the contribution from the higher order terms small. Our results are compared with the experimental data of Ref. 59 and 60. The agreement between the experimental data and our predictions are good except for ψ_γ near 0° and 180°.

As for nonsymmetric cases, we have calculated the proton-proton bremsstrahlung cross section for an incident proton energy of 156-MeV by using the choice of $\Omega_1^e = \Omega_2$. The proton polar angles are $\bar{\theta}_1 = 15^\circ$, $\bar{\theta}_2 = 18^\circ$, 21°, 24° and 27°. These cross sections are compared with the Orsay data (61). From Table V.1, it is seen that our results are in better agreement with the experimental data than the results of Brown (62) or CLSG (40). But, because of the ambiguity in choosing the elastic kinematics for the expansion of the bremsstrahlung amplitude, it is difficult to obtain a meaningful interpretation of our results. Thus, the only conclusion one can draw is that in order to have a consistent soft-photon expansion, the R-type cross section is to be prefered. Although there is nothing wrong with H-type cross sections, they should be compared only with full potential

model calculations.

TABLE V.1
Comparison of ppγ calculations with the experimental data of ORSAY at 156 MeV.

θ_1 (deg.)	θ_2 (deg.)	θ_γ (deg.)	Brown ($\mu b/sr^2 \cdot rad$)	CLSG ($\mu b/sr^2 \cdot rad$)	This Paper ($\mu b/sr^2 \cdot rad$)	Experiment ($\mu b/sr^2 \cdot rad$)
15	18	126.5	1.22	1.03	0.87	1.17± 0.27
15	21	133	1.48	1.21	0.94	0.95± 0.13
15	24	135.2	1.41	1.16	0.96	0.63± 0.14
15	27	133.7	1.45	1.20	0.94	0.68± 0.09

(b) Proton-proton Bremsstrahlung above 300 MeV Incident proton Energy

In general, off-shell effects are larger for higher incident proton energy than for lower ones. Recently, the bremsstrahlung cross sections for the scattering by protons of a 730-MeV proton beam has become available (45). These data were reported as R-type cross sections in the laboratory system for 16 photon angles. Locations of photon counters are shown in Table I of Ref. 45. To analyze these data by using the soft-photon approximation of LN and the Feshbach-Yennie approximation, we have applied the results of section B and C. The effect of the expansion of the phase space factor has also been studied up to order k^2. The results are shown in Figs. V.8 through V.13. In these figures, solid curves are the results obtained by using the Feshbach-Yennie approximation. The dashed (dotted) curves represent the results of our calculations using the first three (two) terms of the expansion of the bremsstrahlung amplitude and using the full phase space factor.

The results for photon counters G1 through G6 are shown in Figs. V.8 and V.9. It is seen that the agreement between our predictions and experiment is good. The difference between the soft-photon approximation of LN, with the full phase space factor, and the Feshbach-Yennie approximation is small. The effect of the terms of order k is small; it

changes the cross section within the experimental error bar.

In Figs. V.10 and V.11, we show the results for photon counters G7 through G10. Here, two more curves are presented for each counter, the dash-dotted curve is the result obtained by using the first three terms of the "expanded cross section" and the other curve (chain-dotted) using the first two terms. By the "expanded cross section" we mean that the cross section is obtained by using the expanded bremsstrahlung amplitude as well as the expanded phase space factor. In general, our predicted cross sections agree well with the data of Ref. 45 only for photon energies below 70-MeV. For $k > 70$-MeV, all of our results are lower than the data of Ref. 45 for these photon counters. At this point, it is worthwhile to give some comparison of our results with those of Ref. 45. Their curve labelled EED is very close to our result using the first two terms in the "expanded cross section". And their curve labelled SPA lies between our solid curve and dashed curve for these photon counters except G7 for which their SPA is very close to our solid curve. By comparing the dashed curve with the dotted curve, we see that the use of the full phase space factor does change the cross sections at large k. But it still can not account for the discrepancies between the experimental data and theoretical results at large k. Having considered the full phase space factor and having included the terms of order k from gauge invariance condition in our calculations,

we may expect other effects to be important in these kinematical regions.

In Fig. V.12, we show the results for photon counters G11 and G12. All of our predicted cross sections are lower than the data of Ref. 45 for counter G11. This feature is similar to that in Ref. 45, but, our result for the Feshbach-Yennie approximation is higher than their SPA for $k > 120$-MeV and our result is different from the data of Ref. 45 by a constant factor which might not have special physical meaning. For photon counter G12, our calculation for the Feshbach-Yennie approximation predicts also a higher cross section for large k than the SPA of Ref. 45 and agrees well with experiment. It should be emphasized that this good agreement does not necessarily imply that the contribution from the terms of order k and higher is negligible for this photon counter. For photon counters G13 through G16, as shown in Fig.V.13, our calculations give similar results which are in good agreement with the experimental data.

Furthermore, the cross sections we presented here are point cross sections. The correction factor S to the point cross section due to the finite size of detectors is given in Table IX of Ref. 45. These correction factors might be different if one does not use EED to calculate them, though the difference due to different bremsstrahlung amplitudes

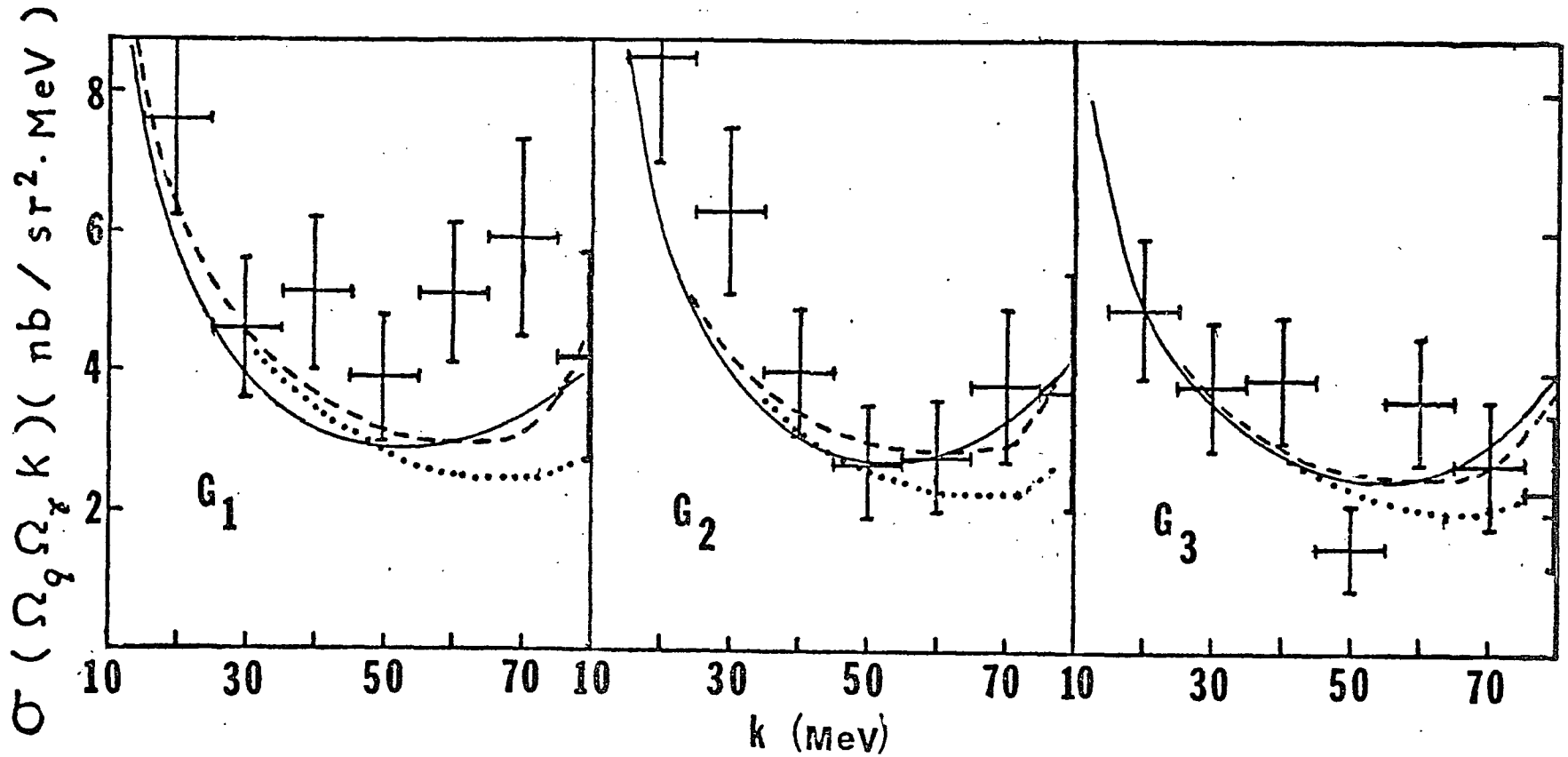

Fig. V.8 The comparison of our ppγ calculations with the experimental data of Ref. 45 for the photon counters G1 through G3. The incident proton energy is 730 MeV and the locations of photon counters are shown in Table V.1. The solid curve represents our results calculated in the Feshbach-Yennie approximation. The dashed curve is our result calculated in the softphoton approximation of LN with the full phase space factor. All three terms in Eq. V.16 are used in this calculation. The dotted curve is the result of the same approximation but the expanded phase space factor is used.

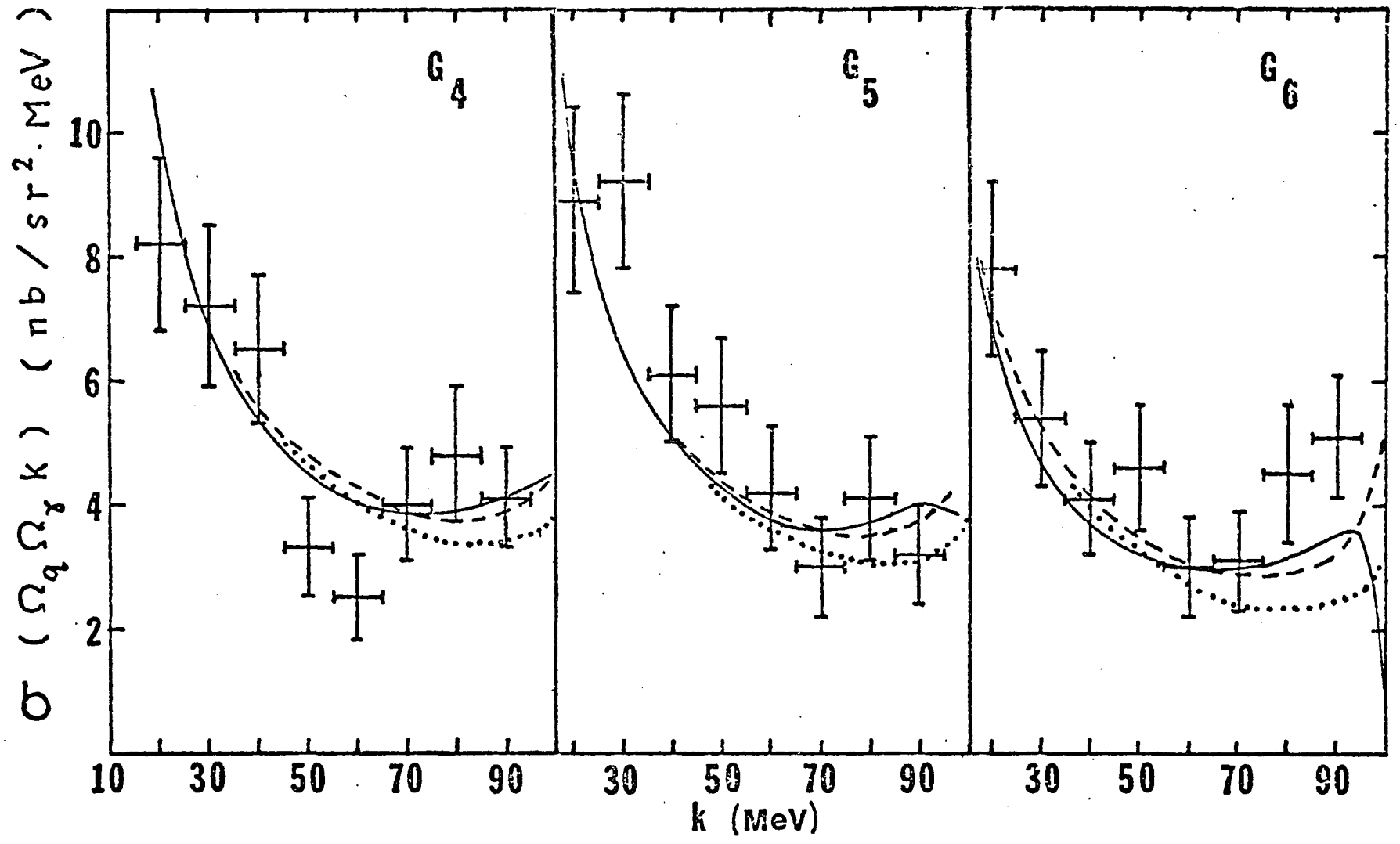

Fig. V.9 Same as Fig. V.8 but for counters G4-G6.

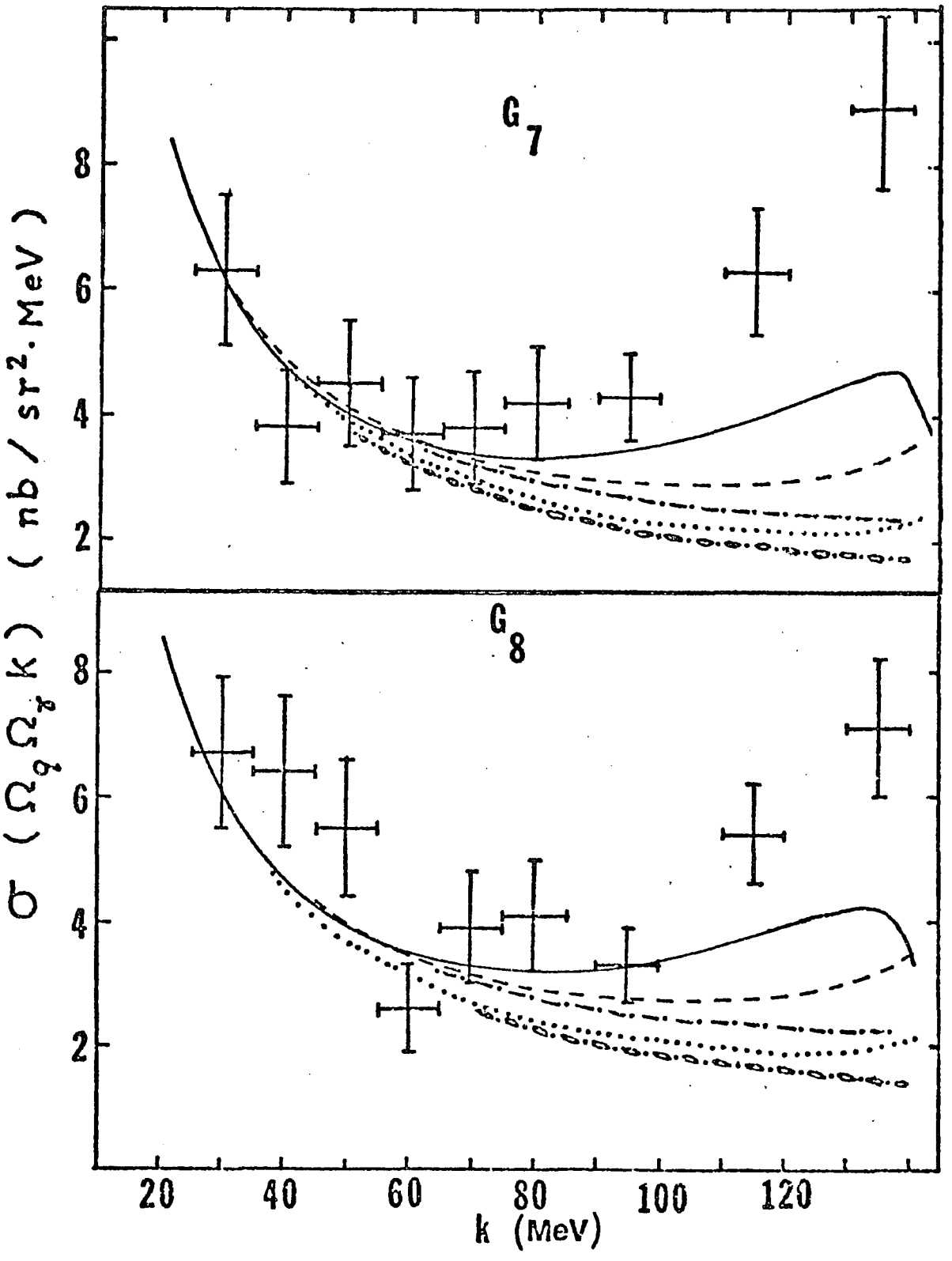

Fig. V.10 Same as Fig. V.8 but for counters G7 and G8. Here the dash-dotted (chain-dotted) curve is obtained by using the expression $\sigma_{-1}/k + \sigma_0$ with the full (expanded) phase space factor.

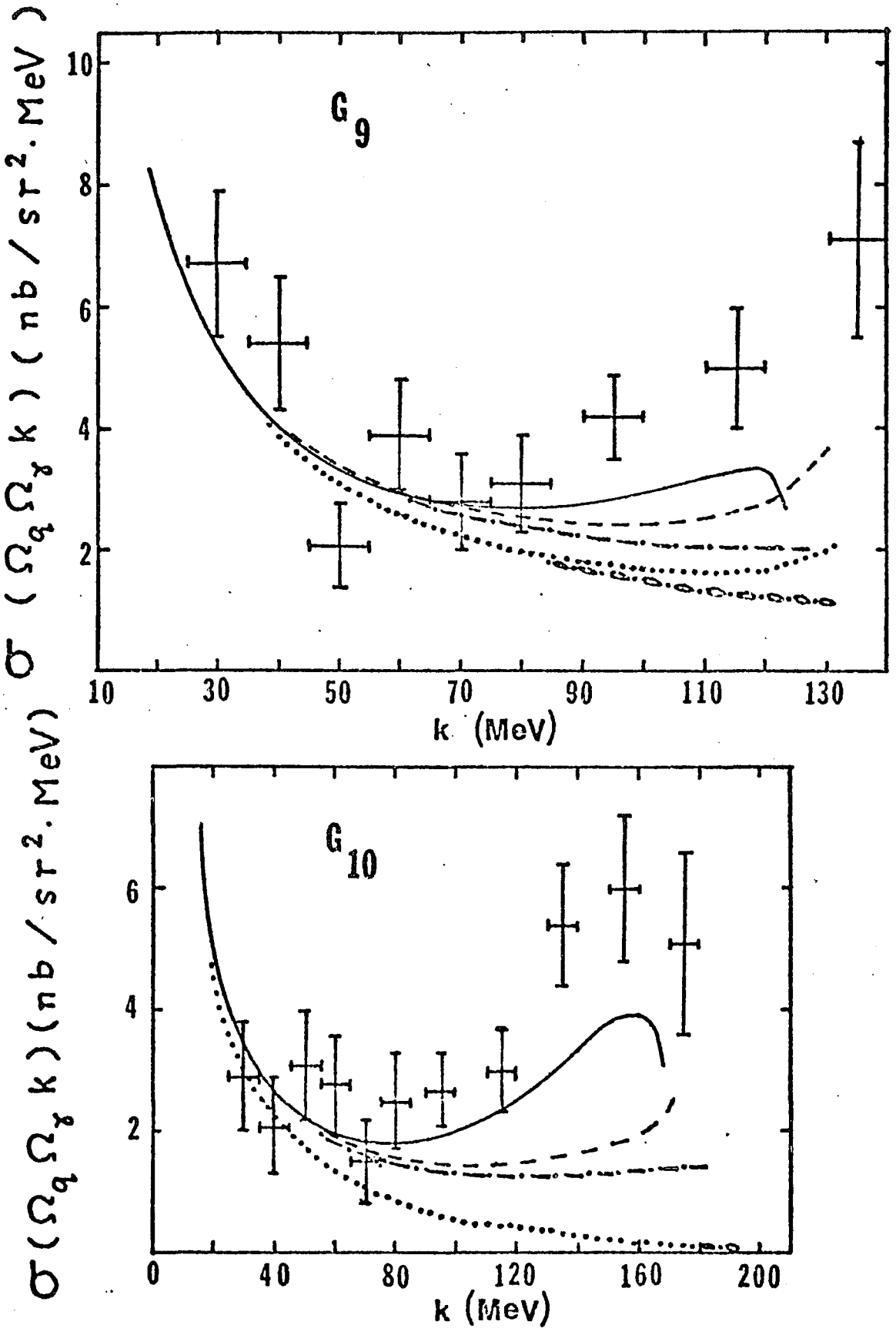

Fig. V.11 Same as Fig. V.10 but for counters G9 and G10.

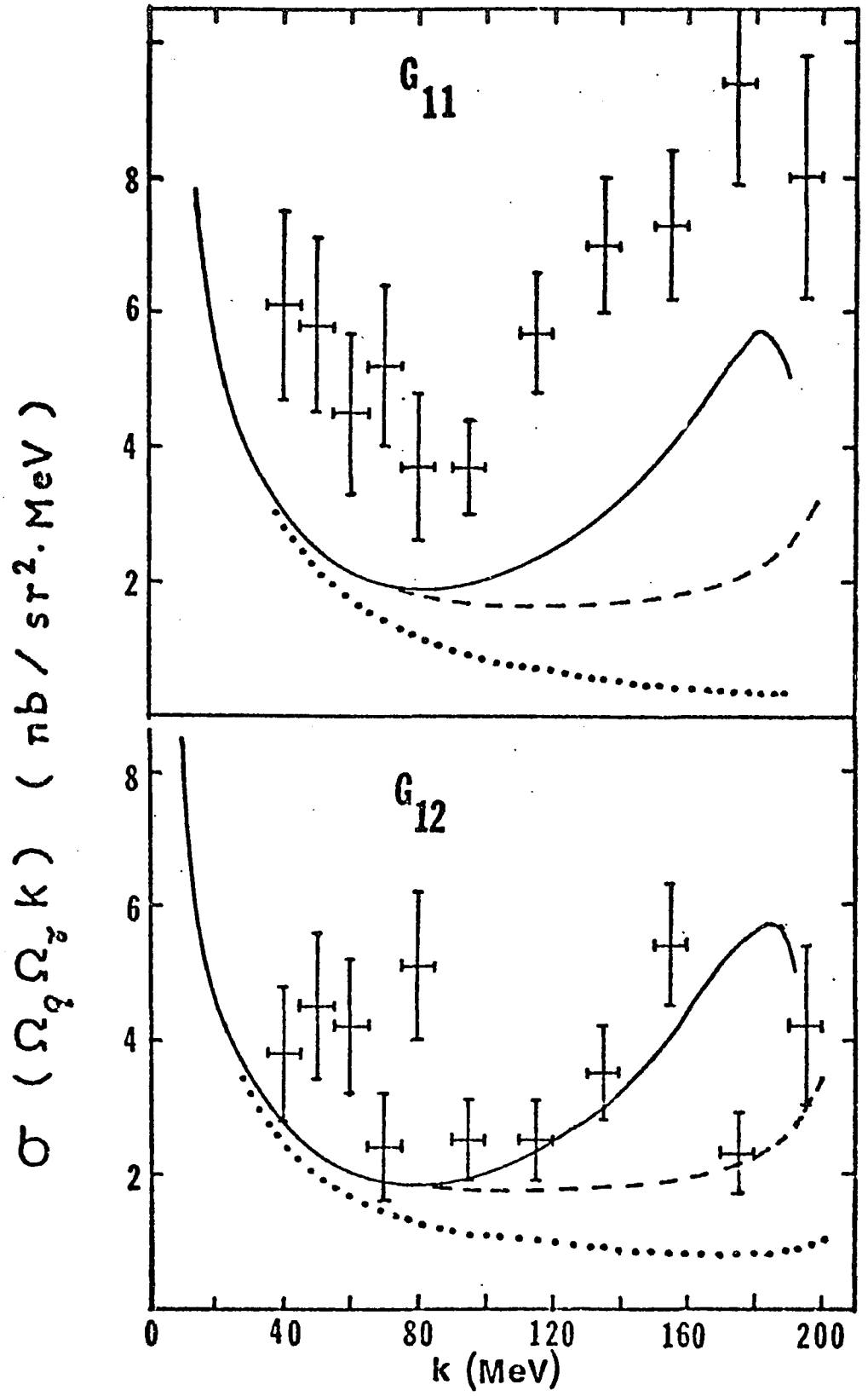

Fig. V.12 Same as Fig. V.8 but for counters G11-G12.

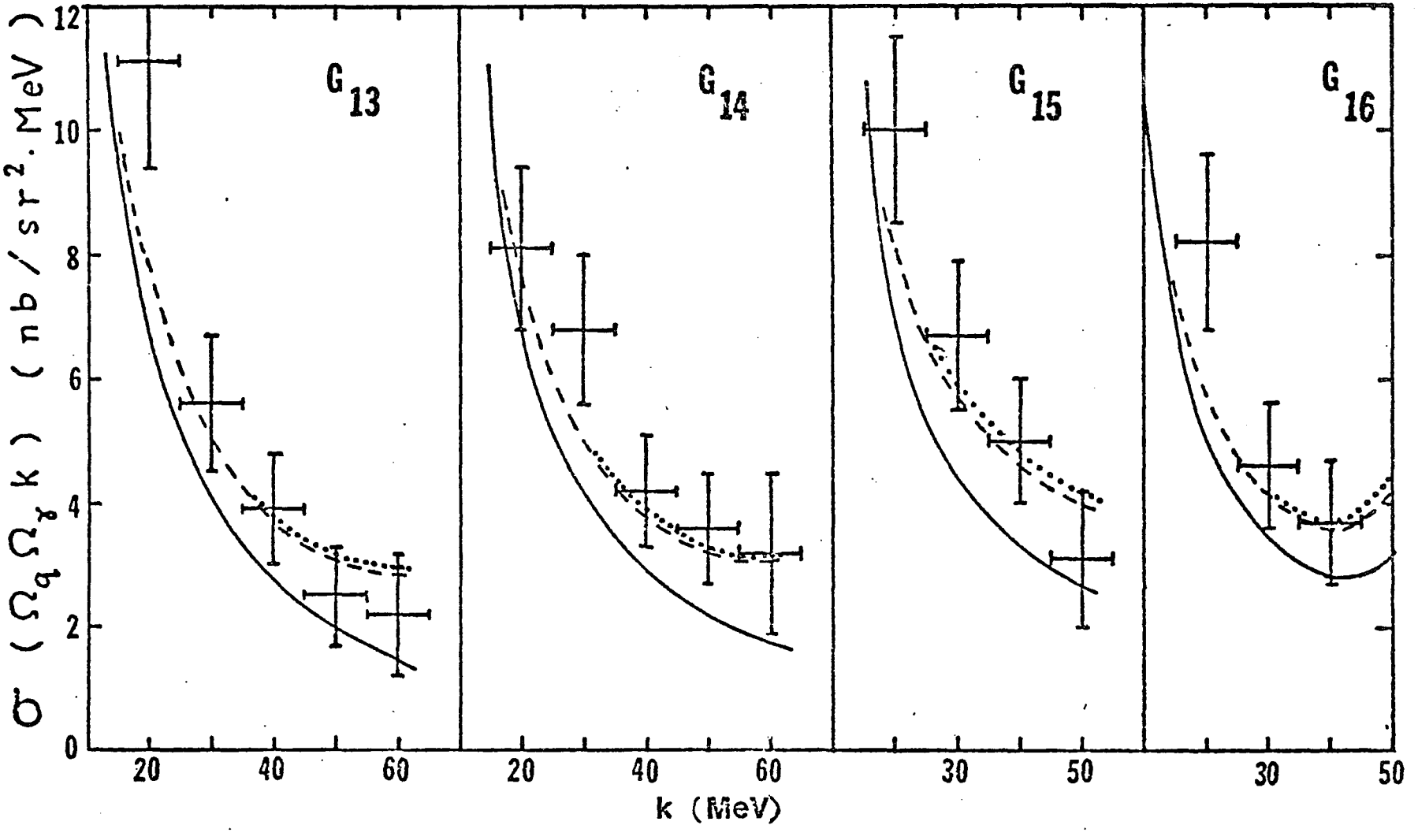

Fig. V.13 Same as Fig. V.8 but for counters G13-G16.

used may be small. Application of these correction factors to our results does not affect our conclusions.

In short, we have calculated the ppγ cross sections by applying the soft-photon approximation of LN and the Feshbach-Yennie approximation. In our soft-photon approximation, the bremsstrahlung amplitude has been completely expanded in powers of photon energy about the on-shell point, k=0. At the incident proton energy of 730-MeV, our results are in good agreement with experiment for most photon counters of Ref. 45. However, for the photon counters G7-G10, our results calculated from the first two terms of the "expanded cross section" are lower than the experimental data at higher photon energies. In an attempt to understand this unexpectedly large discrepancy between theory and experiment, we have studied the effect of the phase space factor on the cross section and have estimated the effect of those terms of order k in our expansion of the bremsstrahlung amplitude. These factors result in about a 20% increase of the calculated cross section at high photon energy for the counters G7-G10. That is, our predicted results are still about 50% lower than experiment. This leads us to expect that other effects such as off-shell effects and isobar effects (63 - 65) may not be negligible in these kinematical regions. We have also compared our result calculated in the Feshbach- Yennie approximation with the data at 730-MeV. Since relativistic effects might not

be small at this incident proton energy, we have taken into account not only the principal term but also the correction terms of the Feshbach-Yennie approximation. The result of this calculation is in better agreement with experiment than that calculated from the soft-photon approximation. But, it is still lower than the experimental data by about 35% at high photon energy for counters G7-G10.

As for the low energy ppγ data, our results for the soft-photon approximation are in good agreement with experiment. However, there exists an ambiguity in choosing the elastic kinematics if the bremsstrahlung amplitude is to be expanded in powers of photon energy for an H-type cross section. The effect of this ambiguity in the cross section is approximately the size of the experimental error for some photon angles at the incident proton energy of 157-MeV, while it is negligible at the energy of 99-MeV and lower.

CHAPTER VI SUMMARY AND CONCLUSION

We have applied two model-independent approaches, the soft-photon approach and the Feshbach-Yennie approach, to study the nuclear bremsstrahlung processes.

In our study of the $p^{12}C\gamma$ process, the bremsstrahlung cross sections near the 1.7-MeV resonance have been calculated using the Feshbach-Yennie apprximation and the results are compared with the experimental data of the Bologna group and the Brooklyn group. We have found that the correction terms in the Feshbach-Yennie approximation are important in the energy region of the $p^{12}C$ resonance. At an energy very far from any resonant state, however, the principal term of the approximation dominates and gives results which are in good agreement with the experimental data. In addition, the time delay for the $p-^{12}C$ reaction has been extracted from the $p^{12}C\gamma$ data and its value is about 10^{-20} second near the resonance.

In our study of the $\pi^{\pm}p\gamma$ processes, we have calculated the bremsstrahlung cross sections at 330 (324) MeV, 298 MeV, and 269 (263) MeV for the coplanar and noncoplanar cases. As in LN, our bremsstrahlung amplitude used in the soft-photon approximation has been expanded completely in powers of the photon energy, about the point of zero photon energy. This approximation gives results which are in very

good agreement with the UCLA data for most of the photon angles. We have also applied the Feshbach-Yennie approximation to the $\pi^{\pm} p\gamma$ processes by taking into account both the principal and correction terms in the calculation of $\pi^{\pm} p\gamma$ cross section. We have found that this approximation always predicts a bump in the bremsstrahlung spectrum near the $\Delta(1236)$ resonance. Most of these bumps are small and our predicted cross sections are in good agreement with the experimental data. However, for some counters, the bumps are too large for the $\pi^{+} p\gamma$ process at 269-MeV. The UCLA data do not permit us to select the best approximation from these two different approximations.

Finally, we have applied both approximations to the $pp\gamma$ process. At an incident proton energy of 730-MeV, our results from both approximations are in good agreement with the experimental data of Ref. 45 for most photon angles. However, for photon counters G7-G10, the results calculated from the first two terms of the soft-photon approximation are too low at high photon energies. The contribution from those terms of order k in our expansion have been estimated. We have found that it increases the calculated cross section at high photon energies for most of the cases but the results are still lower than the experimental data. The Feshbach-Yennie approximation gives better agreement but theory is still lower than the experimental data. Therefore, we expect that other effects, such as the isobar

effects (63-65), are important in these kinematical regions. For the low energy ppγ process, we have obtained results which are in good agreement with the experimental data. However, we have shown that there exists an ambiguity in the determination of the elastic kinematics from a given bremsstrahlung process if the soft-photon expansion is to be applied to an H-type cross section.

APPENDIX A. INVARIANT FUNCTIONS AND HELICITY AMPLITUDES FOR PROTON-PROTON SCATTREING

The invariant functions $\{F_\alpha\}$, $\alpha = 1, 2, 3, 4, 5$ used in Eq.V.2 can be written in terms of phase shifts by inverting the equations given in GGMW. In Nyman's work, $\{F_\alpha\}$ have been written as linear combinations of $\{f_\alpha\}$ of GGMW. The required relations are then obtained by putting $\{f_\alpha\}$ in terms of partial wave amplitues f_0^J, f_1^J, f_{11}^J, f_{12}^J and f_{22}^J which are explicit functions of phase shifts. Unfortunately, the method of including the Coulomb amplitude is not clearly given there. Because of this and also because of increased simplicity in numerical calculation, another approach has been used in our work.

First, we invert Eq.4.17 of GGMW and solve for F_α directly. The results are

$$F_1 = C\Big[(p^2-3E^2)E\phi_1 + (p^2+3E^2)E(\phi_4-\phi_3-\phi_2) - \frac{4\beta E^2}{m y}(m^2+2E^2)\phi_5\Big],$$

$$F_2 = C\Big[-4E^2\frac{E}{1+\beta}\phi_3 - 4E^2\frac{E}{1-\beta}\phi_4 - \frac{8E^4}{my}\phi_5\Big],$$

$$F_3 = C\Big[-4mE^2\frac{\beta}{y}\phi_5 - E(E^2+p^2)\phi_1 - Em^2(\phi_2+\phi_3 - \phi_4)\Big],$$

$$F_4 = C\left[\frac{4E^3}{1+z}\phi_3 + \frac{4E^3}{1-z}\phi_4 + \frac{8E^2m}{y}\phi_5\right],$$

$$F_5 = C\left\{(3p^2-E^2)E\phi_1 - (3p^2+E^2)E\phi_2 + \left[\frac{8E^2}{1+z} - (3p^2+E^2)\right]E\phi_3 + \left[-\frac{8E^2}{1-z} + (3p^2+E^2)\right]E\phi_4 - \frac{4zE^2}{my}(p^2+E^2)\phi_5\right\}, \qquad (A.1)$$

where $C = \frac{\pi}{2E^2p^2}$, $y = \sin\theta$, $z = \cos\theta$, $E^2 = p^2 + m^2$.

Then the required relations are obtained through the use of expressions of ϕ_α in Ref. 48. One of these expressions is shown below, demonstrating the way on which the exact Coulomb amplitude is included

$$\phi_1 = \frac{1}{2}f_{cs} + \frac{z}{2}f_{ca} + \sum_{J\,even}\left\{(2J+1)h_J + Jh_{J-1,J} + (J+1)h_{J+1,J} + 2(J^2+J)^{1/2}h^J\right\}d^J_{00}, \qquad (A.2)$$

where

$$f_{cs} = f_c(\theta) + f_c(\pi-\theta)\ ;\quad f_{ca} = f_c(\theta) - f_c(\pi-\theta),$$

and f_c's is the usual Coulomb amplitude. The usual partial wave amplitudes are

$$h'_l = \frac{1}{2ik}\left(e^{2i\delta_l} - 1\right)e^{2i\Phi_l}\ ,\quad h'_{lJ} = \frac{1}{2ik}\left(e^{2i\bar{\delta}^N_{lJ}} - 1\right)e^{2i\Phi_l},$$

$$h'_{J\pm1,J} = \frac{1}{2ik}\left(\cos 2\bar{\epsilon}^N_J\, e^{2i\bar{\delta}^N_{J\pm1,J}} - 1\right)e^{2i\Phi_{J\pm1}},$$

$$h'^J = \frac{1}{2k} \sin 2\bar{\epsilon}^N_J \exp\left(i\,\bar{\delta}^N_{J-1,J} + i\,\bar{\delta}^N_{J+1,J}\right),$$

where $\bar{\delta}^N$'s are nuclear bar phase shifts and $\bar{\epsilon}^N$ are mixing parameters. For an incident energy above the threshold for pion-production, we include the inelasticity parameters ρ_J, ρ_{JJ}, etc. as in Ref. 48 so that

$$\begin{aligned} h_l &= h'_l \cos\rho_J, \qquad h_{l,J} = h'_{l,J} \cos\rho_{l,J}, \\ h_{J\pm1,J} &= h'_{J\pm1,J} \cos\rho_{J\pm1,J}, \qquad h^J = h'^J e^{i\alpha}. \end{aligned} \tag{A.3}$$

Since $\{\phi_\alpha\}$ have been properly antisymmetrized, the conditions imposed on the Feynman amplitude by the Pauli priciple have been satisfied. This can be checked easily as follows. By changing z into $-z$ in Eq.A1 and using the following relations,

$$\begin{aligned} \phi_i(-z) &= \phi_i(z), \quad i = 1, 2, 5, \\ \phi_3(-z) &= -\phi_4(z), \end{aligned}$$

we obtain $F_\alpha(z) = (-1)^\alpha F_\alpha(-z)$ which is exactly the restrictions imposed on the F_α's by the Pauli principle as shown in GGMW.

APPENDIX B. PHASE SPACE FACTORS, THE R-TYPE CROSS SECTION, AND THE H-TYPE CROSS SECTION

The R-type and the H-type cross sections have been introduced by Liou (24). The H-type cross section is $\sigma_1^H \equiv \sigma(\Omega_1, \Omega_2, x)$, $x = q_f$, E_q, p_f, E_p, k, θ_γ, or ϕ_γ. The independent variables for the H-type cross section are θ_q, ϕ_q, θ_p, ϕ_p, and x. The R-type cross section is $\sigma^R \equiv \sigma(\Omega_\gamma, k, y, z)$. The independent variables for the R-type cross section are θ_γ, ϕ_γ, γ, k, and z, where y can be either ϕ_q or ϕ_p, and $z = q_f$, E_q, p_f, E_p, θ_q or θ_p.

The phase space factor for an R-type cross section has been derived in LN and has been expanded in powers of photon energy up to order k. Here, we expand this phase space factor to one order higher, i.e., to order k^2. Following LN, we write the phase space factor F for the cross section $\sigma(\Omega_q, \Omega_\gamma, k)$ as

$$F = \frac{\left[(p_i \cdot q_f)^2 - (mM)^2\right]^{3/2}}{M^2 \left|(p_i \cdot q_f)(p_f \cdot q_f) - m^2 (p_i \cdot p_f)\right|} \quad . \tag{B.1}$$

Then, we expand $\left|(p_i \cdot q_f)(p_f \cdot q_f) - m^2 (p_i \cdot p_f)\right|^{-1}$ and $\left[(p_i \cdot q_f)^2 - (mM)^2\right]^{3/2}$ using Eq. II.6. After some manipulations, we obtain

$$F = F^{(0)} + F^{(1)} + F^{(2)} \quad , \tag{B.2}$$

$$F^{(0)} = \frac{N^{3/2}}{N_R M^2} \quad , \qquad F^{(1)} = F^{(0)} \left[H + \frac{3}{N} (p_i \cdot \bar{q}_f)(p_i \cdot R) \right] ,$$

$$F^{(2)} = F^{(0)} \left\{ \frac{3H}{N}(p_i\cdot\bar{q}_f)(p_i\cdot R) + \frac{3}{2}(p_i\cdot R)^2\left[\frac{1}{N} + \frac{1}{N^2}(p_i\cdot\bar{q}_f)^2\right] + H^2 \right.$$
$$\left. - \frac{1}{N_R}\left[(p_i\cdot R)(\bar{p}_f\cdot k) - (p_i\cdot\bar{q}_f)(R+k)\cdot R - \bar{q}_f\cdot(R+k)(p_i\cdot R)\right]\right\},$$

where

$$H \equiv \frac{1}{N_R}\left[(p_i\cdot\bar{q}_f)\,\bar{q}_f\cdot(R+k) - (\bar{p}_f\cdot\bar{q}_f)(p_i\cdot R) - m^2 p_i\cdot(R+k) - (p_i\cdot\bar{q}_f)(\bar{p}_f\cdot R)\right],$$

$$N \equiv (p_i\cdot\bar{q}_f)^2 - m^2M^2.$$

As for an H-type cross section, we used the phase space factor of Refs. 26 and 66. It has the following form:

$$F' = \frac{p_1^2 p_2^2}{f E_1 E_2}\left|\sin\theta_\gamma\right|\left[(\cos\phi_\gamma - \sin\phi_\gamma\cot\phi_o)^2 + \left(\frac{\cos\theta_\gamma}{\sin\theta_\gamma} - \frac{\tan\theta_o\sin\phi_\gamma}{\sin\phi_o}\right)\right], \qquad \text{(B.3)}$$

$$f = (\cos\phi_\gamma - \sin\phi_\gamma\cot\phi_o)\left[\frac{\tan\theta_o\cos\phi_\gamma}{\sin\phi_o}J_1 - \frac{1}{\sin\theta_\gamma} \times (A_1B_1 + A_2B_2 + A_3k)\right] - (\sin\phi_\gamma + \cos\phi_\gamma\cot\phi_o) \times\left[\frac{\cos\theta_\gamma}{\sin\theta_\gamma} - \frac{\tan\theta_o\sin\phi_\gamma}{\sin\phi_o}\right]J_1,$$

$$A_1 = \sin\phi_\gamma\left[p_1'\sin\theta_1\sin\phi_1\cos\theta_2 - p_1'\sin\theta_2\sin\phi_2\cos\theta_1\right.$$

$$+ p\sin\theta_2 \sin\phi_2\Big] + \cos\phi_\gamma\Big[p\sin\theta_2\cos\phi_2 - p_1'\sin\theta_2\cos\phi_2$$

$$\times \cos\theta_1 + p_1'\sin\theta_1\cos\phi_1\cos\theta_2\Big],$$

$$A_2 = \sin\phi_\gamma\Big[p_2'\sin\theta_1\sin\phi_1\cos\theta_2 - p_2'\sin\theta_2\sin\phi_2\cos\theta_1$$

$$- p\sin\theta_1\sin\phi_1\Big] + \cos\phi_\gamma\Big[- p\sin\theta_1\cos\phi_1 - p_2'\sin\theta_2\cos\phi_2$$

$$\times \cos\theta_1 + p_2'\sin\theta_1\cos\phi_1\cos\theta_2\Big],$$

$$A_3 = \sin\phi_\gamma\Big[\sin\theta_1\sin\phi_1\cos\theta_2 - \sin\theta_2\sin\phi_2\cos\theta_1\Big] - \cos\phi_\gamma$$

$$\times\Big[\sin\theta_2\cos\phi_2\cos\theta_1 - \sin\theta_1\cos\phi_1\cos\theta_2\Big],$$

$$J_1 = \beta_1 k\sin\theta_2\sin(\phi_\gamma-\phi_2) + \beta_2 k\sin\theta_1\sin(\phi_1-\phi_\gamma) - k$$

$$\times\Big[\sin\theta_1\sin\theta_2\sin\theta_\gamma\sin(\phi_1-\phi_2) + \sin\theta_2\cos\theta_1\cos\theta_\gamma$$

$$\times\sin(\phi_\gamma-\phi_2) + \sin\theta_1\sin\theta_2\cos\theta_\gamma\sin(\phi_1-\phi_\gamma)\Big],$$

$$\beta_1 = p_1'/(\vec{p}_1'^{\,2}+1)^{1/2}, \qquad \beta_2 = p_2'/(\vec{p}_2'^{\,2}+1)^{1/2}.$$

Note that, in the H-type cross section, we have used $\vec{\phi} = \frac{1}{2}(\phi_1 + \phi_2)$ and $\vec{k}' = \vec{k} - \alpha\vec{q}$, where $\vec{q}$ is the momentum of the limitting γ-ray with $\theta_\gamma = \theta_0$ and $\phi_\gamma = \phi_0$. Here, we choose α such that $\vec{k}'$ lies in the xz-plane and has polar angle ψ_γ (39).

APPENDIX C. EXTERNAL BREMSSTRAHLUNG AMPLITUDE FOR THE NNγ PROCESS IN THE SOFT-PHOTON APPROXIMATION OF LN

In the soft-photon approximation of LN, the dependent variables for an R-type cross section are expanded about the on-shell point, k = 0, and so are the bremsstrahlung amplitudes. The external bremsstrahlung amplitude for a NNγ process is given by Eq. V.5. To expand this amplitude, we use the expressions of the invariant functions given by Eq. V.9, which has been expanded completely about k = 0. Expanding also the propagators and electromagnetic vertex functions, we finally obtain the expanded external bremsstrahlung amplitude as a sum of $M_\mu(1/k)$, $M_\mu(k^0)$ and $M_\mu(k)$, which are of order k^{-1}, k^0 and k, respectively:

$$M_\mu^E = M_\mu^E(\tfrac{1}{k}) + M_\mu^E(k^0) + M_\mu^E(k), \tag{C.1}$$

$$M_\mu^E(\tfrac{1}{k}) = \sum_{\alpha=1}^{5} \Big\{ \bar{u}_{q_f} \mathcal{F}_\alpha^e q_\alpha \Big[\frac{\not{z}\,\bar{q}_f^\mu}{\bar{q}_f\cdot k} - \frac{\not{z}\,q_i^\mu}{q_i\cdot k} \Big] u_{q_i}\, \bar{u}_{p_f} \gamma^\alpha u_{p_i}$$

$$+ \bar{u}_{q_f} \gamma_\alpha u_{q_i}\, \bar{u}_{p_f} \mathcal{F}_\alpha^e \gamma^\alpha \Big[\frac{\not{z}\,\bar{p}_f^\mu}{\bar{p}_f\cdot k} - \frac{\not{z}\,p_i^\mu}{p_i\cdot k} \Big] u_{p_i} \Big\},$$

$$M_\mu^E(k^0) = \sum_\alpha \Big\{ \bar{u}_{q_f} \Big[\mathcal{F}_\alpha^e A_0^\mu - \frac{\partial \mathcal{F}_\alpha^e}{\partial t} 2(\bar{p}_f - p_i)\cdot(R+k) \frac{\not{z}\,\bar{q}_f^\mu}{\bar{q}_f\cdot k}$$

$$+ 2\not{z}\,\bar{q}_f^\mu \frac{\partial \mathcal{F}_\alpha^a}{\partial \Delta_a} \Big] \gamma_\alpha u_{q_i}\, \bar{u}_{p_f} \gamma^\alpha u_{p_i} + \bar{u}_{q_f} \gamma_\alpha$$

$$\Big[\mathcal{F}_\alpha^e B_0^\mu + \frac{\partial \mathcal{F}_\alpha}{\partial s} 2(\bar{q}_f + \bar{p}_f)\cdot k \frac{\not{z}\,q_i^\mu}{q_i\cdot k} + \frac{\partial \mathcal{F}_\alpha}{\partial t} \cdot$$

$$\times 2(\bar{p}_f - p_i)\cdot(R+k)\frac{z q_i^\mu}{q_i\cdot k} + \frac{\partial \mathcal{F}_\alpha^b}{\partial \Delta_b} 2 z q_i^\mu \Big] u_{q_i}\, \bar{u}_{p_f}\, g^\alpha u_{p_i}$$

$$+ \bar{u}_{q_f} g_\alpha u_{q_i}\, \bar{u}_{p_f} \Big[\mathcal{F}_\alpha^e C_0^\mu + \frac{\partial \mathcal{F}_\alpha}{\partial t} 2(\bar{q}_f - q_i)\cdot R \frac{z \bar{p}_f^\mu}{\bar{p}_f\cdot k}$$

$$+ \frac{\partial \mathcal{F}_\alpha^c}{\partial \Delta_c} 2 z \bar{p}_f^\mu \Big] g^\alpha u_{p_i} + \bar{u}_{q_f} g_\alpha u_{q_i}\, \bar{u}_{p_f}\, g^\alpha \Big[\mathcal{F}_\alpha^e$$

$$\times D_0^\mu + \frac{\partial \mathcal{F}_\alpha}{\partial s} 2(\bar{q}_f + \bar{p}_f)\cdot k \frac{z p_i^\mu}{p_i\cdot k} + 2 z p_i^\mu \frac{\partial \mathcal{F}_\alpha^d}{\partial \Delta_d}$$

$$- \frac{\partial \mathcal{F}_\alpha}{\partial t} 2(\bar{q}_f - q_i)\cdot R \frac{z p_i^\mu}{p_i\cdot k} \Big] u_{p_i} \Big\},$$

$$M_\mu^E(k) = \sum_\alpha \Big\{ \bar{u}_{q_f} \Big[\mathcal{F}_\alpha^e A_1^\mu - \frac{\partial \mathcal{F}_\alpha}{\partial t} 2(\bar{p}_f - p_i)\cdot(R+k) A_0^\mu$$

$$+ \frac{\partial \mathcal{F}_\alpha^a}{\partial \Delta_a} 2\left(q_f\cdot k A_0^\mu + R\cdot k\, \bar{q}_f^\mu\right) + \frac{\partial \mathcal{F}_\alpha}{\partial t} \frac{\bar{q}_f^\mu}{\bar{q}_f\cdot k}(R+k)^2 \Big] g_\alpha u_{q_i}$$

$$\times \bar{u}_{p_f} g^\alpha u_{p_i} + \bar{u}_{q_f} g_\alpha \Big[-\frac{\partial \mathcal{F}_\alpha}{\partial s} 2(\bar{q}_f + \bar{p}_f)\cdot k B_0^\mu - \frac{\partial \mathcal{F}_\alpha}{\partial t}$$

$$\times 2(\bar{p}_f - p_i)\cdot(R+k) B_0^\mu - \frac{\partial \mathcal{F}_\alpha^b}{\partial \Delta_b} 2 q_i\cdot k B_0^\mu - \frac{\partial \mathcal{F}_\alpha}{\partial t}$$

$$\times (R+k)^2 \frac{q_i^\mu}{q_i\cdot k} \Big] u_{q_i}\, \bar{u}_{p_f}\, g^\alpha u_{p_i} + \bar{u}_{q_f} g_\alpha u_{q_i}\, \bar{u}_{p_f}$$

$$\times \Big[\mathcal{F}_\alpha^e C_1^\mu + \frac{\partial \mathcal{F}_\alpha}{\partial t} R^2 \frac{\bar{p}_f^\mu}{\bar{p}_f\cdot k} + \frac{\partial \mathcal{F}_\alpha^c}{\partial \Delta_c} 2\Big(\bar{p}_f\cdot k\, C_0^\mu - R\cdot k$$

$$\times \frac{\bar{p}_f^\mu}{\bar{p}_f\cdot k}\Big) - \frac{\partial \mathcal{F}_\alpha}{\partial t} 2(\bar{q}_f - q_i)\cdot R\, C_1^\mu \Big] g^\alpha u_{p_i} +$$

$$+\bar{u}_{q_f} g_\alpha u_{q_i} \bar{u}_{p_f} g^\alpha \Big[-\frac{\partial \mathcal{F}_\alpha}{\partial s} 2(\bar{q}_f+\bar{p}_f)\cdot k\, D_o^\mu - \frac{\partial \mathcal{F}_\alpha}{\partial t} 2(\bar{q}_f - q_i)\cdot R$$

$$\times D_o^\mu - \frac{\partial \mathcal{F}_\alpha^d}{\partial \Delta_d} 2 p_i\cdot k\, D_o^\mu - \frac{\partial \mathcal{F}_\alpha}{\partial t} R^2 \frac{p_i^\mu}{p_i\cdot k} \Big] u_{p_i} ,$$

$$A_o^\mu \equiv \frac{z R^\mu}{\bar{q}_f\cdot k} - \frac{z(k\cdot R)\,\bar{q}_f^\mu}{(\bar{q}_f\cdot k)^2} + \frac{\lambda_z}{2m}\Big(\gamma^\mu - \frac{\bar{q}_f^\mu \not{k}}{\bar{q}_f\cdot k}\Big) + (z+\lambda_z)\frac{\gamma^\mu \not{k}}{2\bar{q}_f\cdot k} ,$$

$$B_o^\mu \equiv \frac{\lambda_z}{2m}\Big(\gamma^\mu - \frac{q_i^\mu \not{k}}{q_i\cdot k}\Big) - (z+\lambda_z)\frac{\gamma^\mu \not{k}}{2 q_i\cdot k} ,$$

$$C_o^\mu \equiv -\frac{Z(R+k)^\mu}{\bar{p}_f\cdot k} + \frac{z(k\cdot R)\,\bar{p}_f^\mu}{(\bar{p}_f\cdot k)^2} + \frac{\lambda_z}{2M}\Big(\gamma^\mu - \frac{\bar{p}_f^\mu \not{k}}{\bar{p}_f\cdot k}\Big) + (z+\lambda_z)\frac{\gamma^\mu \not{k}}{2\bar{p}_f\cdot k} ,$$

$$D_o^\mu \equiv \frac{\lambda_z}{2M}\Big(\gamma^\mu - \frac{p_i^\mu \not{k}}{p_i\cdot k}\Big) - (z+\lambda_z)\frac{\gamma^\mu \not{k}}{2 p_i\cdot k} ,$$

$$A_1^\mu \equiv \frac{(k\cdot R)^2\,\bar{q}_f^\mu}{(\bar{q}_f\cdot k)^3} - \frac{(k\cdot R)\,R^\mu}{(\bar{q}_f\cdot k)^2} - \frac{\lambda_z}{2m}\Big[\frac{R^\mu \not{k}}{\bar{q}_f\cdot k} - \frac{(k\cdot R)\,\bar{q}_f^\mu \not{k}}{(\bar{q}_f\cdot k)^2}\Big]$$

$$-(1+\lambda_z)\frac{k\cdot R\,\gamma^\mu \not{k}}{2(\bar{q}_f\cdot k)^2} ,$$

$$C_1^\mu \equiv -\frac{(k\cdot R)(R+k)^\mu}{(\bar{p}_f\cdot k)^2} + \frac{(k\cdot R)^2\,\bar{p}_f^\mu}{(\bar{p}_f\cdot k)^3} + \frac{\lambda_z}{2M}\Big[\frac{(R+k)^\mu \not{k}}{\bar{p}_f\cdot k}$$

$$-\frac{(k\cdot R)\,\bar{p}_f^\mu \not{k}}{(\bar{p}_f\cdot k)^2}\Big] + (1+\lambda_z)\frac{(k\cdot R)\,\gamma^\mu \not{k}}{2(k\cdot \bar{p}_f)^2} . \qquad (C.2)$$

BIBLIOGRAPHY

1. M.I. Sobel and A.H. Cromer, Phys. Rev. 158, 1157, (1967); Phys. Rev. 132, 2698 (1963).

2. M.K. Liou, in proceedings of the International Conference on Few-Body Problems in Nuclear and Particle Physics (Quebec, 1975), and references therein.

3. E.M. Nyman, Phys. Reports 9, 179 (1974).

4. R.M. Eisberg, D.R. Yennie and D.H. Wilkinson, Nucl. Phys. 18, 338 (1960).

5. H. Feshbach and D.R. Yennie, Nucl. Phys. 37, 150 (1962).

6. L.A. Kondratyuk and L.A. Ponomarev, SJNP 7, 82 (1968).

7. F.E. Low, Phys. Rev. 110, 974 (1958).

8. Y. Ueda, Phys. Rev. 145, 1214 (1966).

9. S.L. Adler and Y. Dothan, Phys. Rev. 151, 1267 (1966); H.W. Fearing, E. Fishbach, and J. Smith, Phys. Rev. D2, 542 (1970).

10. T.H. Burnett and N.M. Kroll, Phys. Rev. Lett. 20, 86 (1968).

11. J.S. Bell and R. Van Royen, Nuovo Cimento 60A, 62 (1969).

12. E.M. Nyman, Phys. Letts. 25b, 135 (1967); Phys. Rev. 170, 1628 (1968).

13. H.W. Fearing, Phys. Rev. C6, 1136 (1972); Phys. Rev. D7, 243 (1973).

14. Low's theorem has been proved in a potential model by L. Heller, P. Signell, M.K. Liou and other authors (see Ref. 2 for references).

15. B.M.K. Nefkens and D.I. Sober, Phys. Rev. D14, 2434 (1976).

16. M.K. Liou and W.T. Nutt, Phys. Rev. D16, 2176 (1977); Nuovo Cimento 46A, 365 (1978), this paper will be refered to hereafter as LN.

17. D.I. Sober, M. Arman, D.J. Blasberg, R.P. Haddock, K.C. Leung, B.M.K. Nefkens, B.L. Schrock and J.M. Sperinde, Phys. Rev. D11, 1017 (1975).

18. K.C. Leung, M. Arman, H.C. Ballagh jr., P.F. Glodis, R.P. Haddock, B.M.K. Nefkens and D.I. Sober, Phys. Rev. D14, 698 (1976).

19. B.M.K. Nefkens, M. Arman, H.C. Ballagh, P.F. Glodis, R.P. Haddock, K.C. Leung, D.E.A. Smith and D.I. Sober, Phys. Rev. D18, 3811 (1978), and the references therein.

20. W. Wolfli, J. Hall, and R. Muller, Phys. Rev. Lett. 27, 271 (1971); A.M. Green and A. Prodon, Nucl. Phys. A183, 225 (1972).

21. C. Maroni, I. Massa and G. Vannini, Phys. Letts. 60B, 344 (1976); Nucl. Phys. A273, 429 (1976).

22. G.J. Jan, C.C. Perng and M.K. Liou, Phys. Letts. 85B, 25 (1979); C.C. Perng, G.J. Jan and M.K. Liou, preprint.

23. M.K. Liou, C.K. Liu, P.M.S. Lesser and C.C. Trail, Phys. Rev. C21, 518 (1980); C.C. Trail, P.M.S. Lesser, A.H. Bond, jr., M.K. Liou and C.K. Liu, Phys. Rev. C21, 2131 (1980).

24. M.K. Liou, Phys. Rev. D18, 3390 (1978).

25. M.K. Liou and C.K. Liu, preprint.

26. L.S. Celenza, M.K. Liou, M.I. Sobel, and B.F. Gibson, Phys. Rev. C8, 838 (1973). This paper is refered to hereafter as CLSG.

27. J.C. Armstrong, M.J. Baggett, W.R. Harris, and V.A. Latcrre, Phys. Rev. 144, 823 (1966); H.L. Jackson and A. Galonsky, Phys. Rev. 89, 370 (1953).

28. E.M. Nyman, Nucl. Phys. A154, 97 (1970).

29. W.E. Fischer and P. Minkowski, Nucl. Phys. B36, 519 (1972).

30. R.P. Haddock and K.C. Leung, Phys. Rev. D9, 2151 (1974).

31. C. Picciotto, Nucl. Phys. B89, 357 (1975); G. Grammer, jr., Phys. Rev. D15, 917 (1977).

32. P. Signell, "Few Body Problem, Light Nuclei, and Nuclear Interactions", Vol. 1, Edited by Guy Paic and Ivo Slaus, 1967.

33. G. Felsner, Phys. Lett. 25B, 290 (1967); F. Partovi, Phys. Rev. C14, 795 (1976).

34. V.E. Barnes et al., CERN Report No. 63-27 (unpublished).

35. M.I. Sobel, Phys. Rev. 138, B1517 (1965); J.H. McGuire, A.H. Cromer and M.I. Sobel, Phys. Rev. 179, 948 (1969).

36. V.R. Brown, Phys. Rev. 177, 1498 (1969).

37. D. Drechsel and L.C. Maximon, Ann. of Phys. 49, 403 (1968).

38. J.H. McGuire, Phys. Lett. 32B, 73 (1970).

39. M.K. Liou and M.I. Sobel, Ann. of Phys. 72, 323 (1972).

40. L.S. Celenza, B.F. Gibson, M.K. Liou and M.I. Sobel, Phys. Lett. 42B, 331 (1972).

41. L. Heller and M. Rich, Phys. Rev. C10, 479 (1974).

42. J.H. McGuire and A.H. Cromer, Phys. Rev. 184, 1018 (1969).

43. H.W. Fearing, AIP Conference Proceedings No. 41, 506, AIP, N.Y. (1978).

44. B.M.K. Nefkens, O.R. Sander and D.I. Sober, Phys. Rev. Lett. 38, 876 (1977).

45. B.M.K. Nefkens, O.R. Sander, D.I. Sober and H.W. Fearing, Phy. Rev. C19, 877 (1979).

46. M.L. Goldberger, M.T. Grisaru, S.W. MacDowell and D.Y. Wong, Phys. Rev. 120, 2250 (1960), this paper is refered to hereafter as GGMW.

47. We used the metric: $g_{\mu\nu} = \begin{pmatrix} 1 & 0 & 0 \\ 0 & -1 & \\ & & -1 \end{pmatrix}$.

48. N. Hoshizaki, Suppl. of the Prog. Theor. Phys. 42, 107 (1968).

49. M.H. Macgregor, R.A. Arndt and R.M. Wright, Phys. Rev. 169, 1128 (1968).

50. M.H. Macgregor, R.A. Arndt and R.M. Wright, Phys. Rev. 169, 1149 (1968).

51. T.H. Jeong et al., Phys. Rev. 118, 1080 (1960).

52. K. Nisimura et al.,INSJ-45. Quoted in K.Nisimura, Suppl. of the Prog. of Theor. Phys. 39,286 (1967).

53. D.E. Young et al., Phys. Rev. 119, 313 (1960).

54. A. Konradi, thesis, University of Rochester 1961. Quoted in R. Wilson, "The Nucleon-Nucleon Interaction" (Interscience, New York 1963).

55. B.A. Ryan, A. Kanofsky, T.J. Derlin, R.E. Mischke and P.F. Shepard, Phys. Rev. D3, 1 (1971).

56. B. Gottschalk, W.J. Shlaer and K.H. Wang, Nucl. Phys. A94, 491 (1967).

57. M.K. Liou and M.I. Sobel, Ann. of Phys. 72, 323 (1971).

58. F. Sannes, J. Trischuk and D.G. Stairs, Phys. Rev. Lett. 21, 1474 (1968); Nucl. Phys. A146, 438 (1970).

59. D.L. Mason, M.L. Halbert and L.C. Northcliffe, Phys. Rev. 176, 1159 (1968).

60. J.V. Jovanovich, L.G. Greeniaus, J. Mckeown, T.W. Millar, D.G. Peterson, W.F. Prickett, K.F. Suen and J.C. Thompson, Phys. Rev. Lett. 26, 277 (1971).

61. A. Willis, V. Comparat, R. Frascaria, N. Marty, M. Morlet and N. Willis, Phys. Rev. Lett. 28, 1063 (1972).

62. V.R. Brown, Phys. Rev. C6, 1110 (1972). This paper is refered to herafter as Brown.

63. L. Tiator, H.J. Weber and D. Drechsel, Nucl. Phys. A306, 468 (1978).

64. A. Szyjewicz and A.N. Kamal, 8-th Int'l Conf. on Few body systems and Nucl. Forces, Graz, Aug. 1978.

65. A.N. Kamal and A. Szyjewicz, Nucl. Phys. A285, 397 (1977); A. Ruckl, Phys. Lett. 64B, 39 (1976).

66. M.K. Liou, Ph. D. thesis, University of Manitoba, Canada 1969.

67. T.K. Dahlblom and A.M. Green, Phys. Lett. 41B, 23, (1972).

68. P.M. Ogden, D.E. Hagge, J.A. Helland, M. Banner, J.F. Detoeuf, and J. Teiger, Phys. Rev. 137, B1115 (1965).